LITHUANIAN UNIVERSITY OF HEALTH SCIENCES

Milda Šeškutė

INNATE ANTIVIRAL RESPONSE IN HUMAN INTESTINAL MODELS: INTRACELLULAR SIGNALLING AND IMMUNOMODULATORY ROLE OF MELATONIN

Doctoral Dissertation
Medical and Health Sciences,
Medicine (M 001)

Kaunas, 2025

Dissertation has been prepared at the Department of Pediatrics of the Faculty of Medicine of the Lithuanian University of Health Sciences during the period of 2020–2024.

Scientific Supervisor

Prof. Dr. Lina Jankauskaitė (Lithuanian University of Health Sciences, Medical and Health Sciences, Medicine – M 001).

Consultant

Assoc. Prof. Dr. Mantas Malinauskas (Lithuanian University of Health Sciences, Natural Sciences, Biology – N 010).

Dissertation is defended at the Medical Research Council of the Lithuanian University of Health Sciences:

Chairperson

Prof. Habil. Dr. Vaiva Lesauskaitė (Lithuanian University of Health Sciences, Medical and Health Sciences, Medicine – M 001).

Members:

Prof. Dr. Juozas Kupčinskas (Lithuanian University of Health Sciences, Medical and Health Sciences, Medicine – M 001);

Assoc. Prof. Dr. Edita Gasiūnienė (Lithuanian University of Health Sciences, Medical and Health Sciences, Medicine – M 001);

Prof. Dr. Vaidotas Urbonas (Vilnius University, Medical and Health Sciences, Medicine – M 001);

Dr. Tsvetelina Velikova (Sofia University St. Kliment Ohridski (Bulgaria), Medical and Health Sciences, Medicine – M 001).

Dissertation will be defended at the open session of the Medical Research Council of the Lithuanian University of Health Sciences on the 26th of August 2025 at 1 p.m. in the auditorium No. 4004 of the Department of Pediatrics of the Hospital of the Lithuanian University of Health Sciences, Kauno klinikos. Address: Eivenių str. 2, LT-50161, Kaunas, Lithuania.

LIETUVOS SVEIKATOS MOKSLŲ UNIVERSITETAS

Milda Šeškutė

ĮGIMTAS ANTIVIRUSINIS ATSAKAS ŽMOGAUS ŽARNYNO MODELIUOSE: SIGNALO LĄSTELĖSE PERDAVIMAS IR IMUNOMODULIACINIS MELATONINO VAIDMUO

Daktaro disertacija
Medicinos ir sveikatos mokslai,
medicina (M 001)

Kaunas, 2025

Disertacija rengta 2020–2024 metais Lietuvos sveikatos mokslų universiteto Medicinos fakulteto Vaikų ligų klinikoje.

Mokslinė vadovė

prof. dr. Lina Jankauskaitė (Lietuvos sveikatos mokslų universitetas, medicinos ir sveikatos mokslai, medicina – M 001).

Konsultantas

doc. dr. Mantas Malinauskas (Lietuvos sveikatos mokslų universitetas, gamtos mokslai, biologija – N 010).

Disertacija ginama Lietuvos sveikatos mokslų universiteto Medicinos mokslo krypties taryboje:

Pirmininkė

prof. habil. dr. Vaiva Lesauskaitė (Lietuvos sveikatos mokslų universitetas, medicinos ir sveikatos mokslai, medicina – M 001).

Nariai:

prof. dr. Juozas Kupčinskas (Lietuvos sveikatos mokslų universitetas, medicinos ir sveikatos mokslai, medicina – M 001);

doc. dr. Edita Gasiūnienė (Lietuvos sveikatos mokslų universitetas, medicinos ir sveikatos mokslai, medicina – M 001);

prof. dr. Vaidotas Urbonas (Vilniaus universitetas, medicinos ir sveikatos mokslai, medicina – M 001);

dr. Tsvetelina Velikova (Šv. Klimento Ohridskio Sofijos universitetas (Bulgarija), medicinos ir sveikatos mokslai, medicina – M 001).

Disertacija bus ginama viešajame Medicinos mokslo krypties tarybos posėdyje 2025 m. rugpjūčio 26 d. 13 val. Lietuvos sveikatos mokslų universiteto ligoninės Kauno klinikų Vaikų ligų klinikos 4004 auditorijoje.
Disertacijos gynimo vietos adresas: Eivenių g. 2, LT-50161 Kaunas, Lietuva.

CONTENTS

ABBREVIATIONS

3D – three-dimensional
α-SMA – alpha-smooth-muscle actin
µg/mL – micrograms per millilitre
µm – micrometre
µM – micromolar
a.u. – arbitrary units
AC – adenililcyclase
ANOVA – analysis of variance
AP-1 – activator protein-1
APC – allophycocyanin
ATCC – American Type Culture Collection
cAMP – cyclic adenosine monophosphate
CCK-8 – Cell Counting Kit-8
CLD – Compact Letter Display
CO_2 – carbon dioxide
COVID-19 – coronavirus disease 2019
DMEM – Dulbecco's modified Eagle medium
dsRNA – double-stranded RNA
ECMV – encephalomyocarditis virus
ELISA – enzyme-linked immunosorbent assay
EM – extracellular matrix
EpCAM – epithelial cell adhesion molecule
FACS – flow cytometry analysis
FBS – fetal bovine serum
FITC – fluorescein isothiocyanate
GAS – γ-activated sequence
GI – gastrointestinal
h – hour
HIV – human immunodeficiency virus
HLVEC – human large vessel endothelial cell basal medium
HSIF – human small intestine fibroblasts
HSV-1 – herpes simplex virus-1
HUVEC – human umbilical vein endothelial cells
IFN – interferon
IFNα – interferon α

IFNβ – interferon β
IFNλ1 – interferon lambda-1 (interleukin (IL)-29)
IFNλ3 – interferon lambda-3
IFNAR1 – interferon-α/β receptor 1
IFNAR2 – interferon-α/β receptor 2
IFNLR1 – interferon lambda receptor 1
IRF1 – interferon regulatory factor 1
IRF3 – interferon regulatory factor 3
IRF7 – interferon regulatory factor 7
IRF9 – interferon regulatory factor 9
IL-2 – interleukin 2
IL-6 – interleukin 6
IL-8 – interleukin 8
ISG – interferon stimulated gene
ISRE – interferon-stimulated response element
JAK – Janus kinase
JAK/STAT – Janus kinase/signal transducer and activator of transcription
LPS – lipopolysaccharide
LSGS – low serum growth supplement
MAVS – mitochondrial antiviral signalling protein
MDA5 – melanoma differentiation-associated protein 5
MEM – minimal essential medium
MFI – median fluorescence intensity
mM – millimolar
MT1 – melatonin receptor type 1A
MT2 – melatonin receptor type 1B
MUC2 – mucin-2
MX1 – myxovirus-resistance protein 1
NEAA – non-essential amino acids
NFκB – nuclear factor kappa B
ng/mL – nanograms per millilitre
NY – New York
OAS1 – 2′-5′-oligoadenylate synthetase 1
OD – optical density
P – phosphate
PBS – phosphate-buffered saline
PE – phycoerythrin

PECAM-1 – platelet endothelial cell adhesion molecule-1
PEX1 – peroxisomal biogenesis factor 1
pg/mL – picograms per millilitre
PKH26 – red lipophilic cell-membrane dye
Poly I:C – polyinosinic polycytidylic acid
PRRs – pattern recognition receptors
P/S – penicillin/streptomycin
R848 – resiquimod (TLR 7/8 agonist)
RIG-I – retinoic acid-inducible gene I
RLR – RIG-I-like receptor
RNA – ribonucleic acid
ROR – retinoid orphan receptor
ROI – regions of interest
RZR – retinoid Z receptor
SD – standard deviation
STAT1 – signal transducer and activator of transcription 1
STAT2 – signal transducer and activator of transcription 2
STAT3 – signal transducer and activator of transcription 3
TANK – TRAF-family-member-associated NF-κB activator
TBK1 – TANK-binding kinase 1
TLR – Toll-like receptor
TLR3 – Toll-like receptor 3
TLR7/8 – Toll-like receptor 7/8
TNF-α – tumour necrosis factor alpha
TRAF6 – TNF-receptor–associated factor 6
TRIF – TIR-domain-containing adapter-inducing IFNβ
TRITC – tetramethylrhodamine isothiocyanate
TYK2 – tyrosine kinase 2
UK – United Kingdom
USA – United States of America
USP18 – ubiquitin-specific protease 18
ZO-1 – zonula occludens-1

INTRODUCTION

Viral gastrointestinal (GI) infections pose a serious global health burden, causing high morbidity and mortality, particularly in young children and older adults [1]. Yet, current management of these infections remains only supportive (e.g. rehydration, antipyretics) and no broadly effective antiviral is available [1].

The human GI tract is not only responsible for the absorption of nutrients but also plays an important role as a site of entry for various pathogens, including viruses, making it one of the major barriers of host protection [2,3]. The GI epithelium senses viral RNA via pattern-recognition receptors (PRRs) such as Toll-like receptor-3 (TLR3), which activate the innate response through transcription factors IRF3 and IRF1 [3,4]. This cascade induces type I and III interferons (IFNs) and ensures primary antiviral response by engaging the Janus kinase/ signal transducer and activator of transcription (JAK/STAT) pathway, and up-regulating IFN-stimulated genes [2,5]. Central to the process is TANK-binding kinase 1 (TBK1; TANK = Tumour-necrosis-factor-receptor-associated-factor (TRAF)-family-member-associated nuclear-Factor-κB (NF-κB) activator), which phosphorylates IRF3 at organelle-specific platforms on mitochondria and peroxisomes [6]. However, it is still not fully defined, how this signalling unfolds in gut epithelium.

The research of GI diseases was recently revolutionized by organoid models. They provide a unique platform to study tissue interactions without using animals in a more physiologically relevant environment [7,8]. Differentiated epithelial cells can retain their major absorptive and secretory characteristics to resemble small intestine *in vivo* [9]. By mimicking the architecture and function of actual organs, organoids allow for more accurate modelling of human GI tract infections and make it a valuable tool for studying host-pathogen and cellular interactions as well as evaluating various potential therapeutic substances [7,8].

In addition, epithelial immune responses can be significantly influenced by neighbouring stromal cells, such as fibroblasts and endothelial cells. Thus, recently evolved co-culture systems have further advanced the study of GI immunity by offering a more physiologically relevant setting to investigate cellular cross-talk and host-pathogen interactions more accurately [10]. Fibroblasts and endothelial cells can contribute to tissue homeostasis in the gut and can modulate immune signalling, supporting the antiviral responses of epithelial cells [10,11]. These findings highlight the importance of studying these interactions in more complex model systems.

Melatonin is classically known as a hormone produced in the pineal gland and due to its circadian properties is most widely used for treating sleep disorders [12]. However, recently it has emerged as an immunomodulatory and antiviral molecule suggesting broader therapeutic potential [13,14]. Studies show that melatonin can modulate immune responses and enhance host defence mechanisms [15], potentially via modulating metabolism in mitochondria which are increasingly recognized for their role in antiviral signalling. However, despite these promising findings, its impact on enteric viral infection remains poorly characterized.

Therefore, in this study we established experimental GI models to investigate antiviral signalling in GI epithelium, compare antiviral pathways in GI co-culture versus epithelial monoculture models and analyse prophylactic and therapeutic potential of melatonin on these antiviral pathways.

AIM AND OBJECTIVES OF THE STUDY

The aim of the study

The aim of the study was to investigate the antiviral signalling of intestinal epithelial cells in experimental GI model and to evaluate the modulatory effects of melatonin.

Objectives of the study

1. To establish experimental GI models suitable for analysing antiviral immune responses.
2. To characterize the key signalling proteins and organelles that mediate enterocyte response to viral infection, including their expression dynamics and interactions.
3. To compare the expression patterns of antiviral signalling proteins in the established GI models.
4. To assess the effects of melatonin on virus-induced enterocyte damage, antiviral signalling, and epithelial regeneration in the established GI models.

SCIENTIFIC NOVELTY AND RELEVANCE OF THE STUDY

Viral GI infections remain a major global health challenge, causing considerable morbidity and mortality even in the era of improved hygiene and medical care. Enteric viruses (noroviruses, rotaviruses and others) initially breach the gut by the faecal–oral route, directly damage enterocytes, and can trigger systemic complications ranging from severe dehydration to encephalitis or death. Although the causative agents for viral GI infections are well-characterized, the host-pathogen interactions at the intestinal mucosa are still poorly understood, leading to a lack of targeted therapies.

To address this gap, the present study deepens our understanding of GI mucosal immunity by employing advanced *in vitro* models. It highlights that type III IFN (IFNλ) signalling is central to the epithelial antiviral response on GI barrier and explores the other components of its signalling axis that can modulate the balance toward apoptosis or regeneration. Additionally, it investigates the GI epithelial antiviral pathways in a complex co-culture system combining intestinal epithelial cells with stromal cells, such as fibroblasts and endothelial cells. This approach allows for insights into gut antiviral response in a more physiologically relevant environment and helps fill the gap in current understanding of the role of stromal cells in GI mucosal defence. To our knowledge, this is the first study in Lithuania aimed to establish an *in vitro* model to study acute viral enteric infection and the first to evaluate the stromal contribution to the epithelial defence.

Moreover, this study explores the role of melatonin as a potential therapeutic agent in viral GI infections that is little studied so far. It shows that melatonin is capable of modulating antiviral responses in the gut protecting cells from damage and promoting their regeneration. The study explores both prophylactic and treatment approaches that could be used in viral GI infections. Additionally, it also provides insights into possible mechanisms underlying the observed protective effects through type III IFN axis modulation.

In summary, this research applies a novel experimental approach using organoid and co-culture models to investigate GI mucosal responses and identifies melatonin as a promising modulator. Beyond refining the pathogenesis of viral enteritis, these findings may guide future development of antivirals, vaccines, and broader applications in mucosal immunology, including cancer research.

1. LITERATURE REVIEW

1.1. Gastrointestinal infections

Globally, viral GI infections are a serious public health issue that contribute to high rates of morbidity and mortality, particularly in young children and the elderly [1,16]. With more than 400,000 paediatric deaths per year, rotavirus continues to be the most common cause of diarrheal illnesses in children under five, despite advancements in sanitation and effective immunization campaigns [6]. In high-income regions like Europe, deaths due to rotavirus gastroenteritis decreased by 90 %, but the overall disease burden still remains substantial [16,17].

Furthermore, there is currently no vaccine to prevent viral GI infections caused by other important viral pathogens like norovirus, adenovirus, sapovirus, or astrovirus [16,18,19]. After the introduction of rotavirus vaccines, norovirus became the most common cause of gastroenteritis in developed countries, whereas sapovirus and astrovirus mainly cause infections in infants [18,20].

Children are especially prone to viral enteritis, as the causative pathogens are primarily transmitted via the faecal-oral route, and hygiene practices in early childhood are not yet fully established [21]. Upon entry into the GI tract, these viruses commonly cause clinical symptoms such as profuse watery diarrhoea, emesis, abdominal pain, and fever [22–24]. Although the illness is typically self-limiting and resolves spontaneously within 2–5 days, the associated fluid loss can be substantial, placing children at significant risk of dehydration. In severe cases, this may lead to hypovolemic shock, coma, or even death [22,23].

Due to frequent fluid loss, viral GI infections place a significant strain on healthcare systems. These infections are one of the major causes for consultations in primary care [25]. Rotavirus accounts for a large proportion (32 %) of emergency department visits and 41 % of hospitalizations due to viral GI infections among paediatric populations in highly developed countries without routine vaccination [17]. According to a recent systematic review, only 37 % of hospitalizations are currently prevented by the rotavirus vaccine in countries with low overall mortality in children [26], highlighting the need for broader preventive strategies.

At present, management for viral GI infections is mainly supportive, such as oral or intravenous rehydration therapy, diet, probiotics, antiemetics, and antipyretics [20–22,27,28]. There are currently no approved antivirals targeting these pathogens, underscoring an urgent need for improved therapeutic methods. The development of a broad-spectrum (“pan-antiviral”)

agent could potentially improve patient outcomes and reduce the economic burden on healthcare [1].

In conclusion, viral GI infections – particularly those caused by rotavirus, norovirus, adenovirus, sapovirus, and astrovirus – remain a major global health challenge. Although typically self-limiting, they generate substantial numbers of outpatient visits and hospitalizations due to complications ranging from dehydration to death. As no specific antivirals are currently available, further research to develop broad-spectrum therapeutic agents is needed to improve patient outcomes and reduce the associated economic burden.

1.2. Pathophysiology of intestinal injury during viral infection

The intestinal mucosa is a complex, multi-layered barrier, consisting of absorptive enterocytes, mucus-secreting goblet cells, enteroendocrine and Paneth cells, together with fibroblasts, endothelial cells and immune populations, that together maintain gut homeostasis [29]. Among them, the single-layer epithelium forms the primary physical and immunological defensive barrier against enteric RNA viruses [30].

Acute GI injury during viral infection develops through several, often overlapping mechanisms that vary with the pathogen. Firstly, viruses can cause direct cytopathic effect in epithelial cells by triggering apoptosis, lysis, or other forms of programmed cell death [31]. A second pathway involves viral toxins; for example, rotavirus synthesizes the enterotoxin non-structural glycoprotein 4, which increases water and electrolyte secretion into the lumen and produces watery diarrhoea [23]. Third, epithelial-barrier may be disrupted when viral RNA during replication activates TLR3, initiating a downstream signalling cascade that may cause a severe mucosal injury, villus atrophy, and erosion, thereby weakening the epithelial barrier [32]. Finally, collateral immune damage can happen due to excessive TLR3 signalling and activation of cytotoxic T lymphocytes or other effector cells, which may destroy enterocytes and exacerbate mucosal injury [32].

In summary, the intestinal epithelium is the primary physical and immunological barrier against enteric pathogens. Viral injury can arise via several mechanisms, such as direct cytopathic effect, viral toxin production, disruption of epithelial integrity and collateral immune-mediated damage.

1.3. Cellular immune response to viral infection

As GI tract is important for many viruses as a site of entry, it plays an important role by protecting the body from viral invasion. Innate immunity is the first line defence against viral pathogens in the gut [30]. Upon invasion,

viruses are sensed by a variety of pathogen-recognition receptors (PRRs) present on the plasma membrane or endosomal compartments [24,30]. Toll-like receptors (TLR) play a major role in recognizing viral double-stranded RNA (dsRNA) and activate downstream innate signalling.

Engagement of TLR3 by viral RNA recruits the adaptor TRIF (TIR-domain-containing adapter-inducing IFNβ) and activates the serine/threonine kinase TANK-binding kinase 1 (TBK1) in either peroxisomes or mitochondria [6]. Upon activation, TBK1 phosphorylates downstream transcription factors, most notably IFN regulatory factor 3 and 1 (IRF3, IRF1) [2,3]. These factors are then translocated to the nucleus and initiate the transcription of type I (IFNβ, IFNα) and type III (IFNλ) IFN. These bind to their receptors and signal through JAK/STAT pathway, leading to the induction of interferon-stimulated genes (ISGs) [2,5,33] (Fig. 1.3.1).

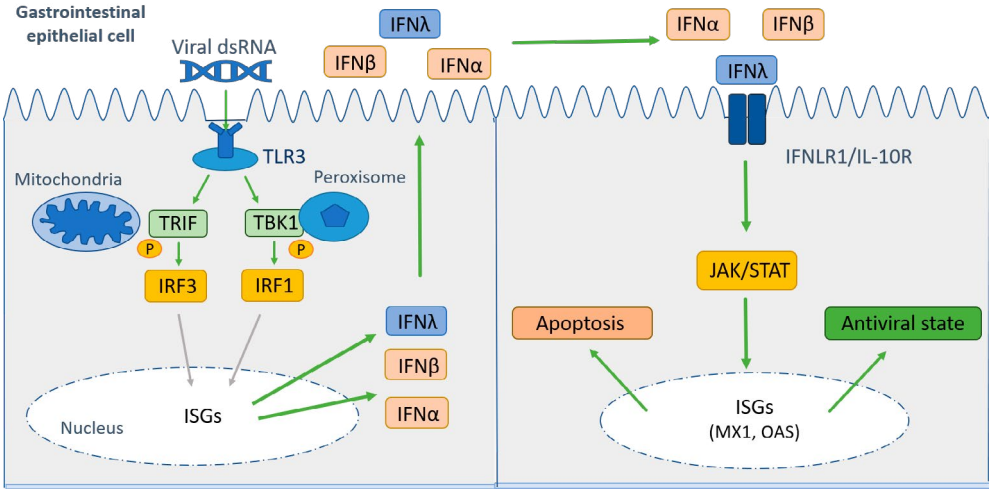

Fig. 1.3.1. *Antiviral response in GI epithelial cell*

Abbreviations: dsRNA – double-stranded RNA; IFN – IFNs; IFNLR1/IL-10R – interferon-λ receptor 1 / interleukin-10 receptor; IRF1 – interferon regulatory factor 1; IRF3 – interferon regulatory factor 3; ISGs – interferon-stimulated genes; JAK/STAT – Janus kinase / signal transducer and activator of transcription pathway; P – inorganic phosphate; TBK1 – TANK-binding kinase 1; TLR3 – Toll-like receptor 3; TRIF – TIR-domain-containing adapter-inducing IFNβ; MX1 – myxovirus-resistance protein 1; OAS – 2′-5′-oligoadenylate synthetase.

Many ISGs can fight viral pathogens by interrupting their life cycle [33]. The classic antiviral ISG-encoded products involve myxovirus-resistance protein 1 (MX1) and 2′-5′-oligoadenylate synthetase (OAS) [34]. OAS proteins, like PRRs may detect foreign viral dsRNA, synthesize 2’,5’-oligomers and

activate latent RNase L, resulting in viral RNA degradation and a boost of innate immune response [33]. MX1 is an effector protein capable of trapping parts of the virus and disrupting its cellular cycle [33].

To sum up, enteric viruses are sensed by membrane-bound and cytoplasmic PRRs, which activate TBK1-IRF signalling and downstream IFN cascades. The described pathway establishes a primary antiviral response resulting in apoptosis of heavily infected cells or, conversely, promotes survival and proliferation of neighbouring epithelium, thereby balancing tissue clearance and regeneration (Fig. 1.3.1). Despite extensive work in immune systems, the dynamics of this signalling cascade in the gut epithelium remain incompletely defined, underscoring the need for gut-specific studies.

1.3.1. Role of interferon in antiviral response

Interferons are a group of cytokines secreted by the host that protect against various pathogens, such as viral, bacterial, fungal and parasitic infections. Human IFNs are classified into three distinct types: type I, II, and III. Type I IFNs were first discovered in the 1950s [35] while type III IFNs were only identified about two decades ago. Although all interferons share structural and functional similarities, each type has unique properties and roles [36,37] (Table 1.3.1.1). Type I IFNs are known to exert more systemic effect by stimulating nearly all nucleated cells in the body, while type III IFNs primarily ensure protection at epithelial surfaces such as the GI and pulmonary tracts, where their specific receptors are expressed [38,39].

Table 1.3.1.1. *Comparison of type I and type III IFN characteristics*

Characteristic	**Type I IFN**	**Type III IFN**
Receptor binding	IFNAR2 (high), IFNAR1 (low)	IFNLR (high) IL-10R (low)
ISG expression kinetics	Rapid, transient	Delayed, prolonged
Antiviral activity	Systemic	Localized to mucosal surfaces
Stimulated cells	Almost all nucleated cells	Epithelial cells mainly
Function in GI tract	Protects from epithelium damage	Increases gut barrier function Protects against epithelium damage
Pro-inflammatory effect	Strong, might induce damage	Mild, protective
Transcription factors	IRF3, AP-1, NF-κB, STATs	IRF3, IRF1, NF-κB, STATs

Abbreviations: GI – gastrointestinal; IFN – interferon; IFNAR1 – interferon-α/β receptor 1; IFNAR2 – interferon-α/β receptor 2; IFNLR – interferon-λ receptor; IL-10R – interleukin-10 receptor; IRF1 – interferon regulatory factor 1; IRF3 – interferon regulatory factor 3; ISG – interferon-stimulated gene; STAT – signal transducer and activator of transcription; AP-1 – Activator Protein-1; NF-κB – nuclear factor kappa B.

Both type I and type III IFNs are key cytokines that help to protect the GI mucosal cells from viral invasion [36,40]. While both induce antiviral defence mechanisms, their kinetics might be different, providing a unique and distinct protection [36]. Type I IFNs typically elicit fast and strong antiviral protection, whereas type III IFNs mediate a more localized and delayed response that might be essential for preserving homeostasis in the gut [5,36,40–43].

When PRRs detect a viral pathogen, IFNs are produced that bind to their specific receptors. Different subtypes of IFNs have different binding properties to the receptors. For example, among type I IFNs, IFNβ1 has the highest binding affinity to interferon-α/β receptor, composed of α-chain (IFNAR1) and β-chain (IFNAR2) subunits; while among type III IFNs, IFNλ3 has the highest affinity for interferon-λ receptor 1 (IFNLR1) [36]. These differences may influence the magnitude and specificity of antiviral response.

Binding to the receptor activates transcription factors and enhances the expression of ISGs that regulate the antiviral response [38]. Despite utilizing distinct receptors, both IFN types end up in a similar JAK/STAT signalling cascade activation to induce ISGs [36] (Fig. 1.3.1.1). Their similar transcriptional regulation involves IFN regulatory factors (IRF3, IRF1), nuclear factor κB (NF-κB), and activator protein-1 (AP-1) [11].

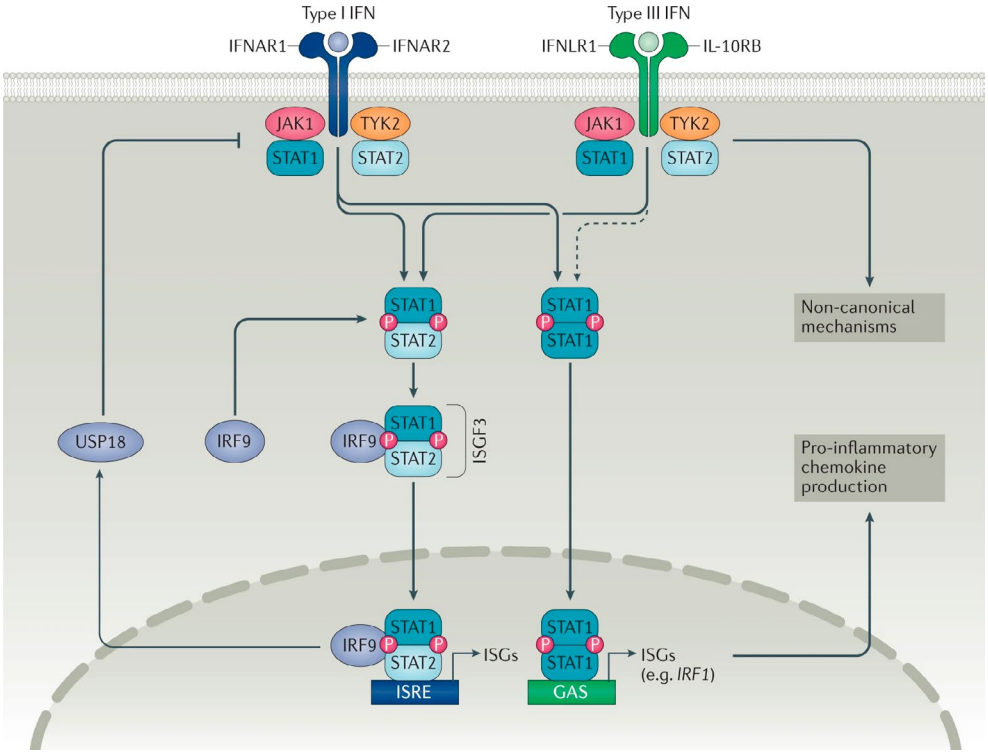

Fig. 1.3.1.1. *Type I and type III IFN signalling pathways*

Adapted from Goel RR et al. Nat Rev Rheumatol. 2021;17(6):349-362 [44].
Abbreviations: IFNAR – interferon-α/β receptor (type I IFN receptor) α-chain; IFNAR2 – interferon-α/β receptor β-chain; IFNLR1 – interferon-λ receptor 1; IL-10RB – interleukin-10 receptor β subunit (shared by IFNλ receptor); JAK – Janus kinase; STAT – signal transducer and activator of transcription; TYK2 – tyrosine kinase 2; P – phosphate (phosphorylated residue); IRF – interferon-regulatory factor; ISRE – interferon-stimulated response element; ISG – interferon-stimulated gene; GAS – γ-activated sequence; USP18 – ubiquitin-specific protease 18.

Type I and type III IFNs are secreted in the extracellular environment where they act in an autocrine and paracrine manner to induce their antiviral activity through the expression of hundreds of ISGs that help to restrict viral invasion in both infected and noninfected cells [37]. Despite the pivotal role of IFNs in pathogen control at the intestinal barrier, their ability to control the virus is incompletely understood [45].

In conclusion, both type I and type III IFNs are essential to the innate antiviral defence of the GI mucosa. Although they signal through similar JAK/STAT pathway, they have different kinetics and tissue range: type I IFNs act rapidly and systemically, whereas type III IFNs elicit a slower, localized response that helps preserve epithelial homeostasis.

1.3.2. Interferon lambda

Type III IFNs, or IFNλ, include several subtypes: IFNλ1, known as IL-29; IFNλ2 (IL-28A); IFNλ3 (IL-28B); and IFNλ4, which is inactive in many individuals [41]. IFNλ1 and IFNλ2/3 have promoters with sites of attachment for IRFs and NFκB transcription factors [41]. When released, IFNλ first binds to its high-affinity specific receptor subunit (IFNLR1), then recruits the low-affinity chain (IL-10R2) [36,41]. This leads to activation of receptor-associated Janus kinases (JAK), which may vary by cell type [36]. Subsequently, JAKs phosphorylate signal transducer and activator of transcription (STAT) proteins, particularly STAT1 and STAT2, which form heterodimers and bind to IRF9 by forming a complex that translocates to the nucleus and activates the transcription of ISGs causing an antiviral state [36,44,45]. All subtypes of IFNλ are capable of inducing the expression of ISGs in order to control viral infections.

The local role of type III IFNs in protecting the gut from viral infections has already been demonstrated by several distinct studies. The IFNLR1 receptor and IFNλ are essential in protecting epithelial cells from GI viruses, including norovirus, rotavirus, enterovirus, or reoviruses in both murine and human cells [11,46,47]. Studies have shown that a lack of IFNLR1 in intestinal epithelial cells makes them highly prone to enteric infections [48]. Type III IFNs were found to provide sufficient protection in the gut against viral infection even in the absence of adaptive immunity, whereas type I IFNs signalling through IFNAR1 is critical to prevent systemic viral dissemination [49].

IFNλ can exhibit both proinflammatory and anti-inflammatory effects [44]. It can promote mucosal healing, enhance the epithelial barrier, and protect the GI from viral infections [44,49]. However, high levels of IFNλ in other tissues might also have detrimental effects. For example, it may disrupt epithelial barrier function in the lungs inducing the risk of tissue damage [44]. Additionally, IFNλ may also lead to Paneth cell death in patients with Crohn's disease or block the restoration of the respiratory epithelium [50]. High levels of type III IFNs have also been associated with increased risk of secondary bacterial infections in the murine respiratory system [51]. However, studies suggest that this effect could be tissue-specific with predominantly protective roles observed in the GI tract.

In summary, type III IFNs signal locally through IFNLR1/IL-10R receptor complex, activate the JAK/STAT pathway, and induce ISGs to establish an antiviral state. In the gut, IFNλ is essential for controlling enteric viruses, strengthening the epithelial barrier, and promoting mucosal healing. However, in other organs, excess IFNλ can disrupt the epithelial integrity, suggesting tissue-specific outcomes. Currently, the mechanisms of these divergent

effects remain unclear, underscoring the need for further research to better understand the role of type III IFNs in intestinal homeostasis.

1.3.3. Organelle-specific antiviral response

There are different ways through which intestinal epithelial cells can exert antiviral responses. Recently, cytosolic organelles were found to be capable of inducing ISG expression upon RIG-I-like receptor (RLR) stimulation.

Upon invasion, viruses can be sensed not only by TLR receptors found on the plasma membrane, but also by cytosolic receptors, such as retinoic acid-inducible gene I (RIG-I) or melanoma differentiation-associated protein 5 (MDA-5), which can activate another antiviral signalling pathway [52]. RIG-I and MDA-5 attract the binding of mitochondrial antiviral signalling protein (MAVS), which downstreams antiviral response through activation of NFκB and IRFs which are then translocated to the nucleus to promote the expression of IFNs and ISGs [52,53].

Mitochondria are known to play an important role in antiviral defence. They are directly responsible for the regulation of cell death by regulating apoptosis [54] and can also regulate TLR signalling through TLR adaptor protein TRAF6 (TNF-receptor-associated factor 6) but the mechanism how mitochondria sense TLR signalling is not clear [54]. Mitochondria also regulate other pathogen-sensing receptors, such as RLR (RIG-I) and MDA5. RIG-I mediates MAVS aggregation on mitochondria which results in activation of TBK1 that phosphorylates IRF3 and subsequent antiviral response [6,54].

In addition, the importance of mitochondria is confirmed by findings that viruses target various chains of mitochondrial metabolism and modulate cell death, but it is still unknown why different viruses cause different effects on mitochondrial function [54].

To conclude, enteric viruses can be sensed not only by membrane-bound TLRs but also by cytosolic RLRs, which activate organelle-specific signalling. Mitochondria serve as key antiviral hubs because MAVS aggregation on their surface may integrate TLR and RLR signalling cues and modulate apoptosis. Despite this central role, the precise mitochondrial mechanisms that shape antiviral outcomes remain incompletely defined.

1.3.3.1. Peroxisome-driven response

Peroxisomes, known to perform key roles in lipid metabolism and oxidation processes, have recently emerged as a key platform regulating the response to viral infections [53,55]. It was found that MAVS is localized not only in mitochondria but also in peroxisomes and might even lead to a different response [52] (Fig. 1.3.3.1.1).

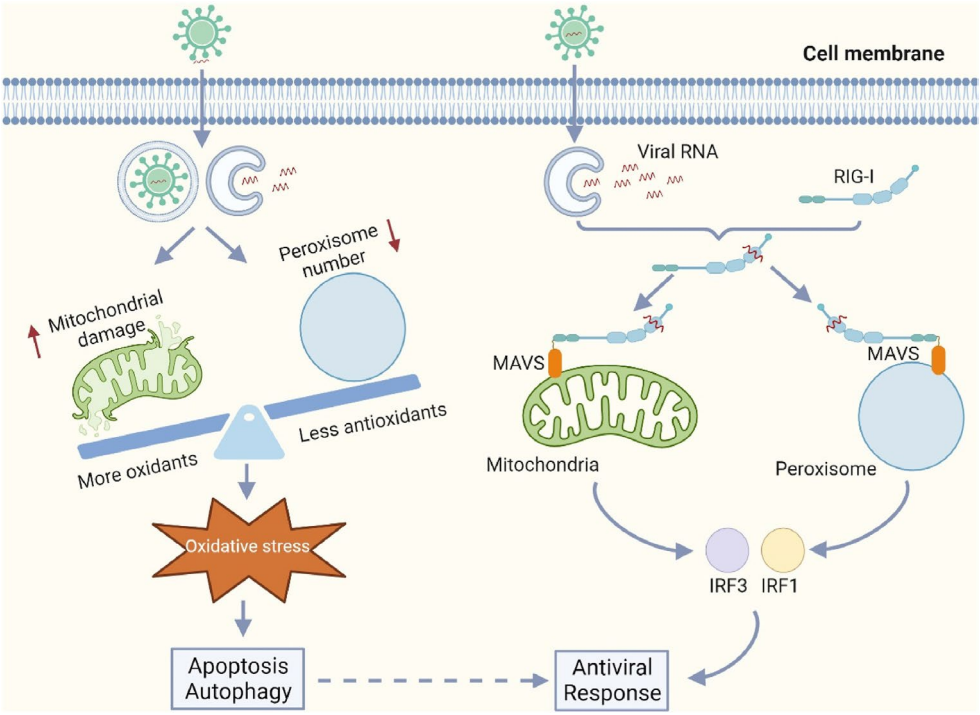

Fig. 1.3.3.1.1. *Organelle-driven antiviral response regulation*

Adapted from Jiang et al., Antiviral Research, 2024, 221:105780 [55].
Abbreviations: RNA – ribonucleic acid; RIG-I – retinoic acid-inducible gene I; MAVS – mitochondrial antiviral-signalling protein; IRF1 – interferon regulatory factor 1; IRF3 – interferon regulatory factor 3.

After viral invasion, peroxisomal MAVS triggers the immediate but temporary upregulation of ISGs in contrast to mitochondrial MAVS, which induces a stable but delayed response. Dixit et al. showed that MAVS-induced viral replication restriction was strongest over the first 24 hours and diminished later [52]. This shows the importance of organelle-specific response as a first-line defence in controlling viral infections.

Peroxisomal response might be explained by morphological changes of the organelles, such as elongation, or close interactions with other compartments, such as endoplasmic reticulum, mitochondria, lysosomes or lipid droplets through exchange of specific metabolites, phospholipids, and signalling molecules [52,53,56]. Even though the mechanism is not entirely clear, peroxisomes are known to elicit less inflammatory response preventing possible collateral damage in the mucosa [52] (Table 1.3.3.1.1).

Table 1.3.3.1.1. *Comparison of mitochondrial and peroxisomal antiviral response*

Aspect	Mitochondria	Peroxisomes
ISG kinetics	Delayed and sustained	Rapid and transient
Inflammation	High	Low
Outcomes	Apoptosis	Cytoprotective
MAVS expression	High	Lower

Abbreviations: ISG – interferon-stimulated genes; MAVS – mitochondrial antiviral signalling protein.

The importance of peroxisomes in antiviral immunity was also confirmed by studies, showing that multiple viruses have developed mechanisms to block peroxisome-driven response. For example, herpes simplex virus 1 (HSV-1) was shown to interfere with downstream peroxisomal signalling, possibly through inhibition of IRF1 and IRF3 [57]. Other studies suggest that viruses, such as enterovirus 71, Zika virus, human immunodeficiency (HIV), dengue virus, etc., might impair peroxisome-driven response by reducing the number of these organelles but the mechanisms are not entirely clear [53,55]. Moreover, even though rotavirus was the first virus shown to involve peroxisomes in modulating its invasion into the host [58], studies regarding GI viruses and peroxisomes are largely lacking [55].

In conclusion, there is compelling data that peroxisomes play an important role in host-virus interactions and modulation of peroxisomal response might have a potential in novel antiviral therapies [53]. However, these mechanisms have only been evaluated in a few studies, and further investigation in this field is needed to fully understand the effect of peroxisomes on immunity regulation.

1.4. Organoid models for the analysis of GI infections

The pathogenesis of viral GI infections, especially immune regulation at mucosal surfaces, is still poorly understood, even though many of the pathogens causing these infections have long been known [45]. This partly results from the limitations of existing experimental models.

As with other diseases, animal models have traditionally been the preferred platform for studying GI diseases. However, while valuable, they pose ethical concerns and often lack translational accuracy due to differences between animal and human tissues, which might lead to misleading conclusions [59]. In addition, some important GI pathogens, like norovirus, cannot be studied in these models as they infect humans only [60,61]. This led to a search for alternative experimental models (Fig. 1.4.1).

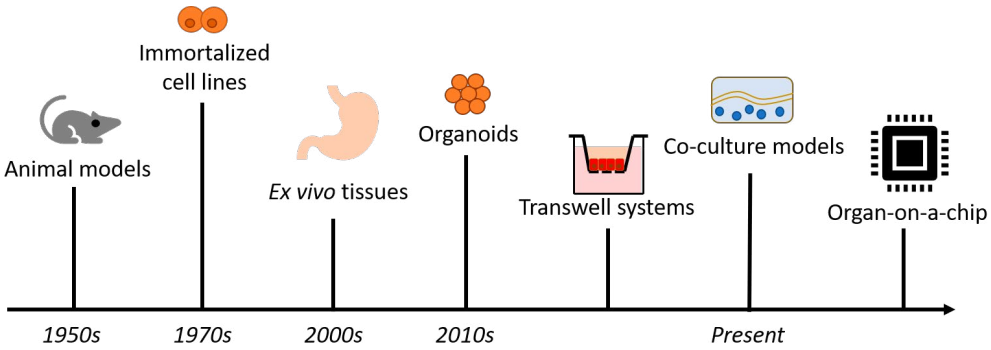

Fig. 1.4.1. *The timeline of evolution of experimental platforms used to analyse GI diseases*

The field was first advanced by immortalized cell lines, most notably the Caco-2 cell line, which has been a gold-standard for *in vitro* GI tract models for over 30 years due to its ability to differentiate and polarize to resemble enterocytes of the small intestine [10,62]. These differentiated epithelial cells were shown to retain their major absorptive and secretory characteristics found *in vivo* [63,64]. However, cell lines can yield inconsistent results due to genetic drift over prolonged culturing, lack a crypt-like structure, and do not reflect the complexity of cellular interactions present in *in vivo* tissues [65].

Later *ex vivo* tissue-based models emerged, involving short-term cultures of intestinal tissue explants mostly obtained from surgical rejections. These models have the advantage of preserving the natural tissue architecture of the intestinal mucosa, including epithelial, immune cells, fibroblasts and endothelial cells. It provides a highly physiological platform for studying host-pathogen interactions, immune responses etc. However, their application is limited by short and restricted availability, as well as donor variability [66], prompting the development of other platforms.

A further breakthrough came with epithelial cultures derived from intestinal crypts surgically resected from intestinal tissue [45]. Primary cultures grown from those isolated crypts or stem cells gave rise to such models as enteroids (from small intestine cells) and colonoids (from large intestine cells) [45]. Enteroids grown in certain conditions in media enriched with growth factors can differentiate into various intestinal epithelial cell subtypes and even form villus-like structures, closely mimicking the architecture of the intestine.

More recently, the study of the GI diseases has been revolutionized by organoid models. Intestinal organoids were first discovered in 2009 [67] and are among the most well-studied. These 3D structures feature a hollow lumen lined with a single layer of intestinal epithelial cells which, under proper conditions, form budding-like structures resembling crypts [61]. Organoids

are capable of self-organizing, proliferating, and differentiating for prolonged periods, allowing for more accurate modelling of human GI tract infections. This enables a detailed analysis of host-pathogen interactions, signalling pathways, and drug responses – all without the use of animals [61,68]. They have enabled the study of GI viruses that were previously considered non-cultivatable, offering novel mechanistic insights into infection [8,60,69]. However, this model also has drawbacks. Infections in these models might be challenging to study due to limited access to the luminal surface of epithelium where many enteric viruses initiate the infection. In addition, cells grown in isolation lack signalling from other cells present in *in vivo* tissues, such as fibroblasts or endothelial cells, which provide mechanical support and immunological protection [61,70,71].

In vivo intestinal epithelial cells lie on a basement membrane supported by extracellular matrix (EM) consisting of fibroblasts, endothelial cells, collagens, glycoproteins, and proteoglycans [10,72] (Fig. 1.4.2). This layer influences the growth and function of enterocytes and is essential for the mucosal integrity [10,72,73]. For example, Zhang et al. [73] showed that adding embryonic fibroblast cells to the Caco-2 cell model created a more physiologically relevant environment with improved permeability characteristics compared to Caco-2 monoculture. Intestinal myofibroblasts are also crucial for supplying growth factors and facilitating signalling between epithelium and stromal cells [61], while endothelial cells contribute to mucosal immunity and intercellular communication [11].

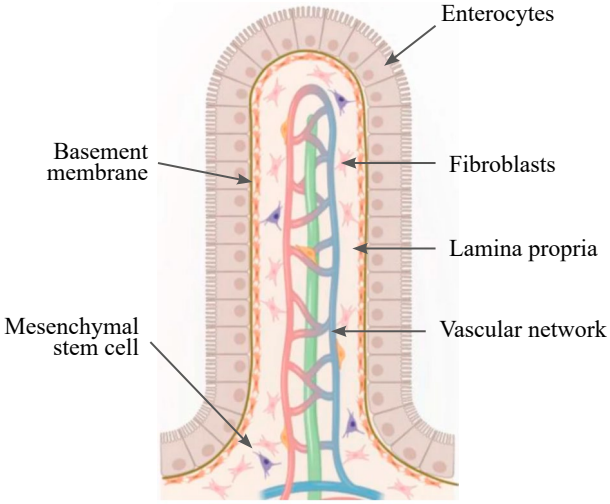

Fig. 1.4.2. *Composition of human small intestinal barrier*

Adapted from Assal et al., Tissue Eng Regen Med, 2024: 21(3):369–377 [59].

More recently, transwell culture systems have gained popularity as a simpler alternative to 3D models. In these platforms, cells are cultured on semi-permeable membranes to mimic the intestinal barrier, allowing apical-basolateral communication [59]. Transwells can be easily enhanced to co-cultures by adding other cells, such as stromal or circulatory immune cells, increasing the physiological relevance [59]. Human colon adenocarcinoma-derived Caco-2 cells remain among the most widely used cells in this context.

Experimental modelling of GI diseases has progressed from animal studies and Caco-2 monocultures to human-derived explants, 3D organoids, and transwell co-cultures. While most of these advanced systems are used in drug discovery or cancer research, their application in infectious disease modelling, especially viral GI infections, is still emerging. Studies utilizing co-culture systems for such infections remain limited [65]. Yet, more advancements in the field are anticipated in the upcoming years through the use of more sophisticated technologies, such as commercially available organ-on-a-chip models [1,65,74] and the incorporation of immune cell populations [61,70,75], which will be crucial for analysing the interactions between the immune system and the gut in response to pathogen invasion.

1.5. Melatonin and its antiviral effect

Melatonin, a hormone primarily synthesized by the pineal gland and well-recognized for its role in regulating the circadian sleep-wake cycle [76], has also demonstrated a broad range of physiological effects beyond chronobiology. Notably, its potent antioxidant properties have attracted increasing scientific interest, positioning melatonin as a promising candidate for therapeutic applications in both non-infectious and infectious disease contexts [77–82].

The first indication that melatonin might influence host defence dates back to 1926, when kittens treated with pineal gland extracts displayed increased resistance to infections [83]. This was followed by observations that pinealectomy caused an impairment in immune response with reversed outcomes following melatonin supplementation after the surgical procedure [83]. Endogenous melatonin concentrations were also found to be associated with the proliferation rate of immune cells [83].

These findings prompted evaluation of the immunomodulatory capacity of exogenously administered melatonin. In animal models, melatonin treatment was found to stimulate both innate and adaptive immune responses, especially under immunosuppression [83].

The observed immune benefits provided rationale to investigate melatonin's efficacy against viral infections. The first antiviral evidence

emerged in 1988, when melatonin treatment protected rodents challenged with encephalomyocarditis virus (ECMV) [84]. Since then, melatonin has demonstrated broad-spectrum antiviral activity, inhibiting the replication of severe acute respiratory syndrome coronavirus 2, Zika, Japanese encephalitis, HSV-1, and several other pathogens [13,81,85–87].

As a result, evidence on the immunomodulatory properties of melatonin leads to its clinical applications. Melatonin has been extensively studied as an adjunctive therapy in cases of sepsis, including neonates, and its protective effect is well-documented [88–90]. Interest in melatonin increased substantially during the COVID-19 pandemic when it was used as an adjunctive therapy for severe COVID-19 patients and was associated with improved outcomes. Melatonin not only exerts diverse physiological functions but also possesses an excellent safety profile, even at high doses [91].

The antiviral effect of melatonin is primarily attributed to its ability to reduce apoptosis and enhance autophagy by mitigating oxidative stress [87,89]. In addition, melatonin exhibits anti-inflammatory and immunomodulatory effects that enhance humoral and/or cellular immune responses [81,83,92]. Melatonin plays an important role in the proliferation and maturation of various immune cells, such as T and B cells, and decreases the production of pro-inflammatory mediators (interleukin (IL)-2, IL-6, IL-8, IFNα, tumour necrosis factor (TNF)-α, NFκB, etc.) [82,92,93] (Fig. 1.5.1) but the knowledge about melatonin's antiviral mechanisms, especially in the GI tract, is still scarce.

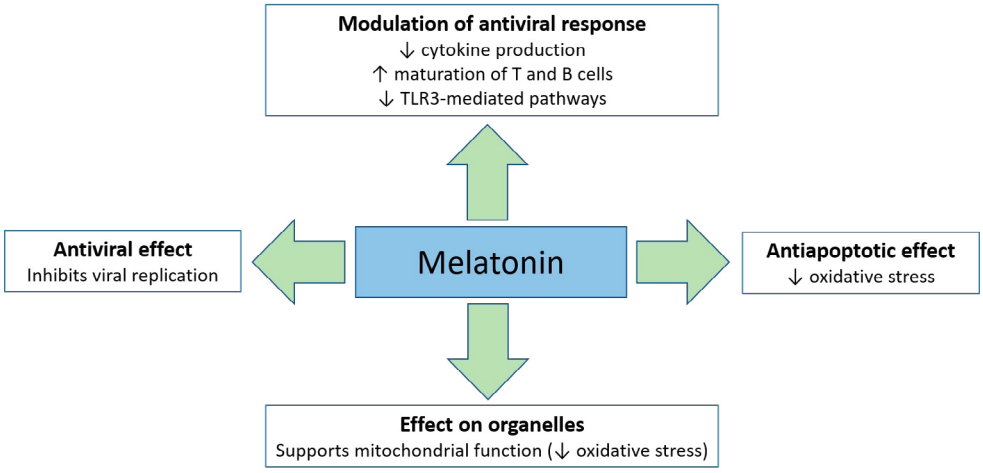

***Fig. 1.5.1**. Summary of antiviral properties of melatonin*

Abbreviations: TLR3 – Toll-like receptor 3.

Melatonin exerts its biological effects primarily through interaction with two specific membrane-bound G protein-coupled receptors in humans: melatonin receptor type 1A (MT1) and melatonin receptor type 1B (MT2) [88,89,94,95]. The receptors are widely expressed in various tissues. MT1 receptors are predominantly expressed in the brain, cardiovascular system, immune system, endocrine organs, and abdominal viscera [94], whereas MT2 receptors are expressed mainly in the immune system, brain and GI tract [94].

In addition, melatonin has been proposed to bind several nuclear receptors, including the retinoid Z receptors RZRα and RZRβ, and the retinoid orphan receptors RORα, RORα2, and RORγ. The expression of these nuclear receptors is subtype-specific and widespread across various tissues [94].

Upon activation, melatonin receptors couple with G protein subunits, leading to the inhibition of adenililcyclase and subsequent reduction in cyclic adenosine monophosphate (cAMP) levels or modulation of intracellular calcium levels which in turn activates calmodulin-dependent pathways [89,94,96]. Both of these signalling cascades ultimately enhance transcriptional activity within the cell (Fig. 1.5.2).

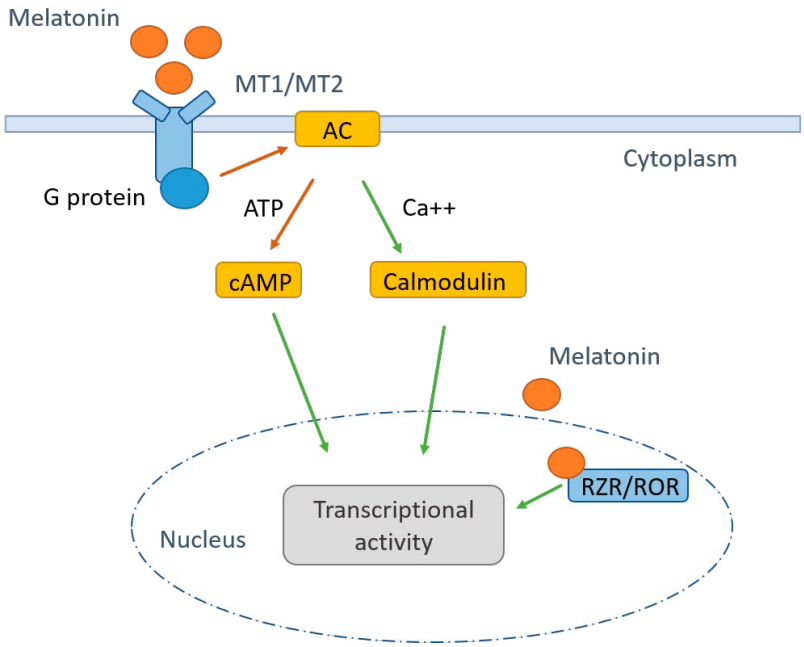

Fig. 1.5.2. *Intracellular signalling regulation by melatonin*

Abbreviations: AC – adenililcyclase; ATP – adenosine triphosphate; Ca^{2+} – calcium ion; cAMP – cyclic adenosine monophosphate; MT1 – melatonin receptor type 1; MT2 – melatonin receptor type 2; RZR/ROR – retinoid-related orphan receptor.

As a hormone, melatonin has an exceptional feature to be produced by a number of extrapineal organs [83,96]. Recent animal studies have shown that melatonin in the gut is produced independently from the pineal gland which shows its importance in this organ system [97,98]. GI melatonin regulates electrolyte and ion transport, GI motility, and epithelial regeneration and has gastroprotective properties [97,99]. As demonstrated in studies involving lymphocytes, the local production of melatonin can be regulated by paracrine and autocrine factors and is not dependent on the circadian rhythm [88,100].

Melatonin concentration in extrapineal tissues is known to be higher than plasma levels, which range from <10 pg/mL during daytime and to around 25–150 pg/mL at night, depending on age [96,101]. Studies suggest that melatonin concentrations in GI tract may surpass those in the plasma by 10 to 100-fold, while levels within the pineal gland are around 400 times higher than in circulation [102]. Lack of circadian fluctuations for extrapineal melatonin production suggests the importance of local production for the cytoprotection from oxidative stress throughout the day [96,102].

To summarize, melatonin is a potent antioxidant and immunomodulator that can enhance antiviral immune responses and protect cells from oxidative stress, apoptosis, and viral replication across a broad spectrum of pathogens. These properties and excellent safety profile make melatonin an attractive agent for viral GI infections, although its mechanisms of action at the GI mucosa still need deeper investigations.

2. MATERIALS AND METHODS

Most of the experiments in this study were performed at the Institute of Pharmacology and Physiology of the Lithuanian University of Health Sciences. No ethical approval was needed for the study as commercially available cell lines were used for the development of GI model.

2.1. Cell maintenance

To develop GI model 3 commercially available cell lines were used:

- Intestinal epithelial cells (**Caco-2**, HTB-37, ATCC, UK),
- Human small intestine fibroblasts (**HSIF**, P10760, Innovative Technologies and Biological Systems, S.L., Spain), and
- Human umbilical vein endothelial cells (**HUVEC**, C0035C, Thermo Fisher Scientific, USA).

All cells were cultured in 150 cm^2 tissue culture flasks (TPP, Techno Plastic Products AG, Switzerland) at 37 °C in a humidified incubator with 5 % CO_2. Each cell type was maintained in its respective growth media (Table 2.1.1) which was replaced every 2–3 days. Cells were passaged at 70–80 % confluency using TrypLE™ Express Enzyme (Gibco, Life Technologies Corporation, Grand Island, NY, USA). Prior to passaging, viable cell numbers were determined using 0.4 % Trypan Blue exclusion and a haemocytometer (Gibco, Life Technologies Corporation, Grand Island, NY, USA). All experiments were conducted using cells between passages 7 and 25.

Table 2.1.1. *Composition of Culture Media for Different Cell Types Used in the Models*

Cells	Medium Composition
Caco-2	MEM+ 10 % FBS (Gibco, Life Technologies NZ Ltd., Auckland, New Zealand) + 1 % NEAA (Gibco, Life Technologies Limited, Paisley, UK) + 1% P/S (Gibco, Life Technologies Limited, Paisley, UK)
HSIF	DMEM (Gibco, Life Technologies Limited, Paisley, UK) + 10 % FBS + 1 % P/S
HUVEC	HLVEC Basal Medium (Gibco, Life Technologies Corp., Grand Island, NY, USA) + 10 % FBS + 1 % P/S + LSGS (Gibco; Cascade Biologics; Life Technologies Corp., Grand Island, NY, USA)

Abbreviations: DMEM – Dulbecco's Modified Eagle Medium; FBS – Fetal Bovine Serum; HLVEC – Human Large Vessel Endothelial Cell Basal Medium; LSGS – Low Serum Growth Supplement; MEM – Minimum Essential Medium; NEAA – Non-essential Amino Acids; P/S – Penicillin/Streptomycin.

2.2. Development of GI model

A series of complementary approaches were employed to develop GI model suitable for investigating viral infection, ranging from Caco-2 monoculture to a complex multicellular co-culture (Fig. 2.2.1). The detailed methodology for each model is provided in the following sections.

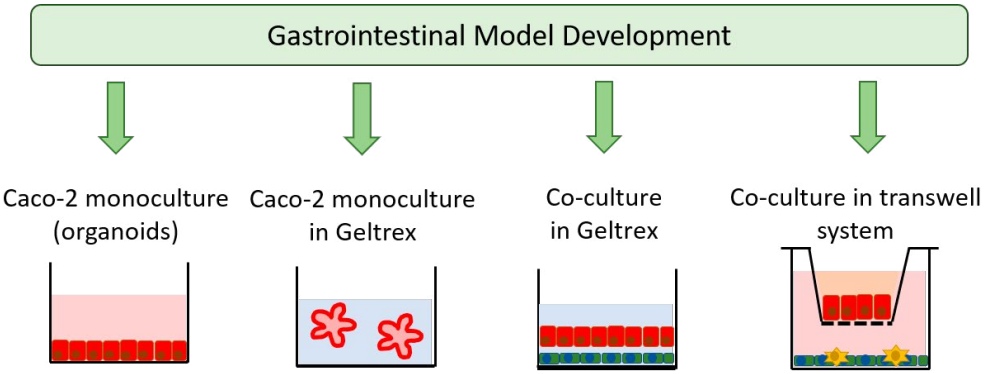

Fig. 2.2.1. *Workflow for developing the GI in vitro models*

2.2.1. Caco-2 monoculture on plastic

Caco-2 cells were used to establish an *in vitro* monoculture GI organoid model, as they have been considered a gold standard in GI research for over 30 years. Caco-2 is an immortalized epithelial cell line derived from a human colorectal adenocarcinoma. When cultured under specific conditions, these cells can differentiate and polarize to resemble enterocytes of the small intestine [62].

Initially, a monoculture model was established by seeding Caco-2 cells at a density of 1×10^4 cells/well into 96-well tissue culture plates and culturing for 21 days to allow for differentiation and polarization to form organoids. The cells were washed with phosphate-buffered saline (PBS, Gibco, Life Technologies Limited, Paisley, UK), and culture medium was replaced every 2-3 days.

2.2.2. Caco-2 monoculture in Geltrex

To simulate more physiologically relevant conditions for cell differentiation and organoid formation, Caco-2 cells were further cultured in media containing various concentrations (2 %, 25 %, 60 %, and 100 %) of Geltrex™ (Gibco, Life Technologies Limited, Paisley, UK). Geltrex is a basement membrane matrix derived from murine Engelbreth-Holm-Swarm tumours which contains

additional EM components such as laminin, collagen, and proteoglycans. They support 3D cellular organization, promote differentiation, and help to maintain phenotypic stability.

Caco-2 cells were harvested using TrypLE™ Express Enzyme, counted with a haemocytometer using 0.4 % Trypan Blue solution, and seeded at slightly higher density (2×10^4 cells/well) into 96-well plates with corresponding Geltrex-medium mixtures. Cells were cultured for 21 days, with medium changes every 2–3 days.

2.2.3. Co-culture GI model

To develop a co-culture model, Caco-2 cells were first cultured with human small intestine fibroblasts (HSIF). Several configurations were evaluated, including:

1. Mixing Caco-2 and HSIF at various ratios on plastic (Fig. 2.2.3.1 A),
2. Culturing Caco-2 cells above HSIF embedded in Geltrex (Fig. 2.2.3.1 B),
3. Culturing Caco-2 in transwells above HSIF in the lower compartment (Fig. 2.2.3.1 C).

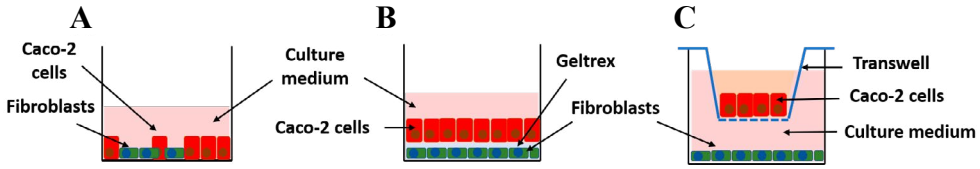

Fig. 2.2.3.1. *Schematic layout of different seeding schemes for Caco-2 and human small intestinal fibroblasts (HSIF) co-culture: (A) Caco-2 and on plastic; (B) Caco-2 cells above HSIF in Geltrex; (C) Caco-2 in transwells above HSIF*

To further enhance the physiological relevance, human umbilical vein endothelial cells (HUVEC) were added to create a triple co-culture model. Several different configurations were tested:

1. All three cell lines were seeded in layers in Geltrex;
2. Caco-2 in transwells above HSIF and HUVEC in the lower compartment.

In the first co-culture method, following cell harvesting and counting, HSIF, HUVEC, and Caco-2 cells (seeded on top) were sequentially layered in 96-well plates. Each cell layer was embedded in either 20 % or 50 % Geltrex, combined with the appropriate culture media mix, at a total density of 1×10^4 cells per layer. After seeding each layer, plates were incubated at 37 °C in a

humidified incubator at 5 % CO_2 for 45 minutes before the next layer was added. Cultures were maintained in a 1:1 mixture of Caco-2 and HSIF culture media throughout the experimental period.

The second, optimized method – used in subsequent experiments – involved seeding all cells into 24-well tissue culture plates (TPP, Techno Plastic Products AG, Switzerland). HSIF and HUVEC cells were first mixed at a 3:1 ratio and seeded at a total density of 3 × 10^4 cells per well a 1:1 mixture of their respective media. Caco-2 cells (1 × 10^4 cells per well in MEM) were then seeded onto 0.4 µm pore-size cell culture inserts (Brand GMBH, Wertheim, Germany), which were placed above the fibroblast-endothelial layer (Fig. 2.2.3.2 A). The co-cultures were maintained at 37 °C in a humidified incubator at 5 % CO_2, with media changes every 2–3 days over a 14-day period.

Prior to seeding, HUVEC cells were labelled with PKH26 fluorescent membrane dye to facilitate identification via fluorescence microscopy (see 2.7 Immunofluorescence section). The presence of HSIF in co-cultures was verified by immunostaining with anti-α-smooth muscle actin (α-SMA) antibody after fixation, following 14 days of co-culture incubation. In parallel, Caco-2 monoculture and dual co-cultures (Caco-2 with either HSIF or HUVEC) were established for the comparative analysis (Fig. 2.2.3.2 B–D).

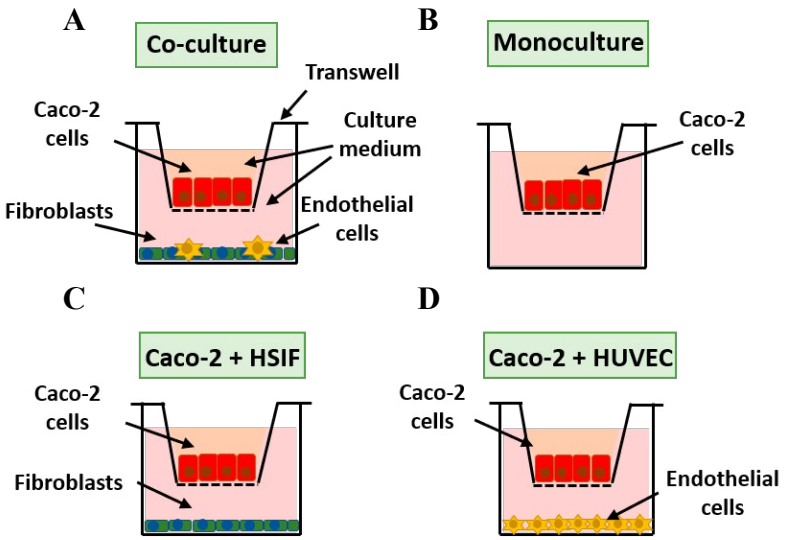

Fig. 2.2.3.2. *Schematic of the seeding layout of the triple co-culture (A) and comparative models (B–D)*

Abbreviations: HSIF – human small intestinal fibroblasts; HUVEC – human umbilical vein endothelial cells.

2.3. Viral-mimic stimulation

2.3.1. Stimulation with Poly I:C

To model virus-induced epithelial damage, Caco-2 cells were stimulated with polyinosinic polycytidylic acid (Poly I:C; Tocris Bioscience™, UK), a synthetic double-stranded viral RNA structural analog and Toll-like receptor 3 (TLR3) agonist. Poly I:C was selected as a surrogate for infection with live virus due to laboratory biosafety constraints.

In monocultures, Caco-2 cells grown in 96-well plates for 21 days, were stimulated with Poly I:C for 24 hours at concentrations of 1, 10 or 50 µg/mL. These concentrations were chosen based on findings in the literature, while optimal timing was determined during the preliminary experiments. Unstimulated cells were used as mock controls.

In co-culture models, only 10 or 100 µg/mL concentrations of Poly I:C were used. Poly I:C was added directly to Caco-2 cells cultured in transwells for 14 days. The cells in the lower compartment (HSIF and/or HUVEC) were not directly stimulated with the TLR3 agonist (Fig. 2.3.1.1).

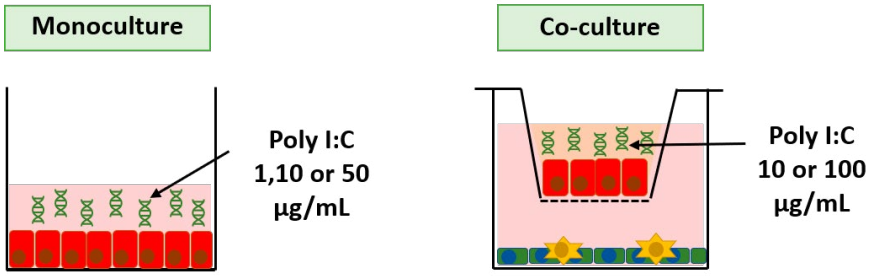

Fig. 2.3.1.1. *Poly I:C stimulation scheme in monoculture and co-culture transwell models*

Abbreviations: Poly I:C – polyinosinic polycytidylic acid.

2.3.2. Stimulation with R848

In the preliminary experiments, 21-day-old Caco-2 monocultures were stimulated with the TLR7/8 agonist resiquimod (R848) to evaluate dose-dependent cellular responses. R848 was applied at concentrations of 50, 100, 500, and 1000 ng/mL. To investigate potential synergistic or additive effects on antiviral signalling pathways, additional experimental conditions including co-stimulation with varying combinations of R848 and the Poly I:C. These treatments were designed to mimic viral single- and double-stranded RNA exposure, thereby enabling a comprehensive evaluation of epithelial innate immune responses under different stimulatory conditions.

2.4. Melatonin treatment

Due to emerging evidence suggesting that melatonin has antiviral properties, it was investigated as a potential antiviral substance to mitigate the cellular damage caused by Poly I:C. Melatonin was prepared according to the manufacturer's instructions (Sigma-Aldrich, USA) and subsequently diluted in MEM with supplements as previously described.

In monoculture experiments, Caco-2 cells were either pretreated with melatonin at concentrations of 1, 10, 50 or 100 µM 24 hours prior to Poly I:C stimulation, or treated with the same concentrations for 24 hours following Poly I:C stimulation by applying it directly to the wells (Fig. 2.4.1).

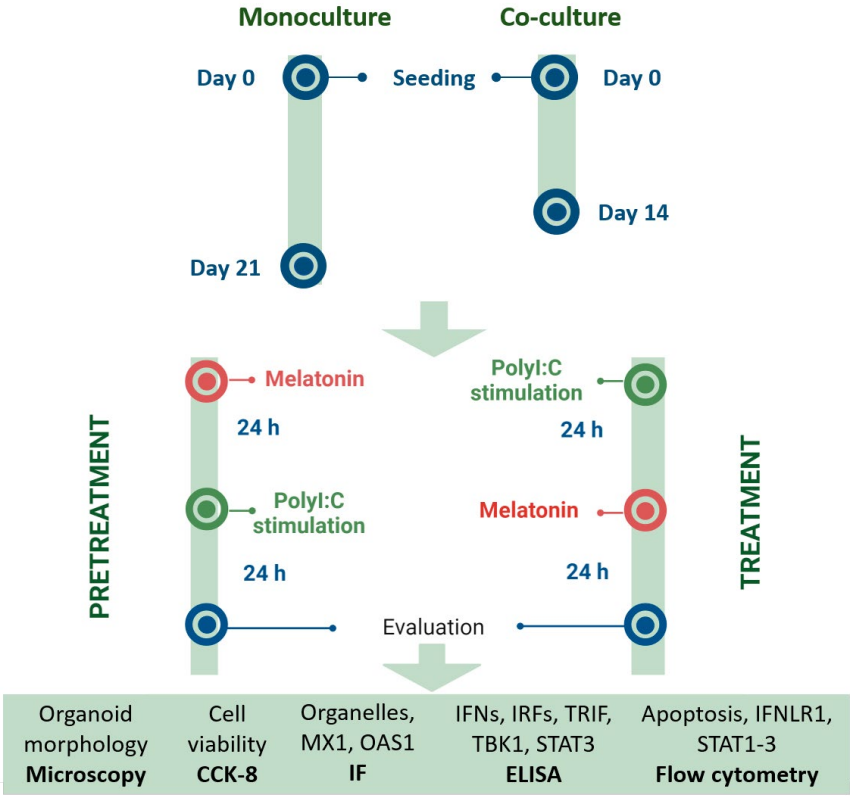

Fig. 2.4.1. *Experimental layout of the study*

Abbreviations: CCK-8 – Cell Counting Kit-8; ELISA – enzyme-linked immunosorbent assay; IF – immunofluorescence; IFNLR1 – interferon-λ receptor 1; IFNs – interferons; IRFs – interferon regulatory factors; MX1 MX1 – myxovirus-resistance protein 1; OAS – 2′-5′-oligoadenylate synthetase. Poly I:C – polyinosinic-polycytidylic acid; STAT1–3 – signal transducer and activator of transcription 1–3; TBK1 – TANK-binding kinase 1; TRIF – TIR-domain-containing adapter-inducing IFNβ.

In co-culture models, cells were similarly either pretreated before or treated after Poly I:C stimulation, but only with 50 μM melatonin, as monoculture experiments showed that this concentration exerted antiviral and barrier-protective effects without signs of cytotoxicity. Melatonin was applied directly on Caco-2 cells cultured in transwells. The cells in the lower compartment (HSIF and HUVEC) were not directly treated with melatonin.

2.5. Microscopy and organoid morphology evaluation

The cell growth in the monoculture and co-cultures was monitored by brightfield microscopy using an inverted microscope (Olympus IX2-SP, Olympus Corporation, Tokyo, Japan) equipped with a digital camera (Olympus DP26, Olympus Corporation, Tokyo, Japan). Imaging was performed on Day 7, 14, 21 in monocultures and on Day 3, 7, 14 in co-cultures. To evaluate organoid growth and morphology in monoculture, live Caco-2 organoids were imaged at 24 hours after Poly I:C stimulation or 24 hours after melatonin application (treatment) in 96-well plates, capturing three non-overlapping random fields per well (technical triplicates) and evaluating three different wells of the same condition (biological triplicates).

All images were acquired using cellSens software (version 1.16, Olympus, Olympus Corporation, Japan). Brightfield images for organoid evaluation were taken at consistent magnification (4×) to allow accurate comparisons. The number and size of Caco-2 organoids were measured using ImageJ software (version 1.53k, National Institutes of Health, Bethesda, MD, USA). The number of organoids was counted manually using ImageJ. For each condition, the mean organoid size was calculated. Image acquisition and analysis parameters were kept identical across samples. The analysis was performed in triplicates using three independent wells per condition.

2.6. Cell viability assays

Cell viability was assessed using Cell Counting Kit-8 (WST-8/ CCK8; Abcam, Cambridge, UK) at 24 and 48 hours after Poly I:C stimulation or melatonin treatment. As instructed by the manufacturer, following medium replacement, 10 μL of the CCK-8 solution was added to each well and incubated for 2 hours. Absorbance was measured at 450 nm wavelength using a Multiscan Go microplate reader (Thermo Fisher Scientific, Waltham, MA, USA) at the Laboratory of Biochemistry of the Lithuanian University of Health Sciences. Control conditions were set as 100 % viability.

2.7. Immunofluorescence

2.7.1. Staining and imaging procedure

Pre-staining, Caco-2 cells were washed with PBS and subsequently fixed with 4 % paraformaldehyde (PFA) for 15 minutes at room temperature. After rinsing with PBS, cells were permeabilized with 0.2 % Triton™ X-100 (Sigma-Aldrich, St. Louis, MO, USA) for 1 hour at room temperature to facilitate antibody access to intracellular markers (ZO-1, vimentin, MUC2). Cells were then blocked with 10 % FBS in PBS for 1 hour at room temperature. After aspirating the blocking solution, cells were incubated overnight at 4 °C with the primary human monoclonal antibodies targeting specific markers (Table 2.7.1.1).

Table 2.7.1.1. *Markers used for immunofluorescent staining*

Marker and manufacturer	Fluorochrome	Dilution
Caco-2 staining		
EpCAM (CD326; Invitrogen, Carlsbad, CA, USA)	FITC	1:1000
ZO-1 (Invitrogen, Rockford, IL, USA)	FITC	1:1000
Vimentin (Invitrogen, Rockford, IL, USA)	APC	1:1000
MUC2 (Santa Cruz Biotechnology, Dallas, Texas, USA)	Alexa Fluor 488	1:100
HSIF and HUVEC staining		
α-SMA (Abcam, Cambridge, UK)	Alexa Fluor 647	1:100
PKH26 (Sigma-Aldrich, St. Louis, USA)	PE/TRITC	1:500
Peroxisomes and mitochondria staining		
PEX1 (Bethyl, Fortis Life Sciences, Boston, MA, USA)	Alexa Fluor 488	1:100
MitoTracker™ (Invitrogen, Eugene, OR, USA)	Deep Red (Cy-5)	200 nM
ISG-encoded protein staining		
MX1 (Invitrogen, Rockford, IL, USA)	Alexa Fluor 488	1:100
OAS1 (Invitrogen, Rockford, IL, USA)	Alexa Fluor 488	1:100

Abbreviations: APC – allophycocyanin; EpCAM – epithelial cell adhesion molecule; ZO-1 – zonula occludens-1; MUC2 – mucin-2; α-SMA – alpha-smooth-muscle actin; PEX1 – peroxisomal biogenesis factor 1; PKH26 – red lipophilic cell-membrane dye; FITC – fluorescein isothiocyanate; PE – phycoerythrin; TRITC – tetramethylrhodamine isothiocyanate; MX1 – myxovirus-resistance protein 1; OAS1 – 2′-5′-oligoadenylate synthetase 1.

For HSIF staining, cells were fixed with 4 % PFA for 15 minutes at room temperature, washed with PBS, permeabilized with 0.2% Triton X-100 for 30 minutes, and blocked with 10 % FBS for 1 hour. Cells were then incubated overnight at 4 °C with conjugated mouse α-SMA antibody.

HUVECs were pre-labelled with PKH26 membrane dye before seeding, according to the manufacturer's protocol, and visualized directly without further staining.

For peroxisomal labelling and detection of ISG-encoded proteins MX1 and OAS1, fixed and permeabilized cells were incubated overnight at 4 °C with the appropriate primary antibodies (Table 2.7.1.1). They were then exposed to fluorophore-conjugated secondary antibodies for 3 hours at room temperature for peroxisomal staining, or overnight at 4 °C for MX1 and OAS1 staining.

For mitochondrial imaging, live cells were incubated with MitoTracker™ for 30 minutes at 37 °C following experimental treatments and immediately imaged without fixation.

After incubation, fixed cultures were washed with PBS and counterstained with DAPI (Sigma-Aldrich, St. Louis, MO, USA) for 10 minutes at room temperature to visualize nuclei.

All fluorescence staining procedures were performed under light-protected conditions. Fluorescent images were acquired using an inverted microscope equipped with a digital camera and an X-cite 120Q fluorescence illuminator (Lumen Dynamics, Ontario, Canada). Images were captured using cellSens software and processed using ImageJ software.

2.7.2. Image analysis

To quantify organelle and ISG-encoded protein (MX1 and OAS1) labelling, images were first separated into their individual channels and converted to grayscale. Non-specific fluorescence was removed by background subtraction, and image quality was enhanced using despeckle filtering and threshold adjustment to delineate organelle structures. Mean fluorescence intensity was quantified in predefined regions of interest (ROIs) and expressed in arbitrary units (a.u.). All imaging and analysis were performed in triplicates using identical acquisition parameters across samples.

2.8. Flow cytometry

Flow cytometry was used to assess cell apoptosis and to quantify the expression of the intracellular and surface proteins, involved in the antiviral signalling pathways. Multicolour flow cytometry analysis (FACS) was performed using a BD FACSMelody™ cell sorter and BD FACSChorus™ software (version 3.0, Becton, Dickinson and Company, Franklin Lakes, New Jersey, USA) at the Clinical and Molecular Gastroenterology Laboratory of the Institute for Digestive Research at the Lithuanian University of Health Sciences.

Following experimental treatments, cells (1–5 × 10^5) were washed with PBS, detached using TrypLE™ Express Enzyme, and centrifuged at 1400 rpm for 5 minutes at 4 °C. The resulting pellets were resuspended in PBS supplemented with 10 % FBS to block unspecific binding sites. Staining procedures were conducted according to the manufacturer's instructions using immunofluorescent antibodies (Fig. 2.8.1, Table 2.8.1).

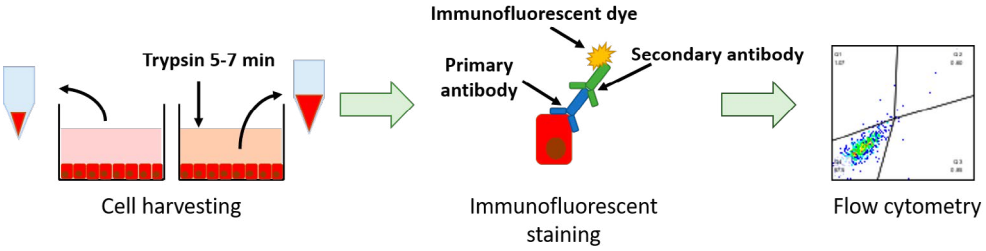

Fig. 2.8.1. *Schematic layout of immunofluorescent staining procedure*

Table 2.8.1. *Immunofluorescent markers used for flow cytometry*

Marker and manufacturer	Location	Fluorochrome	Isotype	Dilution
IFNLR1 (Invitrogen, Rockford, IL, USA)	Extracellular	Alexa Fluor™ 488	-	0.25 µg/10^6 cells
PECAM-1 (CD31; Invitrogen, Life Technologies Corp., Carlsbad, CA, USA)	Extracellular	eFluor™ 450	-	5 µL/test
Phospho-STAT1 (Tyr701; eBioscience™, Life Technologies Corporation, Carlsbad, CA, USA)	Intracellular	eFluor™ 660	Rabbit IgG	5 µL/test
Phospho-STAT2 (Tyr689; Invitrogen, Rockford, Illinois, USA)	Intracellular	FITC	Mouse IgG1κ	10 µl/10^6 cells
Phospho-STAT3 (Tyr705; eBioscience™, Life Technologies Corporation, Carlsbad, CA, USA)	Intracellular	eFluor™ 450	Mouse IgG2bκ	5 µL/test

Abbreviations: IFNLR1 – interferon lambda receptor 1; STAT – signal transducer and activator of transcription; FITC – fluorescein isothiocyanate; PE – phycoerythrin; PECAM-1 – platelet endothelial cell adhesion molecule-1.

For IFNLR1 staining, the cells were additionally fixed with 4 % PFA after trypsinization, then incubated with a primary monoclonal IFNLR1 antibody, followed by a secondary antibody for at least 60 and 30 minutes, respectively,

at 4 °C. In co-culture settings, endothelial cells were pre-labelled with PECAM-1 for 30 minutes before the staining steps.

For intracellular marker detection, the cells were permeabilized with a 0.2 % Triton™ X-100 solution for 10–15 minutes, followed by incubation with fluorophore-labelled antibodies (Table 2.8.1) for at least 30 minutes at 4 °C.

Apoptotic cells were identified using the Annexin V-FITC/propidium iodide (PI) apoptosis detection kit (Invitrogen, Life Technologies Corporation, Eugene, OR, USA). Briefly, after the treatments, all supernatants were collected, and all cells ($1–5 \times 10^5$) were harvested using TrypLE™ Express Enzyme, washed in ice-cold PBS, and centrifuged at 1400 rpm for 5 minutes at 4 °C. The cells were then resuspended in 100 µL annexin-binding buffer and stained with Annexin V and PI for at least 15 minutes on ice in the dark. An additional 100 µL of annexin-binding buffer was added to the cell suspension prior to immediate analysis.

Flow cytometric acquisition was performed immediately following staining. Data were analysed using FlowJo v10.10 software (Becton, Dickinson and Company, Franklin Lakes, New Jersey, USA). Median fluorescence intensity (MFI) values were used to quantify protein expression levels. The percentage of cells positive for each marker was determined based on thresholds set using matched isotype controls or unstained cells. All experiments were conducted in triplicate using standardized acquisition settings.

2.9. ELISA assays

The antiviral response was evaluated by quantifying interferons (IFNλ1, IFNβ, and IFNα) in cell culture supernatants, and key signalling molecules involved in the antiviral pathways, including IFN regulatory factors (IRF1 and IRF3), signal transducer and activator of transcription 3 (STAT3), as well as the adaptor protein Toll-like receptor adaptor molecule 1 (TRIF) and the kinase TANK-binding kinase 1 (TBK1), in cell lysates using commercially available human enzyme-linked immunosorbent assay (ELISA) kits. The detection limits of measured analytes are presented in Table 2.9.1.

Table 2.9.1. *Analytes measured by ELISA and their detection limits*

Analyte and manufacturer	Sample type	Detection limit
IFNλ1 (Abcam, Cambridge, UK)	Supernatant	13.72 ng/mL
IFNβ (Abcam, Cambridge, UK)	Supernatant	9.38 pg/mL
IFNα (Invitrogen, Bender MedSystems GmbH, Vienna, Austria)	Supernatant	7.8 pg/mL
IRF1 (ELK Biotechnology; Denver, USA)	Cell lysate	0.32 ng/mL
IRF3 (ELK Biotechnology; Denver, USA)	Cell lysate	0.16 ng/mL
TRIF (ELK Biotechnology; Denver, USA)	Cell lysate	78.13 pg/mL
TBK1 (ELK Biotechnology, Denver, USA)	Cell lysate	0.32 ng/mL
phospho-STAT3 (Tyr705; Invitrogen, Thermo Fisher Scientific, Life Technologies Corp., Carlsbad, CA, USA)	Cell lysate	Semi-quantitative

Abbreviations: IFNα – interferon-α; IFNβ – interferon-β; IFNλ1 – interferon-λ1; IRF1 – interferon regulatory factor 1; IRF3 – interferon regulatory factor 3; phospho-STAT3 (Tyr705) – phosphorylated signal transducer and activator of transcription 3 (tyrosine 705); TBK1 – TANK-binding kinase 1; TRIF – TIR-domain-containing adapter-inducing IFNβ.

After desired treatments (Poly I:C stimulation or melatonin treatment), cell supernatants and cell lysates were collected. Cell supernatants were immediately stored at −80 °C until the day of analysis. Cell lysates were prepared using Cell Lysis buffer II (Invitrogen, Thermo Fisher Scientific; Bender MedSystems GmbH, Vienna, Austria) following trypsinization with TrypLE™ Express Enzyme and immediately stored until analysis at −80 °C.

According to the manufacturer's instructions, the analysed cytokines were incubated with specific monoclonal antibodies and subsequently with horseradish peroxidase. Optical density (OD) values were measured using a Multiscan Go microplate reader at the Laboratory of Biochemistry of the Lithuanian University of Health Sciences and concentrations were calculated from standard curves. All assays were performed in triplicate for statistical robustness.

2.10. Statistical analysis

Statistical analysis was performed using IBM SPSS Statistics (version 29.0.2.0, IBM Corp., Armonk, NY, USA) and GraphPad Prism software (version 10.4.2, GraphPad Software, Boston, MA, USA). The data are presented as mean and standard deviation (SD) of at least three independent experiments.

Pairwise comparisons between two independent conditions were evaluated with an unpaired Student's t-test. For comparisons involving more than two treatment conditions within a single culture model, one-way analysis of variance (ANOVA) was applied, followed by Bonferroni adjustment for

post-hoc multiple testing. To assess the main and interactive effects of culture model and treatment regimen on each dependent variable, a two-way ANOVA was conducted, followed by Bonferroni-corrected post-hoc comparisons. Correlations between variables were assessed using the Pearson's correlation coefficient. The statistical significance was defined as p-value < 0.05. Levels of significance were indicated as follows: * $p < 0.05$, ** $p < 0.01$, and *** $p < 0.001$.

Graphs were generated using GraphPad Prism 10.0 software. Statistical significance in protein expression over time between mock- and Poly I:C-stimulated groups was assessed using the Compact Letter Display (CLD) method, where different letters indicate significant differences: lowercase letters denote $p < 0.05$, and uppercase letters denote $p < 0.01$. Illustrations were created using Microsoft PowerPoint (Office Standard 2019, version 1808).

OpenAI (ChatGPT) was used to assist in editing the text in terms of wording and formatting, and to improve clarity. All AI-generated content was critically reviewed and verified to ensure accuracy, scientific integrity, and alignment with current evidence and ethical standards.

2.11. Funding

The study was funded by the Research Council of Lithuania (IPTAVI project, No. S-MIP-23-110) as well as the Science Fund of the Lithuanian University of Health Sciences.

3. RESULTS

3.1. Development of viral GI model

Three different GI models were established during the study, two of which were selected for further experimentation. Each model is described in detail below.

3.1.1. Caco-2 monoculture on plastic

Firstly, Caco-2 cells were cultured as a monolayer for 21 days, during which they differentiated and formed polarized epithelial structures – intestinal organoids. The development of organoids was verified using microscopy (Fig. 3.1.1.1 A-D). As shown in Fig. 3.1.1.2, organoid formation was confirmed by the presence of specific markers, such as ZO-1, EpCAM, and vimentin.

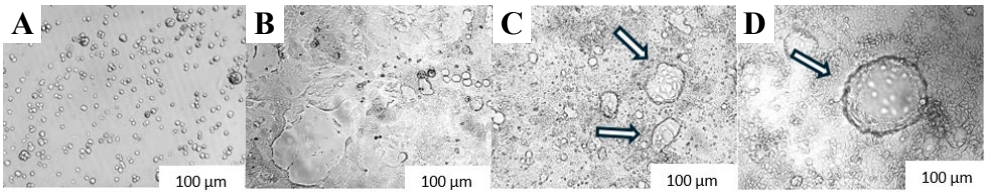

Fig. 3.1.1.1. *Microscopy of Caco-2 cell culture on (A) Day 0, (B) Day 7, (C) Day 14, (D) Day 21, showing the formation of GI organoids (marked by arrows)*

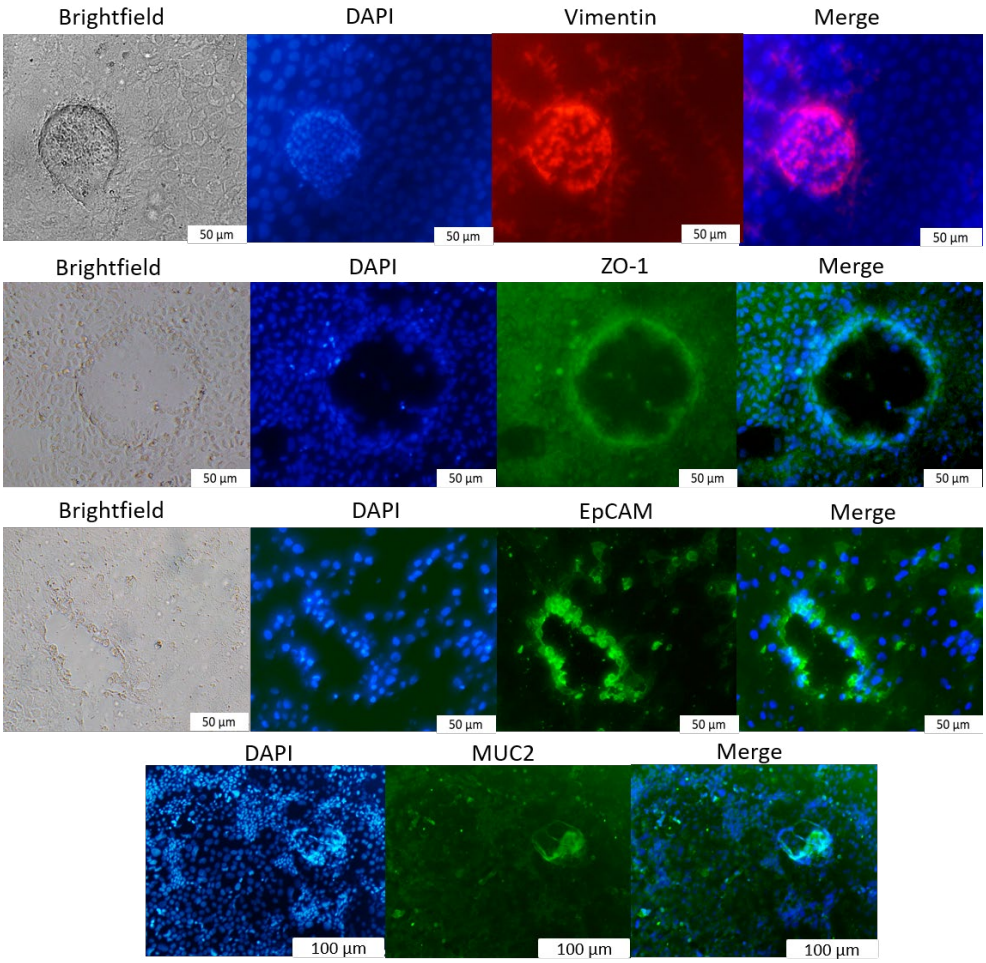

Fig. 3.1.1.2. *Microscopy images of organoids formed in Caco-2 monoculture and the presence of specific markers (vimentin, ZO-1, EpCAM and MUC2)*

Abbreviations: DAPI – 4′,6-diamidino-2-phenylindole; EpCAM – epithelial cell adhesion molecule; ZO-1 – zonula occludens-1 (tight-junction protein); MUC2 – mucin-2.

After 21 days, we exposed the cells to varying concentrations of Poly I:C for different durations to determine optimal viral-mimic conditions (Fig. 3.1.1.3). It was found that 24 hours of stimulation was the most optimal, while 1, 10, and 50 µg/mL concentrations were chosen for further experiments.

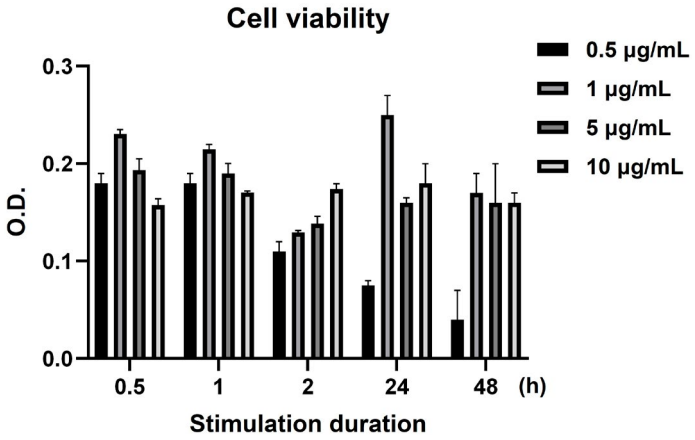

Fig. 3.1.1.3. *Cell viability at various timepoints after application of various concentrations of Poly I:C (n = 3)*

Abbreviations: O.D. – optical density.

3.1.2. Caco-2 monoculture in Geltrex

Culturing the cells in a 3D Geltrex matrix instead of on plastic significantly improved Caco-2 organoid formation and morphology (Fig. 3.1.2.1 A). Caco-2 organoids developed budding-like structures more readily than those grown on plastic, especially at lower Geltrex concentrations (Fig. 3.1.2.1 A-C).

However, the 3D Geltrex model proved unsuitable for further antiviral experiments. CCK-8 viability measurements were unreliable as the dye was retained in the matrix, and Poly I:C could not be fully removed after stimulation, raising the risk of unintended, prolonged TLR3 stimulation. Alternative approaches reported by other groups (e.g., mechanical organoid extraction or lumen microinjections [60,61,103]) were impractical with our resources. We therefore opted to discontinue the use of Geltrex and transitioned to a transwell-based co-culture system, as described in the following sections. This alternative setup allowed for more controlled stimulation conditions and reproducible results.

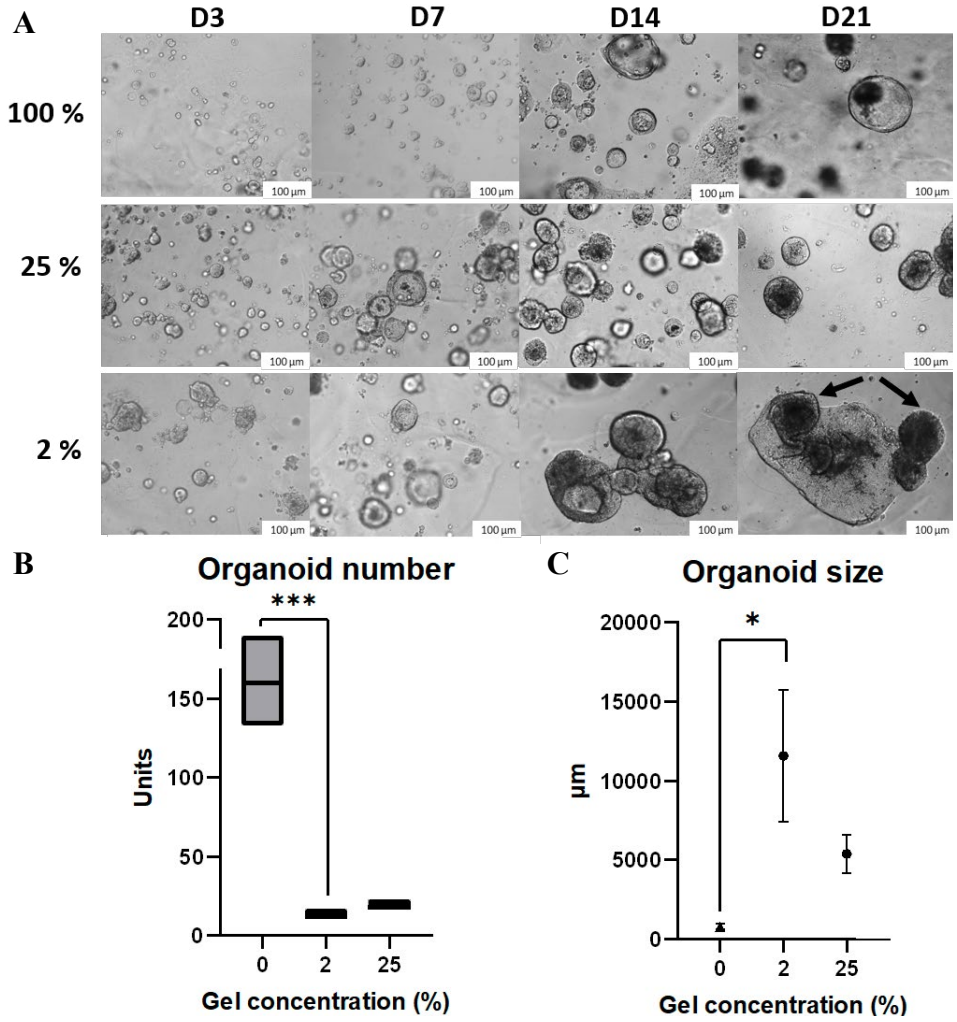

Fig. 3.1.2.1. *(A) Representative images of brightfield microscopy of Caco-2 monoculture at Day 3, Day 7, Day 14 and Day 21 showing the formation of intestinal organoids in different Geltrex concentrations (black arrows show budding-like structures). Comparison of organoid number (B) and size (C) at 24 hours after Poly I:C stimulation in different Geltrex concentrations after 21 days of culturing (n = 3)*

* indicates $p < 0.05$, and *** $p < 0.001$.

3.1.3. Development of co-culture model

3.1.3.1. Caco-2 and HSIF co-culture

Although epithelial-cell monoculture is a well-established platform for investigating GI immune mechanisms, the inclusion of stromal cell populations enhances physiological fidelity by more closely recapitulating *in vivo* conditions. That is why we proceeded to develop a co-culture model.

We first tried to improve our model by adding intestinal fibroblasts (HSIF) only. We tried mixing them with Caco-2 at various ratios and culturing on plastic, culturing Caco-2 cells above HSIF embedded in Geltrex (Fig. 3.1.3.1.1 and 3.1.3.1.2) and culturing Caco-2 in transwells above HSIF in the lower compartment. HSIF enhanced the growth of Caco-2 cells but did not result in better organoid formation (Fig. 3.1.3.1.1). However, prolonged culturing requiring organoid formation (21 days) in the transwell model led to overgrowth and structural disruption of the organoids. We therefore chose to keep the transwell configuration but shortened the differentiation period to 14 days. This arrangement, which preserves paracrine communication between cell types, offered the best balance for subsequent experiments due to increased but more stable growth, better reflection of physiological GI layers as well as readily accessible epithelial layer.

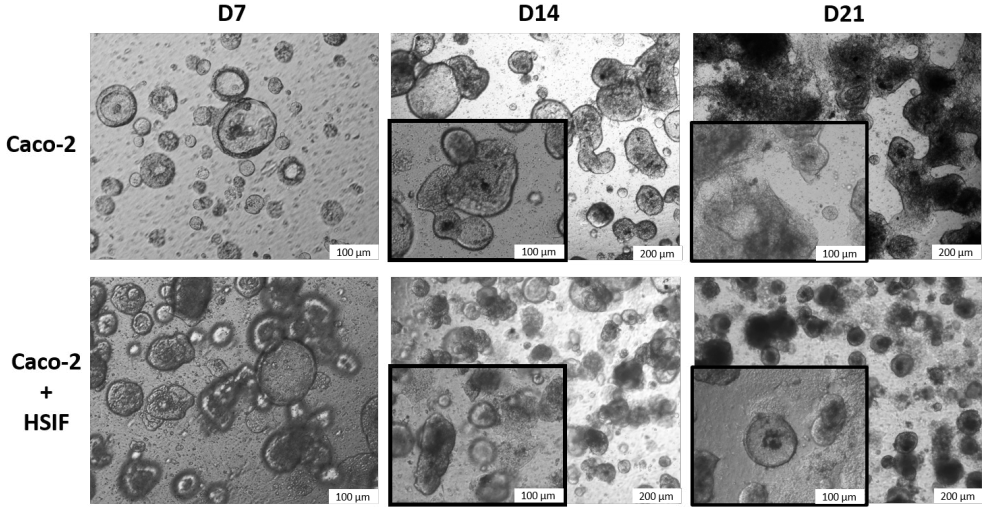

Fig. 3.1.3.1.1. *Brightfield images showing the development of Caco-2 organoids in Caco-2 monoculture above Geltrex and Caco-2 co-culture above HSIF seeded in Geltrex at Day 7, Day 14 and Day 21*

Abbreviations: HSIF – human small intestinal fibroblasts.

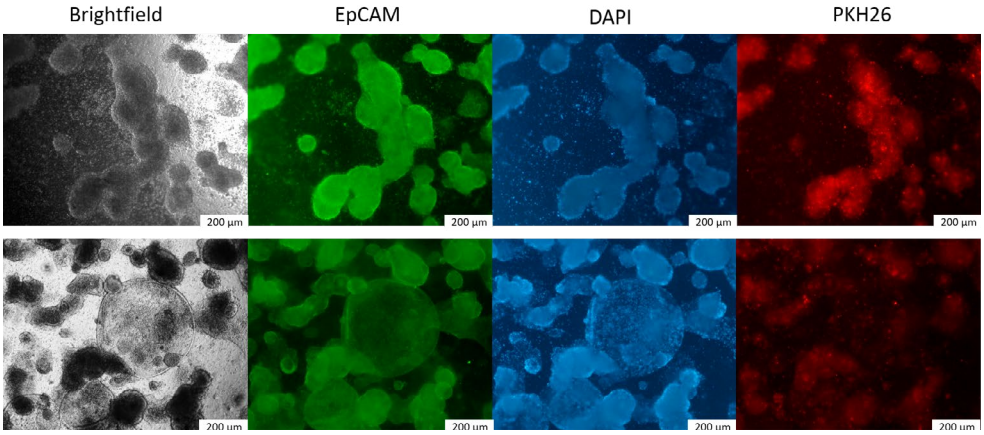

Fig. 3.1.3.1.2. *Representative immunofluorescence images of Caco-2 organoids 21 days after culturing above HSIF seeded in Geltrex*

Abbreviations: EpCAM – epithelial cell adhesion molecule; DAPI – 4′,6-diamidino-2-phenylindole; PKH26 – red fluorescent cell-membrane linker dye.

3.1.3.2. Caco-2, HSIF and HUVEC co-culture

The model was further enhanced by introducing endothelial (HUVEC) cells. Caco-2 cells were initially cultured above HSIF and HUVEC layers embedded in Geltrex. However, this setup did not result in improved organoid formation (Fig. 3.1.3.2.1).

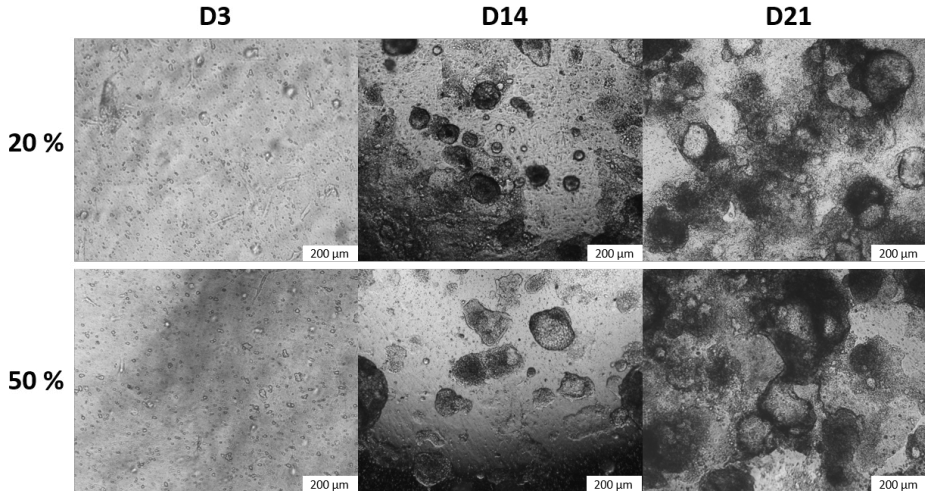

Fig. 3.1.3.2.1. *Brightfield images of Caco-2 culture above HSIF and HUVEC layers embedded in Geltrex (20 % and 50 %) at Day 3, Day 7, and Day 21*

Thus, we switched to transwell systems and grew HSIF and HUVEC cells in the lower compartment. This slightly enhanced cell growth rate in the co-culture models compared to monoculture as seen by microscopy images (Fig. 3.1.3.2.2). This observation was corroborated by a 32 % increase in viability in Caco-2 cells co-cultured with HSIF and HUVEC compared to monoculture (1.68 ± 0.2 vs. 1.13 ± 0.03, respectively; $p = 0.031$).

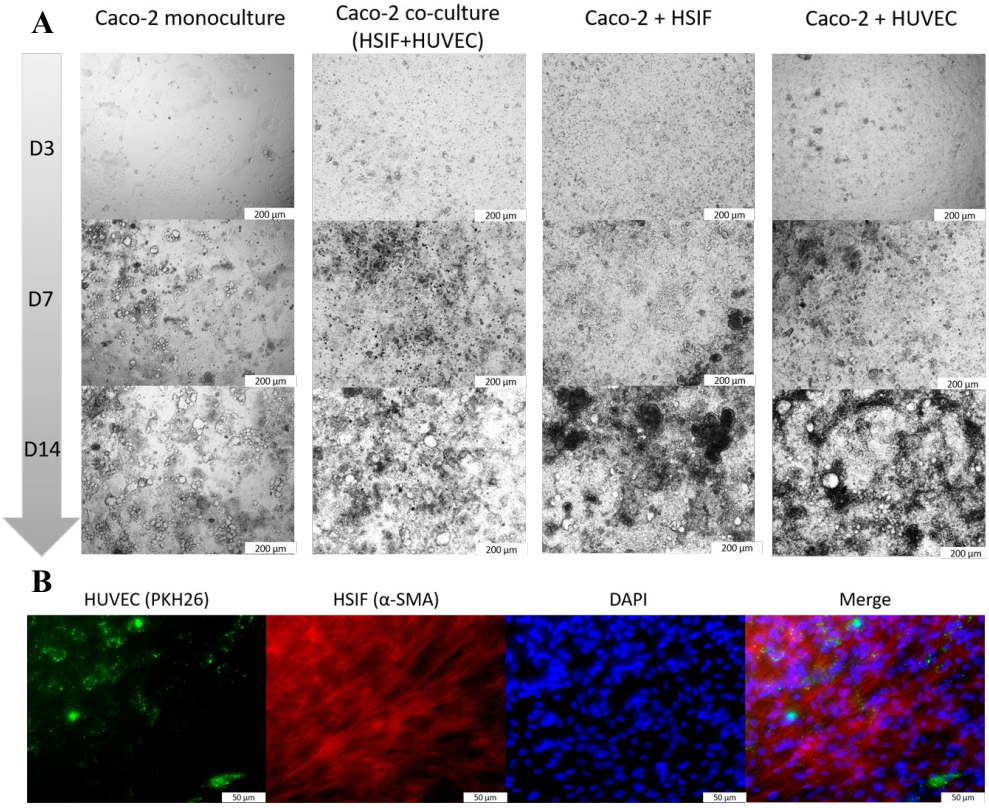

Fig. 3.1.3.2.2. *(A) Brightfield images showing the growth of Caco-2 cells in monoculture or co-cultures with HSIF and (or) HUVEC cells from Day 3 to Day 14 (images were acquired at 10× magnification). (B) Immunofluorescence images demonstrating the presence of HSIF and HUVEC cells in the co-culture model. HUVEC were labelled with PKH26 (green), HSIF were stained with α-SMA (red), and nuclei were counterstained with DAPI (blue) (images were acquired at 20× magnification)*

Abbreviations: α-SMA – alpha-smooth muscle actin; DAPI – 4′,6-diamidino-2-phenylindole; HSIF – human small intestinal fibroblasts; HUVEC – human umbilical vein endothelial cells; PKH26 – red fluorescent cell-membrane linker dye.

3.1.4. Viral-mimic damage induction in Caco-2 monoculture

3.1.4.1. Poly I:C stimulation

Subsequently, we quantified the effect of Poly I:C on cell viability (CCK-8 assay) and on both the number and size of Caco-2 organoids (brightfield microscopy). Poly I:C induced a dose-dependent decline in viability (Fig. 3.1.4.1.1 A): at 50 µg/mL Poly I:C (highest concentration) viability reduced to 84 % of the mock control (p = 0.003). Similarly, both the number and size of the organoids were also reduced (Fig. 3.1.4.1.1 B-D). The number of organoids reduced by approximately 35 %, while the size decreased by about 55 % at the highest Poly I:C concentration. Collectively, these results confirmed successful induction of viral-mimic-mediated epithelial damage in this model.

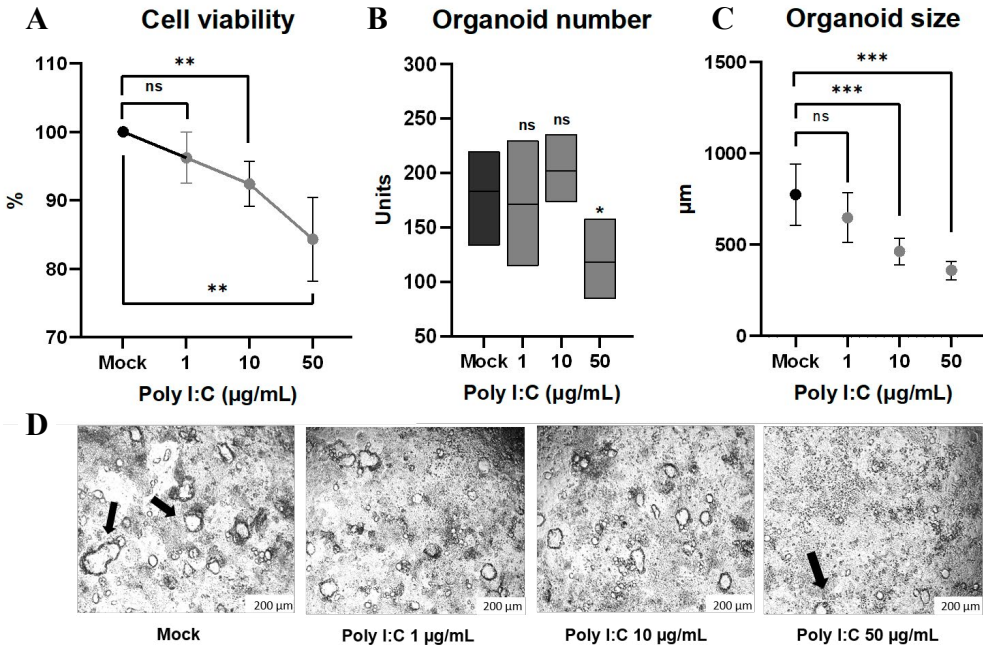

Fig. 3.1.4.1.1. *The effect of Poly I:C on Caco-2 monoculture: (A) cell viability (CCK-8) (n = 3), (B) organoid number (n = 3), (C) organoid size (n = 3). (D) Representative brightfield images of Caco-2 monoculture 24 hours after Poly I:C stimulation (arrows indicate organoids)*

ns indicates $p > 0.05$, * $p < 0.05$, ** $p < 0.01$, and *** $p < 0.001$. Abbreviations: Poly I:C – polyinosinic polycytidylic acid.

In line with reduced cell viability, Poly I:C induced a dose-dependent increase in Caco-2 apoptosis. Even the lowest dose of Poly I:C induced significantly higher apoptosis compared to mock, while in cells stimulated with high-dose Poly I:C apoptosis increased around twice (Fig. 3.1.4.1.2).

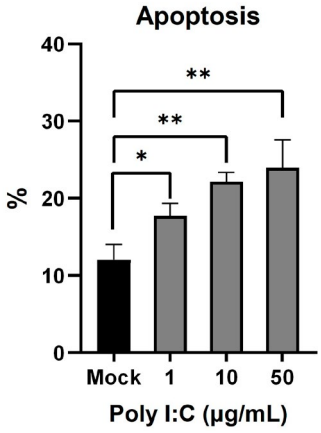

Fig. 3.1.4.1.2. *Apoptosis induced by Poly I:C after 24 hours by flow cytometry (n = 3)*

* indicates $p < 0.05$, and ** $p < 0.01$. Abbreviations: Poly I:C – polyinosinic polycytidylic acid.

3.1.4.2. R848 stimulation

Stimulation with R848 induced a dose-dependent decrease in cell viability and an increase in apoptosis (Fig. 3.1.4.2.1 A–B). Notably, alterations in culture morphology were also observed (Fig. 3.1.4.2.1 C); although numerous organoid-like structures formed, their growth was impaired as they failed to mature into larger, well-developed organoids over time. Similar morphological disruptions and cytotoxic effects were observed with various combinations of R848 and Poly I:C mix.

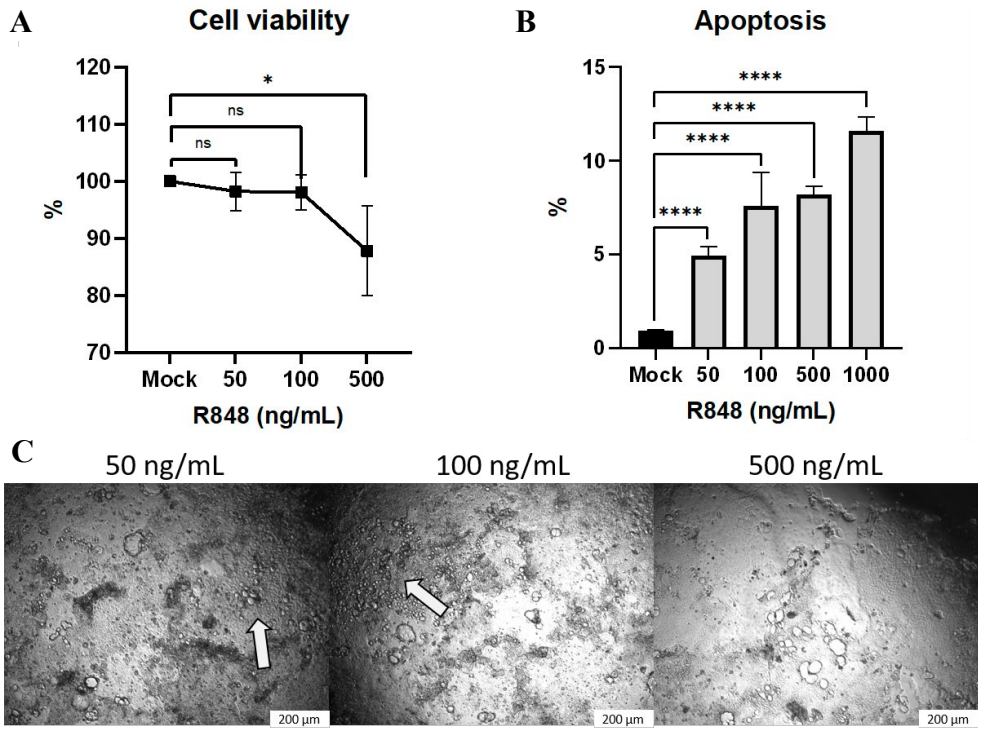

Fig. 3.1.4.2.1. *Results of Caco-2 monoculture stimulated with different concentrations of R848: (A) cell viability (n = 3), (B) apoptosis (n = 3), (C) brightfield microscopy (arrows show multiple cystic structures formation)*

ns indicates $p > 0.05$, * indicates $p < 0.05$, and *** indicates $p < 0.001$. Abbreviations: R848 – resiquimod.

3.1.5. Viral-mimic damage induction in co-culture model

In the co-culture model, epithelial cells displayed greater resilience to Poly I:C. Caco-2 cell viability tended to be better preserved in triple co-culture (Caco-2 + HSIF + HUVEC) compared to the monoculture and dual co-cultures (Caco-2+HSIF or Caco-2+HUVEC) (Fig. 3.1.5.1 A). To impose stronger viral-mimic stress, the Poly I:C concentration was increased to 100 µg/mL. At this dose viability fell to roughly 75–80 % in dual co-cultures, whereas the triple co-culture remained near mock-treated levels.

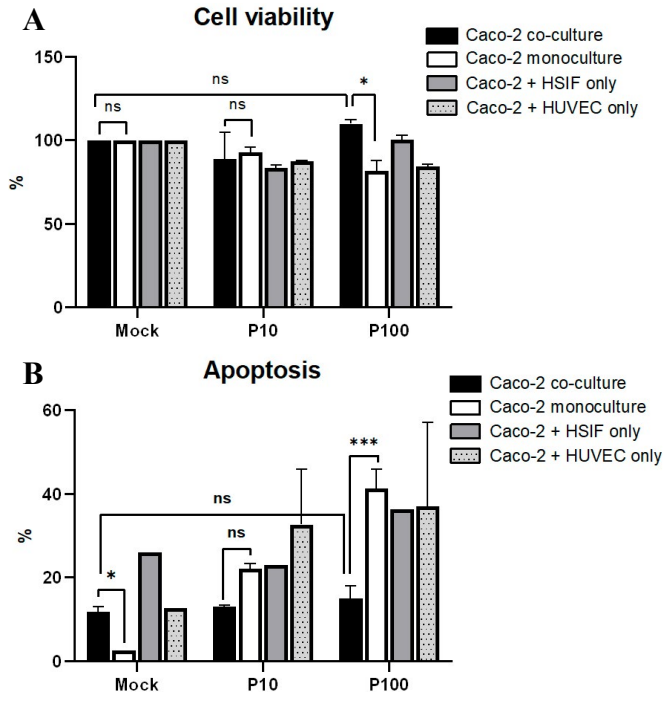

Fig. 3.1.5.1. *Comparison of cell viability (A) and apoptosis (B) in co-culture models after Poly I:C stimulation (n = 3)*

ns indicates $p > 0.05$, * indicates $p < 0.05$, and *** indicates $p < 0.001$. Abbreviations: P10 – Poly I:C 10 μg/mL; P100 – Poly I:C 100 μg/mL; HSIF – human small intestinal fibroblasts; HUVEC – human umbilical vein endothelial cells.

Under this high-dose challenge (100 μg/mL), apoptosis levels reached approximately 35–40 % in the monoculture and both dual co-cultures, yet remained close to baseline in the triple co-culture (15.05 % vs 12.1 %, p>0.05; Fig. 3.1.5.1 B). Collectively, these data indicate that the simultaneous presence of fibroblasts and endothelial cells enhanced epithelial resistance to Poly I:C-induced cytotoxicity and conferred effective protection against apoptosis.

3.2. Antiviral response in monoculture model

3.2.1. IFN expression

3.2.1.1. Poly I:C stimulation

After establishing the viral GI model, we proceeded to quantify the antiviral response by measuring the expression of key antiviral cytokines, including type I IFNs (IFNβ and IFNα) and the type III IFN (IFNλ1).

Poly I:C induced a clear dose-dependent increase in IFNλ1 expression in Caco-2 cells (Fig. 3.2.1.1.1 A). Significantly elevated IFNλ1 levels were already observed after 6 hours after stimulation at every Poly I:C concentration tested (Fig. 3.2.1.1.1 B). In contrast, the expression of IFNβ or IFNα was not detected under identical conditions (Fig. 3.2.1.1.1 C, D).

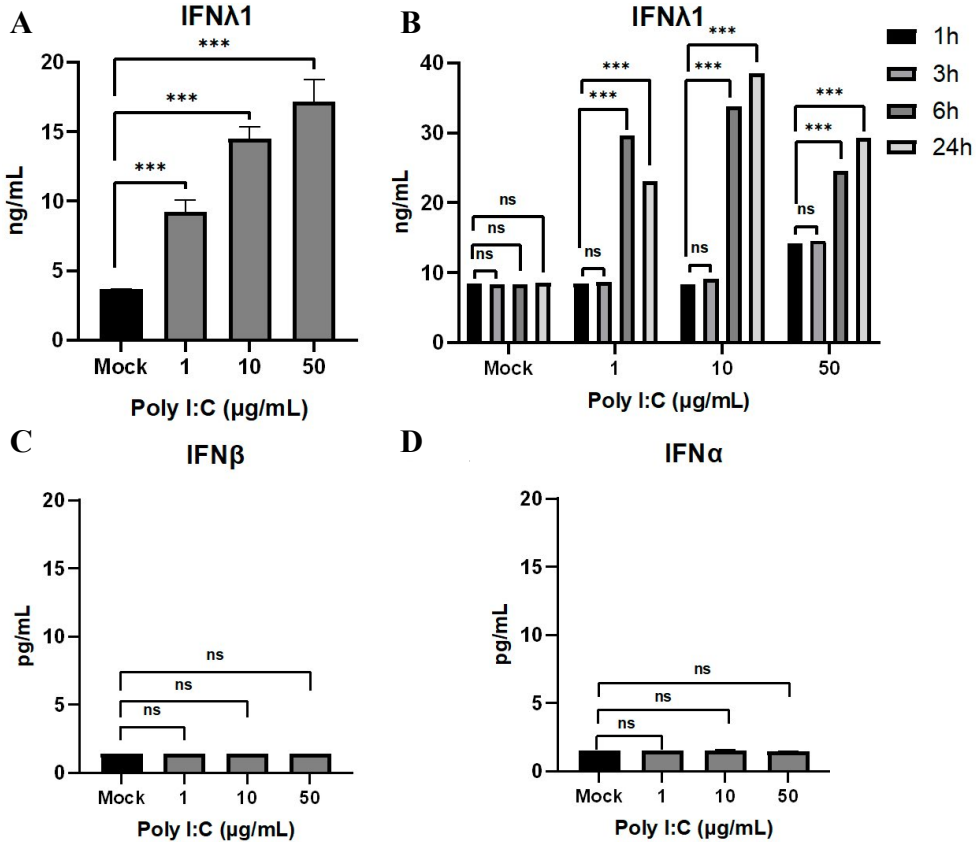

Fig. 3.2.1.1.1. *IFN levels in Poly I:C-stimulated Caco-2 cells measured by ELISA: (A) IFNλ1 levels 24 h after stimulation with various concentrations of Poly I:C (n = 3); (B) IFNλ1 release at different timepoints after stimulation with Poly I:C (n = 3); (C) IFNβ and (D) IFNα levels 24 h after stimulation with Poly I:C (n = 3)*

ns – indicates $p > 0.05$, *** indicates $p < 0.001$. Abbreviations: Poly I:C – polyinosinic polycytidylic acid; IFNλ1 – interferon λ1; IFNβ – interferon β; IFNα – interferon α; h – hour.

3.2.1.2. R848 stimulation

No significant increase in IFNλ1 expression was observed in R848-stimulated cultures compared to untreated controls, regardless of the duration

of stimulation (Fig. 3.2.1.2.1). Co-stimulation with Poly I:C and R848 elicited an antiviral response comparable to that induced by Poly I:C alone, suggesting that the observed effects were primarily attributable to Poly I:C. However, these conditions also resulted in pronounced morphological abnormalities inconsistent with typical organoid architecture as shown in section 3.1.4.2.

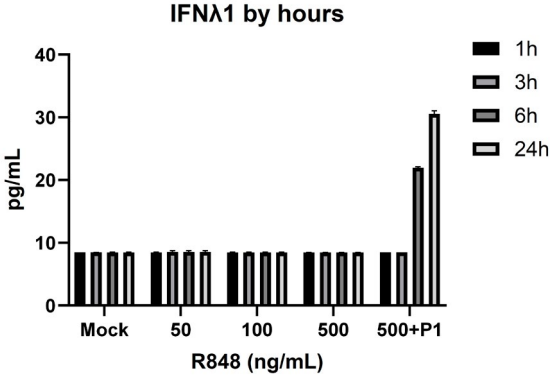

Fig. 3.2.1.2.1. *IFNλ1 levels (ELISA) at different timepoints after stimulation of R848 only and R848 and Poly I:C mix (n = 3)*

Abbreviations: R848 – resiquimod; h – hour; P1 – Poly I:C 1 μg/mL.

Given the lack of additive immunostimulatory effects and the detrimental impact on culture integrity and organoid formation, further experiments involving R848, either alone or in combination with Poly I:C, were discontinued.

3.2.2. IFNLR1 expression

To further evaluate type III IFN axis, we quantified the expression of the IFNλ receptor 1 (IFNLR1) by flow cytometry. Poly I:C increased or retained IFNLR1 expression 24 hours after stimulation (Fig. 3.2.2.1), indicating that Caco-2 cells upregulate the receptor in response to the viral mimic and are thereby primed for subsequent IFNλ signalling.

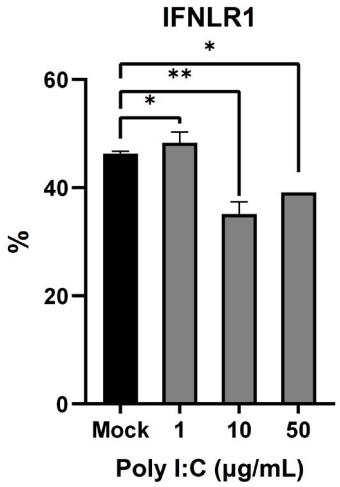

Fig. 3.2.2.1. *Surface IFNLR1 expression in Caco-2 monocultures 24 h after Poly I:C stimulation, determined by flow cytometry (n = 3)*

* indicates $p < 0.05$, ** indicates $p < 0.01$. Abbreviations: Poly I:C – polyinosinic polycytidylic acid; IFNLR1 – interferon λ receptor 1.

3.2.3. STAT expression

To examine downstream signalling, we quantified the cellular levels of phosphorylated STAT1, STAT2 and STAT3 by flow cytometry. Poly I:C treatment significantly upregulated the expression of all three STAT proteins relative to mock-treated cells (Fig. 3.2.3.1 A–C). Thus, viral-mimic exposure not only induced IFNλ production but also upregulated key downstream proteins, consistent with activation of the type III IFN signalling axis.

Taken together, the results show that Poly I:C effectively triggered a robust antiviral response in this epithelial monoculture by engaging the type III IFN pathway, as evidenced by IFNλ secretion, upregulation of its receptor IFNLR1, and activation of STAT-dependent downstream signalling.

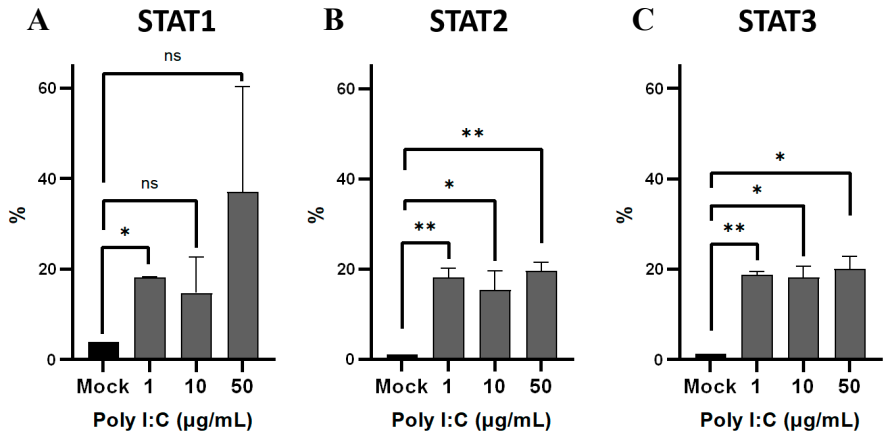

Fig. 3.2.3.1. *Expression of STAT1 (A), STAT2 (B), and STAT3 (C) proteins by flow cytometry in Caco-2 monoculture 24 hours after Poly I:C stimulation (n = 3)*

ns indicates $p > 0.05$, * indicates $p < 0.05$, ** indicates $p < 0.01$. Abbreviations: Poly I:C – polyinosinic polycytidylic acid; STAT1 – signal transducer and activator of transcription 1; STAT2 – signal transducer and activator of transcription 2; STAT3 – signal transducer and activator of transcription 3.

3.3. Antiviral response in co-culture model

Given the results from the monoculture, we next investigated the antiviral response in co-culture model, expanding our analysis of the type III IFN signalling pathway to upstream regulators (e.g., IRF1, IRF3, TRIF, and TBK1) and organelle-specific contributions (mitochondria and peroxisomes) in order to provide a mechanistic explanation to the induction of IFNλ1 response.

3.3.1. IFN kinetics and expression

As IFNλ1 proved pivotal in the monoculture, we first quantified its secretion in the co-culture model. Time-course ELISA revealed a clear dose- and time-dependent rise (Fig. 3.3.1.1 A). Higher Poly I:C dose induced earlier IFNλ1 responses with levels reaching 34.34 ± 0.34 and 34.98 ± 0.02 ng/mL at 4 and 6 hours after 100 µg/mL compared to 19.96 ± 0.04 and 26.08 ± 0.08 ng/mL at the same timepoints after 10 µg/mL stimulation. Mock-treated controls remained static (19.57 ± 0.013 ng/mL, $p < 0.001$).

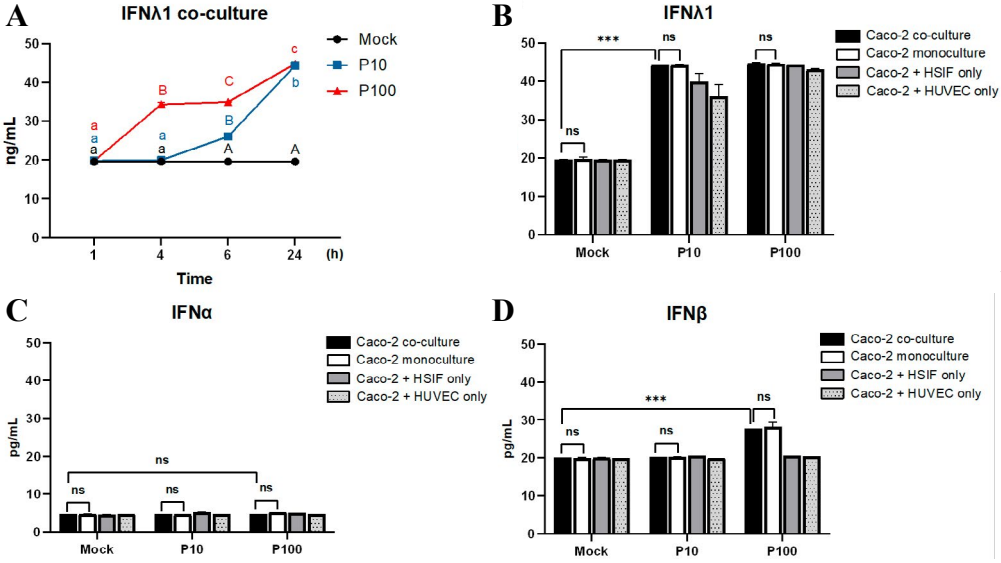

Fig. 3.3.1.1. *Levels of IFNs by ELISA in co-culture and monoculture models 24 hours after Poly I:C stimulation: (A) levels of IFNλ1 over time in co-culture (different letters show statistical significance: different lowercase letters indicate $p < 0.05$, uppercase – $p < 0.01$) ($n = 3$); (B) IFNλ1 levels ($n = 3$); (C) IFNα levels ($n = 3$); (D) IFNβ levels ($n = 3$)*

ns indicates $p > 0.05$, *** indicates $p < 0.001$. Abbreviations: P10 – Poly I:C 10 μg/mL; P100 – Poly I:C 100 μg/mL; Poly I:C – polyinosinic polycytidylic acid; IFNλ1 – interferon λ1; IFNβ – interferon β; IFNα – interferon α; h – hour; HSIF – human small intestinal fibroblasts; HUVEC – human umbilical vein endothelial cells.

Across all models, at 24 hours after stimulation Poly I:C provoked a strong IFNλ1 response exceeding 40 ng/mL at both doses, with the triple co-culture exhibiting the highest levels, though the differences between models were modest (Fig. 3.3.1.1 B). Mock-treated cells maintained baseline IFNλ1 levels (~20 ng/mL), confirming that stimulus was required for the induction. These data demonstrate that each culture model is fully competent to mount a vigorous type III IFN response.

As in the monoculture, IFNα was not detected in the co-cultures (Fig. 3.3.1.1 C). IFNβ, by contrast, showed a modest increase only at the 100 μg/mL Poly I:C dose (28.18 ± 1.19 pg/mL in the Caco-2 monoculture and 27.84 ± 0.23 pg/mL in the triple co-culture), with no detectable expression after low-dose stimulation (Fig. 3.3.1.1 D). The lack of induction at lower concentrations clarifies why earlier experiments failed to detect IFNβ and indicates that the type I IFN participates in the antiviral programme, but less vigorously than IFNλ1.

Taken together, these findings show that the co-culture not only withstands viral-mimic stress more effectively than the monoculture but also displays a slightly distinct pattern of IFN regulation.

3.3.2. Regulation of IRF3 and IRF1

To clarify the upstream control of the robust IFNλ1 response, we measured the transcription factors IRF3 and IRF1. Poly I:C provoked a rapid rise in IRF3 that peaked as early as after 4 hours in the co-culture (42.45 ± 0.63 ng/mL at 100 µg/mL) (Fig. 3.3.2.1 A), whereas in monoculture the maximum was delayed until 24 hours (55.3 ± 3.3 ng/mL) (Fig. 3.3.2.1 B). IRF1 had different dynamics remaining nearly constant in co-culture but increasing steadily in monoculture in a dose-dependent fashion and peaking at 24 hours (Fig. 3.3.2.1 C–D).

At the 4-hour time point, IRF3 expression increased in a dose-dependent manner across all models, with the greatest induction observed in the triple co-culture (42.45 ± 0.62 ng/mL), compared to monoculture (28.01 ± 0.01 ng/mL) and the dual co-cultures with HSIF (22.13 ± 0.18 ng/mL) or HUVEC (18.85 ± 0.21 ng/mL) ($p < 0.001$; Fig. 3.3.2.1 E). In contrast, after high-dose Poly I:C, IRF1 levels in monoculture were more than twice as high as in triple co-culture (29.3 ± 2.54 vs. 14.2 ± 1.63 ng/mL, $p = 0.02$) (Fig. 3.3.2.1 F).

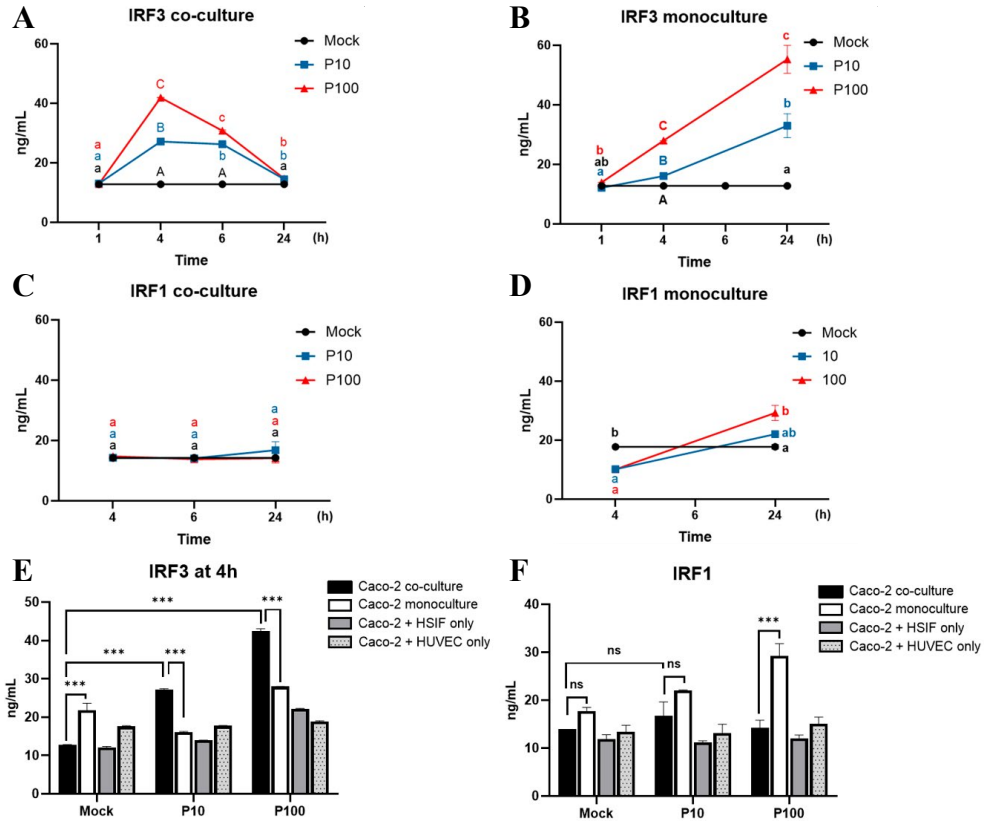

Fig. 3.3.2.1. *Levels of IRFs measured by ELISA in co-culture and monoculture models after Poly I:C stimulation: IRF3 expression over time in co-culture with HSIF and HUVEC (A) and monoculture (B) (n = 3); IRF1 expression over time in co-culture with HSIF and HUVEC (C) and monoculture (D) (different letters show statistical significance: different lowercase letters indicate $p < 0.05$, uppercase – $p < 0.01$) (n = 3); (E) IRF3 levels after 4 hours of Poly I:C stimulation (n = 3); (F) IRF1 levels after 24 hours of Poly I:C stimulation (n = 3)*

ns indicates $p > 0.05$, and *** indicates $p < 0.001$. Abbreviations: P10 – Poly I:C 10 μg/mL; P100 – Poly I:C 100 μg/mL; IRF1 – interferon regulatory factor 1; IRF3 – interferon regulatory factor 3; HSIF – human small intestinal fibroblasts; HUVEC – human umbilical vein endothelial cells.

These data indicate that fibroblasts and endothelial cells accelerate IRF3 activation while simultaneously dampening IRF1 induction, potentially modulating downstream type III IFN signalling in the co-culture model.

3.3.3. TRIF-TBK1 signalling axis activation

To explore the upstream arm of the innate immune cascade that culminates in IRF3 activation, we quantified TBK1 and TRIF in monoculture and co-culture after a viral-mimic challenge.

In Caco-2 monoculture, TBK1 rose in a clear dose-dependent manner and peaked at 24 hours (70.8 ± 0.2 ng/mL at 100 μg/mL Poly I:C) (Fig. 3.3.3.1 A). By contrast, the triple co-culture exhibited a primed activation state, with baseline TBK1 levels already high (~45 ng/mL) and remaining relatively unchanged over the 24-hour period (Fig. 3.3.3.1 B). At the earliest time points (1 and 4 hours), TBK1 was about two-fold higher in the co-culture than in monoculture (38.8 ± 0.23 vs 17.3 ± 0.01 ng/mL at 1 hour after 100 μg/mL Poly I:C; $p < 0.001$) (Fig. 3.3.3.1 C, D). Elevated TBK1 levels were also seen in mock-treated co-cultures which implies basal pre-activation driven by fibroblast- or endothelial-derived signals.

TRIF likewise increased in a dose-dependent manner and was significantly higher in the triple co-culture than in monoculture ($p < 0.001$) (Fig. 3.3.3.1 E). TBK1 and TRIF levels were tightly correlated ($r = 0.998$, $p < 0.001$), indicating a coordinated engagement of the TRIF–TBK1 axis, which likely accelerates IRF3 phosphorylation and the ensuing IFNλ1 response. Together, these data suggest that signals from fibroblasts and endothelial cells activate epithelial TBK1 and amplify TRIF–TBK1 signalling upon viral-mimic stimulation, contributing to the more rapid IFNλ1 production observed in the co-culture model.

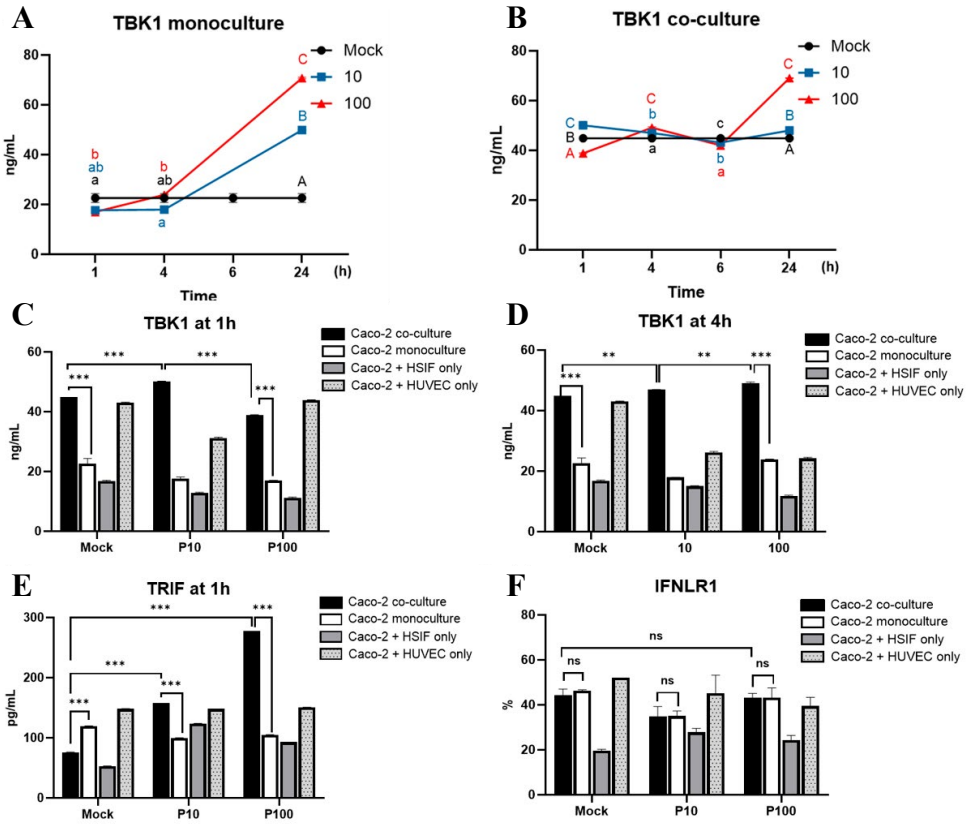

Fig. 3.3.3.1. *TBK1 expression in co-cultures compared to monocultures by ELISA: TBK1 expression over time in monoculture (A) and co-culture with HSIF and HUVEC (B) (different letters show statistical significance: lowercase letters indicate $p < 0.05$, uppercase – $p < 0.01$) (n = 3); Comparison of TBK1 expression among cultures at 1 (C) and 4 hours (D) after Poly I:C stimulation (n = 3). (E) Comparison of TRIF expression among cultures at 1 hour after Poly I:C stimulation (n = 3). (F) Comparison of IFNLR1 expression among cultures at 24 hours after Poly I:C stimulation by flow cytometry (n = 3)*

ns indicates $p > 0.05$, ** indicates $p < 0.01$, and *** indicates $p < 0.001$. Abbreviations: P10 – Poly I:C 10 μg/mL; P100 – Poly I:C 100 μg/mL; IFNLR1 – interferon-λ receptor 1; TBK1 – TANK-binding kinase 1; TRIF – TIR-domain-containing adapter-inducing IFNβ; HSIF – human small intestinal fibroblasts; HUVEC – human umbilical vein endothelial cells.

3.3.4. IFNLR1 expression

To determine whether receptor availability modulates downstream IFNλ1 signalling, we measured surface IFNLR1 in all models after Poly I:C challenge. Under mock conditions, IFNLR1 expression was similar in monoculture and the triple co-culture (46.0 ± 0.3 % vs 42.8 ± 2.2 % respectively), but markedly lower in the Caco-2 + HSIF dual co-culture (19.7 ± 0.4 %; $p < 0.001$) (Fig. 3.3.3.1 F). Poly I:C induced a modest decline in receptor expression in most models, and both triple co-culture and monoculture still displayed high IFNLR1 levels at the highest dose tested (46.3 ± 3.1 % and 44.1 ± 1.6 %, respectively).

Collectively, these data indicate that the co-culture preserves both signalling capacity (via early TBK1 activation) and receptor responsiveness (via sustained IFNLR1 surface expression). The combination of both probably underlies the stronger, more durable type III IFN response seen in the GI epithelium of the triple co-culture model.

3.3.5. Mitochondrial and peroxisomal activation comparison

To further examine the antiviral pathway, we assessed organelle-specific responses, focusing on mitochondria and peroxisomes, which are known to play key roles in cellular immunity. Activation of the organelles was evaluated by quantitative analysis (Fig. 3.3.5.1 A, B) of fluorescence microscopy (Fig. 3.3.5.1 C, D) and revealed distinct activation patterns between models.

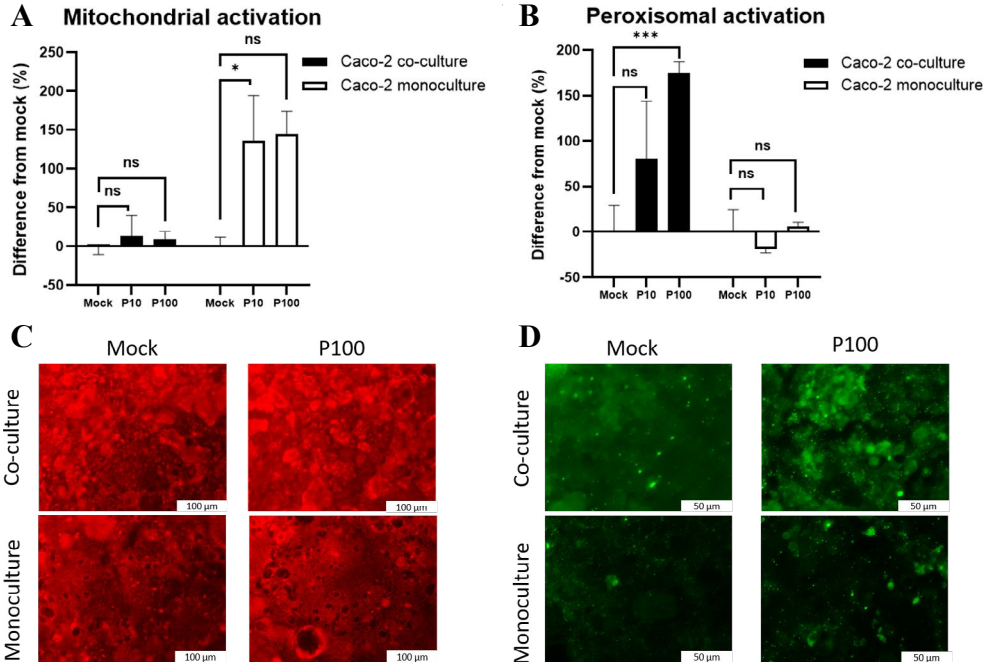

Fig. 3.3.5.1. *Mitochondrial and peroxisomal activation by immunofluorescent staining in co-culture compared to monoculture: quantification of mitochondrial (A) and peroxisomal (B) activation intensity, expressed as the difference from mock-treated controls (n = 3); (C) representative immunofluorescence images of mitochondrial activation detected by MitoTracker staining; (D) representative immunofluorescence images representing peroxisomal activation detected by PEX-1 staining*

ns indicates $p > 0.05$, * indicates $p < 0.05$, and *** indicates $p < 0.001$. Abbreviations: P10 – Poly I:C 10 µg/mL; P100 – Poly I:C 100 µg/mL.

In the Caco-2 monoculture, Poly I:C boosted mitochondrial activity by nearly two-fold (9.32 ± 0.9 a.u. in mock vs. 23.1 ± 4.46 a.u. and 21.86 ± 2.27 a.u. after 10 and 100 µg/mL of Poly I:C, $p = 0.01$ and $p = 0.008$, respectively) (Fig. 3.3.5.1 A). In contrast, the triple co-culture exhibited higher baseline mitochondrial activation (29.57 ± 2.1 a.u.) with no significant change after stimulation, suggesting reduced reliance on mitochondrial antiviral signalling pathways (Fig. 3.3.5.1 A).

The activation of peroxisomes had an opposite trend. Triple co-culture displayed a marked, dose-dependent increase in peroxisomal activity (~110-170 % over mock) (Fig. 3.3.5.1 B, D), whereas monocultures showed little or even slightly negative change (Fig. 3.3.5.1 B, D).

Peroxisomal activation closely correlated with IRF3 induction ($r = 0.894$ at 4 hours in all models; $r = 0.949$ at 4 hours in co-culture) and TBK1 and TRIF levels ($r = 0.949$, $p = 0.002$ and $r = 0.947$, $p = 0.002$, respectively) (Fig. 3.3.8.1). These correlations were weak in monoculture.

The data indicate that the co-culture favours peroxisome–TBK1–IRF3 axis, providing a robust yet less cytotoxic antiviral route than the mitochondria-centred pathway dominant in monoculture. This is consistent with sustained TBK1 levels and reduced apoptosis observed in the co-culture model.

3.3.6. STAT3 signalling

Phosphorylated STAT3 (Tyr705) followed a distinct pattern. In Caco-2 monocultures, STAT3 increased to 172.8 ± 12.5 % of mock after high-dose Poly I:C (Fig. 3.3.6.1), whereas in the triple co-culture it remained close to baseline. This pattern suggests that STAT3 activation is largely confined to epithelial monoculture.

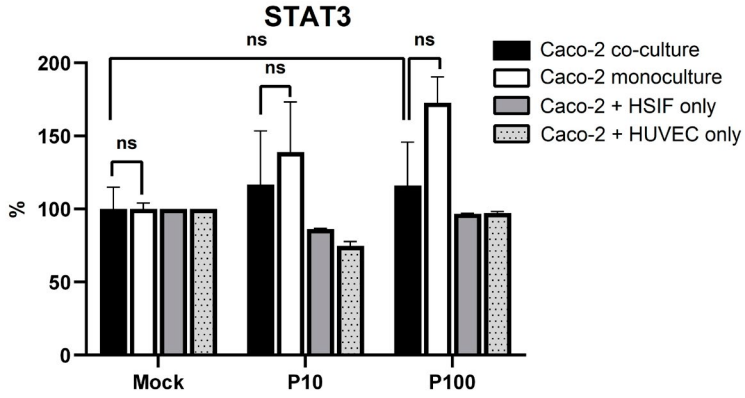

Fig. 3.3.6.1. *Comparison of STAT3 expression by ELISA in co-culture and monoculture 24 hours after Poly I:C stimulation (n = 3)*

ns indicates $p > 0.05$. Abbreviations: P10 – Poly I:C 10 μg/mL; P100 – Poly I:C 100 μg/mL; STAT3 – signal transducer and transcription activator 3; HSIF – human small intestinal fibroblasts; HUVEC – human umbilical vein endothelial cells.

3.3.7. The expression of ISG-encoded proteins

To evaluate the downstream activation of the type III IFN signalling axis, the expression of two canonical interferon-stimulated gene (ISG) products − MX1 and OAS1 was quantified using immunofluorescence analysis. High-dose Poly I:C stimulation (100 μg/mL) significantly upregulated MX1 protein expression (19.33 ± 0.83 a.u.) compared to mock-treated controls

(10.01 ± 2.03 a.u., $p < 0.001$) (Fig. 3.3.7.1 A). In contrast, OAS1 levels were significantly reduced following Poly I:C stimulation (3.3 ± 1.05 a.u. vs. 5.7 ± 0.5 a.u. in mock, $p < 0.023$) (Fig. 3.3.7.1 B), potentially reflecting translational inhibition resulting from excessive intracellular dsRNA levels.

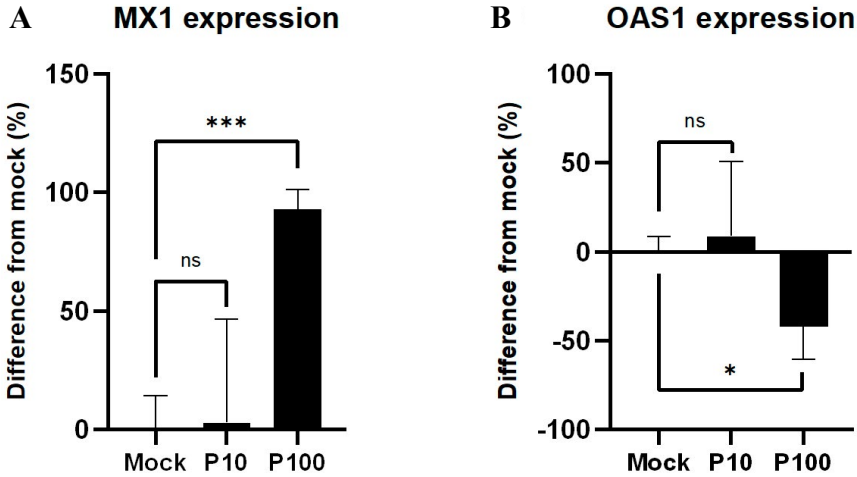

Fig. 3.3.7.1. *The expression of ISG-encoded proteins (MX1 and OAS1) by fluorescent microscopy 24 hours after Poly I:C stimulation in co-culture (n = 3)*

ns indicates $p > 0.05$, * indicates $p < 0.05$, and *** indicates $p < 0.001$. Abbreviations: P10 – Poly I:C 10 μg/mL; P100 – Poly I:C 100 μg/mL; MX1 – myxovirus-resistance protein; OAS1 – 2′-5′-oligoadenylate synthetase 1.

Correlation analysis revealed that MX1 intensity positively correlated with peroxisomal activation ($r = 0.456$, $p = 0.043$) and TBK1 expression ($r = 0.578$, $p = 0.03$), while showing a strong negative correlation with mitochondrial activation ($r = -0.664$, $p = 0.005$). OAS1 expression was positively associated with both TBK1 ($r = 0.808$, $p = 0.003$) and STAT3 ($r = 0.623$, $p = 0.041$), and inversely correlated with apoptosis ($r = -0.818$, $p = 0.002$) (Fig. 3.3.8.1). These findings support the notion that peroxisome-associated IFNλ1 signalling promotes a non-cytotoxic antiviral state, whereas mitochondrial stress is more closely linked to apoptotic responses.

3.3.8. Correlation analysis of antiviral signalling pathway

In Caco-2 monoculture, IRF1 was tightly linked to IRF3 ($r = 0.691$, $p = 0.003$), STAT signalling ($r = 0.755$, $p < 0.001$) and mitochondrial activation ($r = 0.705$, $p = 0.0049$), indicating a stress-associated response rather than antiviral.

By contrast, in the triple co-culture, IRF3 levels showed strong, time-dependent correlation with IFNλ1 ($r = 0.865$, $p = 0.013$ at 4 hours; $r = 0.987$, $p < 0.001$ at 24 hours) and its upstream kinase TBK1 ($r = 0.999$, $p < 0.001$ at 4 hours; $r = 0.852$, $p = 0.016$ at 24 hours) (Fig. 3.3.8.1). These results underscore a coordinated IRF3–TBK1–IFNλ1 signalling axis preferentially engaged in the presence of stromal cells.

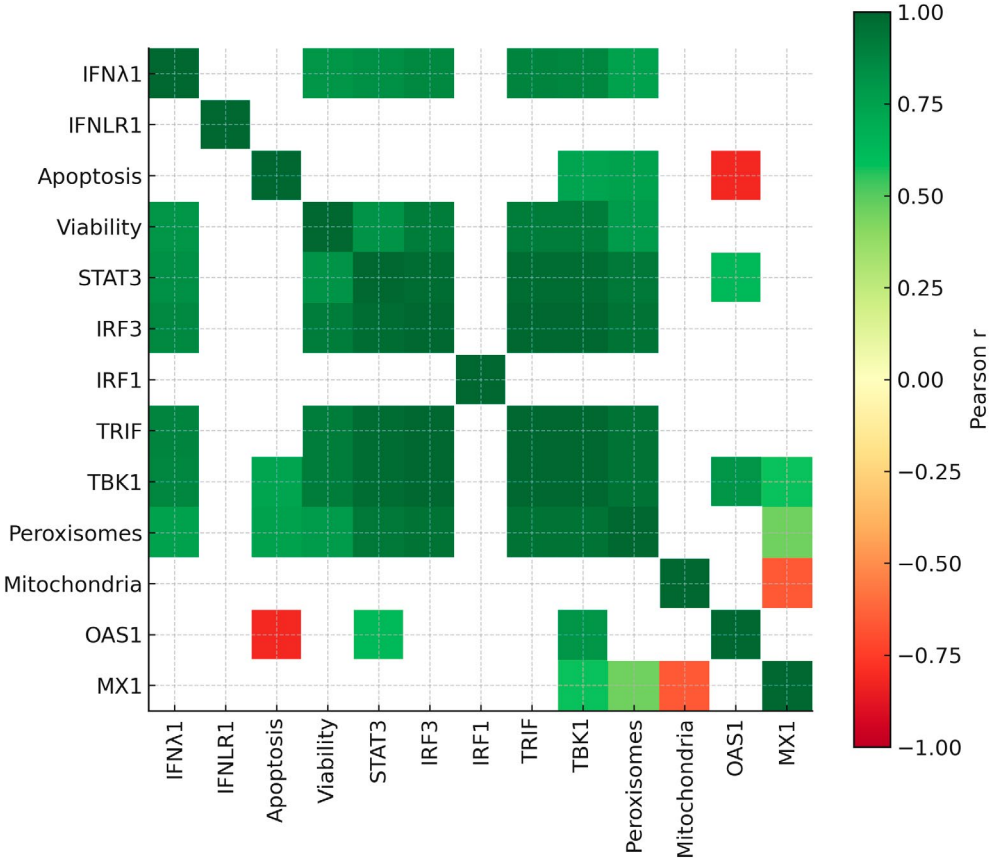

Fig. 3.3.8.1. *Heat-map showing the strength of significant Pearson correlations (r) among antiviral signalling cytokines and signalling organelles in the co-culture model. Darker green indicates stronger positive correlations; darker red – stronger negative correlations; white cells denote non-significant ($p > 0.05$) values*

Abbreviations: IFNλ1 – interferon λ1; IFNLR1 – interferon λ receptor 1; STAT3 – signal transducer and transcription activator 3; IRF1 – interferon regulatory factor 1; IRF3 – interferon regulatory factor 3; TBK1 – TANK-binding kinase 1; TRIF – TIR-domain-containing adapter-inducing IFNβ; MX1 – myxovirus-resistance protein 1; OAS1 – 2′-5′-oligoadenylate synthetase 1.

Taken together, these results show that stromal cells reshape the antiviral response in Caco-2 cultures, leading to a faster, stronger and more precisely regulated type III IFN response while limiting potentially cytotoxic pathways driven by excessive IRF1 and STAT3 activation.

3.4. The effect of melatonin in monoculture

Following the antiviral signalling analysis, we continued our study to search for possible antiviral substances. Given the emerging evidence of melatonin's potential antiviral properties, its current use in clinical practice for other indications, and its well-established safety profile, we decided to investigate its ability to mitigate the cellular damage caused by Poly I:C.

3.4.1. Melatonin safety evaluation in unstimulated Caco-2 cells

We first assessed the cytotoxicity of melatonin in unstimulated Caco-2 monoculture. A 24-hour exposure to various melatonin concentrations produced no significant effect on either cell viability or organoid morphology confirming that melatonin is non-toxic under baseline conditions (Fig. 3.4.1.1 A–C).

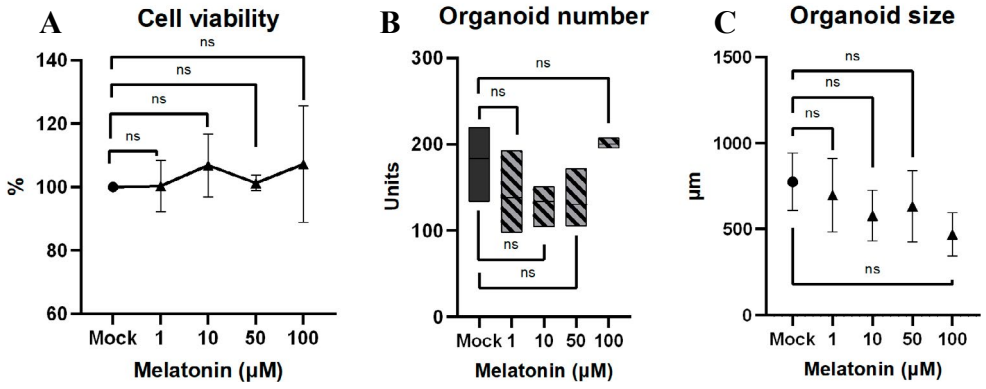

Fig. 3.4.1.1. *The effect of melatonin on unstimulated Caco-2 cell monoculture after 24 hours: (A) cell viability by CCK-8 (n = 3), (B) organoid number (n = 3), and (C) organoid size (n = 3)*

ns indicates $p > 0.05$.

3.4.2. Caco-2 apoptosis and viability

As melatonin can exhibit both prophylactic and therapeutic antiviral properties, we tested two different strategies: 1) pretreatment – melatonin applied 24 hours before Poly I:C stimulation, and 2) treatment – melatonin applied 24 hours after Poly I:C stimulation, to assess its potential to promote cell regeneration after epithelial injury.

Pretreatment of Caco-2 cells with low melatonin concentrations (1 μM and 10 μM) significantly increased viability (119.9 ± 0.09 % in pretreated cells compared to 92.37 ± 2.84 % in melatonin-naive cells after 10 μg/mL Poly I:C, $p < 0.001$), whereas higher concentrations (50 μM and 100 μM) had little effect (Fig. 3.4.2.1A). By contrast, treatment with melatonin after Poly I:C exposure failed to rescue viability, suggesting that postexposure administration could be too late to exert antiapoptotic effects (Fig. 3.4.2.1A).

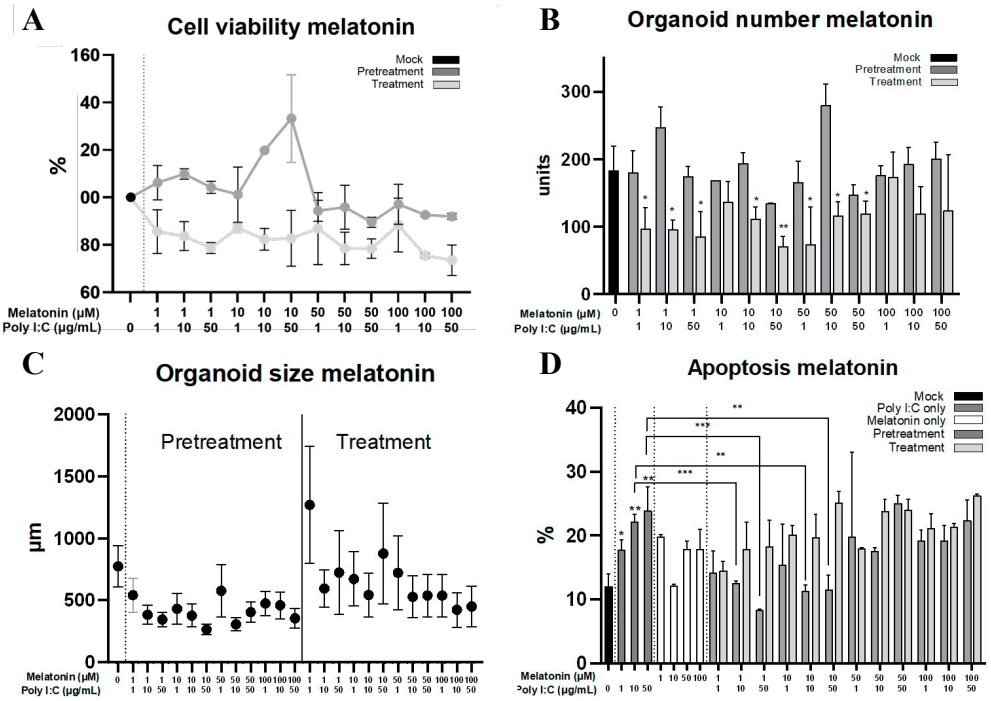
A
Cell viability melatonin
Mock
Pretreatment
Treatment
%
Melatonin (µM)
Poly I:C (µg/mL)
B
Organoid number melatonin
Mock
Pretreatment
Treatment
units
Melatonin (µM)
Poly I:C (µg/mL)
C
Organoid size melatonin
Pretreatment
Treatment
µm
Melatonin (µM)
Poly I:C (µg/mL)
D
Apoptosis melatonin
Mock
Poly I:C only
Melatonin only
Pretreatment
Treatment
%
Melatonin (µM)
Poly I:C (µg/mL)

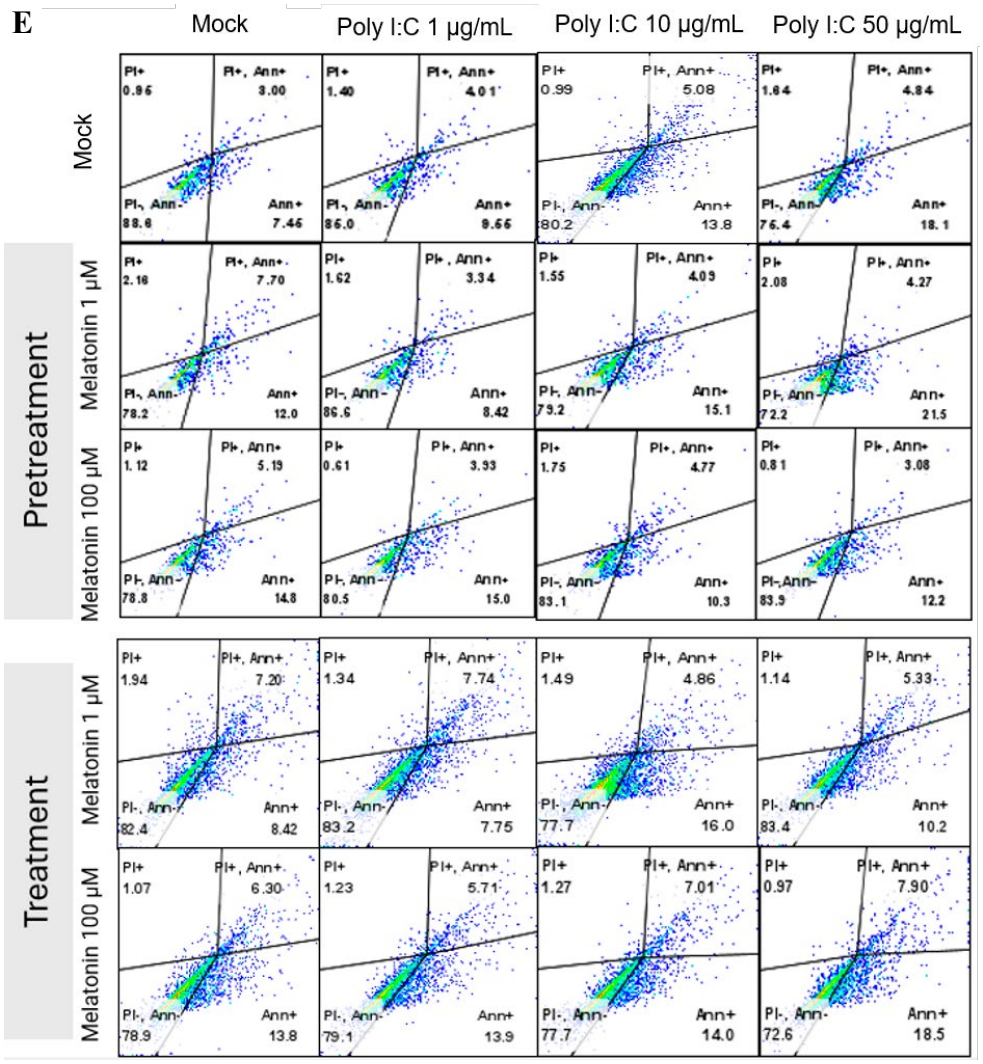

Fig. 3.4.2.1. *Effect of melatonin (1–100 µM) given before (pretreatment) or after (treatment) Poly I:C stimulation on Caco-2 cells: (A) viability (n = 3); (B) organoid count (n = 3); (C) organoid size (n = 3); (D) apoptosis (n = 3); (E) scatter-plots comparing apoptosis at 1 µM and 100 µM against Poly I:C-only and mock controls*

* indicates $p < 0.05$, ** indicates $p < 0.01$, and *** indicates $p < 0.001$. Abbreviations: Poly I:C – polyinosinic polycytidylic acid.

Melatonin given before Poly I:C did not prevent organoid damage. Although the organoid count remained close to control values after 50 µg/mL Poly I:C, average size fell markedly (Fig. 3.4.2.1 B, C, Fig. 3.4.2.2). When melatonin was added after Poly I:C, the total number of organoids decreased, particularly at lower melatonin doses, but the remaining ones were noticeably larger than those in untreated Poly I:C cultures, hinting at a delayed, partial protective effect (Fig. 3.4.2.1 B, C, Fig. 3.4.2.2).

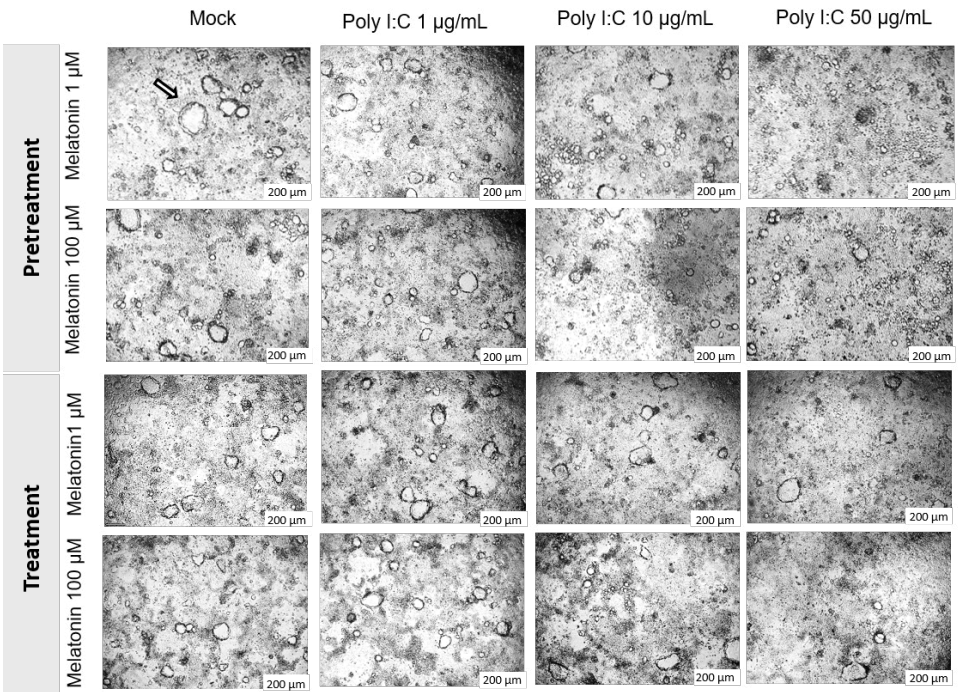

Fig. 3.4.2.2. *Brightfield images of Caco-2 monoculture 24 hours after exposure to 1 or 100 µM melatonin applied either before (pretreatment) or after (posttreatment) stimulation with 1, 10, or 50 µg/mL Poly I:C: higher Poly I:C doses reduce organoid (shown by arrow) size and number, whereas melatonin pre-treatment preserves organoid abundance even at the highest Poly I:C concentration compared with controls*

Abbreviations: Poly I:C – polyinosinic polycytidylic acid.

Melatonin pretreatment tended to reduce apoptosis after Poly I:C challenge, most noticeably at 1 µM and 10 µM (Fig. 3.4.2.1 D, E). In contrast, administering higher melatonin doses after Poly I:C exposure did not reduce apoptosis in comparison to the Poly I:C-only control.

3.4.3. IFNλ1 levels

Melatonin on its own did not trigger IFNλ1 production in Poly I:C-unstimulated Caco-2 cultures (Fig. 3.4.3.1 A). Pre-treating cells with melatonin before Poly I:C exposure also left IFNλ1 expression unchanged relative to melatonin-naïve controls. By contrast, adding melatonin after Poly I:C markedly lowered IFNλ1 levels: when the viral mimic was used at 1 or 10 µg/mL, treatment after it reduced IFNλ1 to values almost indistinguishable from mock levels (Fig. 3.4.3.1 A). This effect was evident across the entire melatonin concentration range tested, suggesting a consistent protective action.

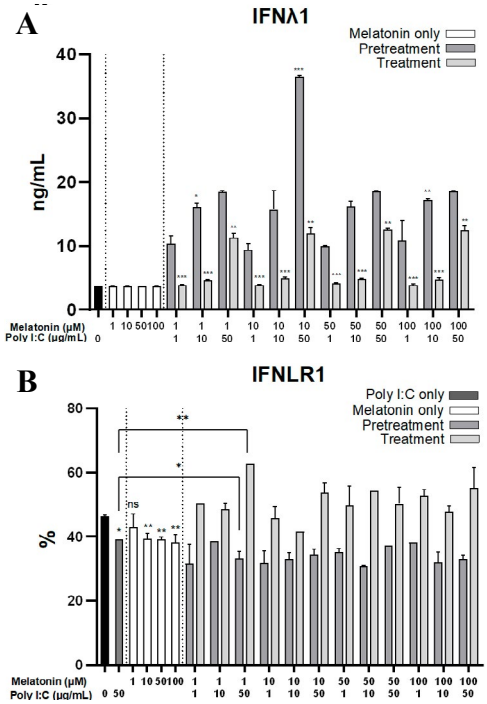

Fig. 3.4.3.1. *Effect of melatonin on type III IFN signalling in Caco-2 cells: (A) IFNλ1 expression (ELISA) after in 1–100 µM melatonin pretreated or treated cells after Poly I:C stimulation compared to mock and Poly I:C-unstimulated melatonin-only treated cells (only significant differences in comparison to melatonin-naïve Poly I:C-stimulated cells are indicated; n = 3); (B) surface IFNLR1 expression (flow cytometry) under the same melatonin regimens, compared to Poly I:C-only and melatonin-only controls (n = 3)*

ns indicates $p > 0.05$, * indicates $p < 0.05$, ** indicates $p < 0.01$, and *** indicates $p < 0.001$. Abbreviations: Poly I:C – polyinosinic polycytidylic acid; IFNλ1 – interferon λ1; INFLR1 – interferon λ receptor 1.

3.4.4. IFNLR1 expression

Melatonin's influence on the type III IFN axis was next explored by measuring surface receptor of IFNλ. Unexpectedly, melatonin alone upregulated IFNLR1 in unstimulated Caco-2 cells. When melatonin was added after Poly I:C, IFNLR1 expression increased further, whereas pretreatment reduced the amount of IFNLR1 (Fig. 3.4.3.1 B and Fig. 3.4.4.1). The effect of melatonin on the receptor was similar across the entire 1–100 µM range.

In the pretreated cells, an inverse association emerged between IFNλ1 production and IFNLR1 expression ($r = –0.475$, $p = 0.03$); no significant link was seen in the treatment group ($p = 0.528$).

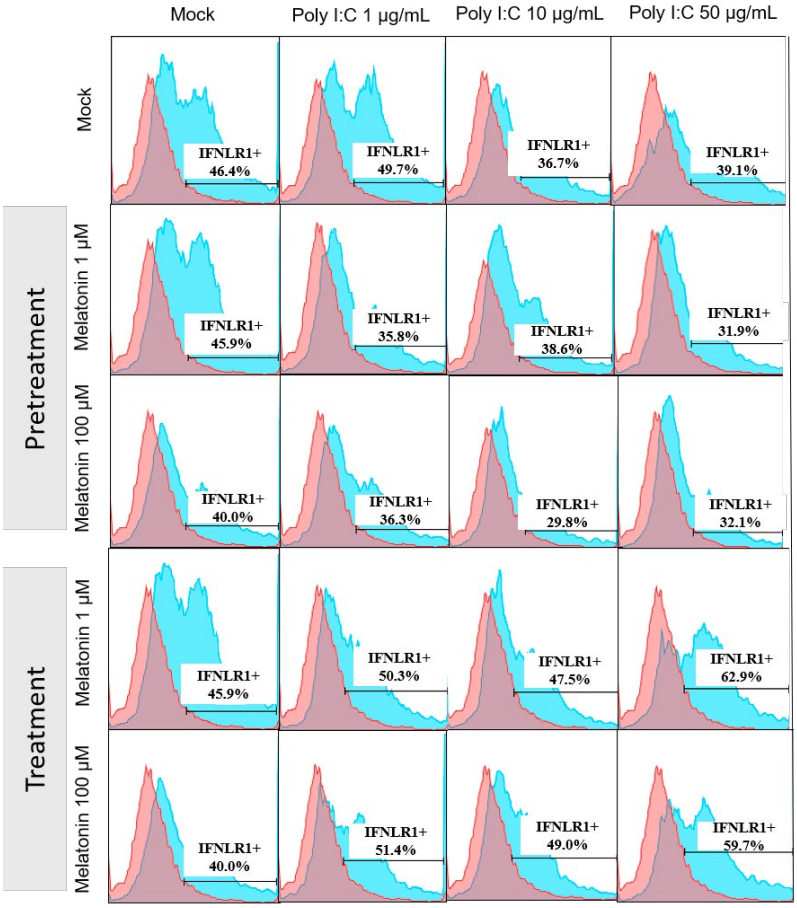

Fig. 3.4.4.1. *Representative histograms illustrating IFNLR1 levels in Caco-2 cells after 1 µM or 100 µM melatonin applied after Poly I:C challenge compared with controls (red histogram shows unstained control, blue – IFNLR1 positive cells)*

Abbreviations: Poly I:C – polyinosinic polycytidylic acid; INFLR1 – interferon λ receptor 1.

3.4.5. Expression of STAT proteins

Melatonin pretreatment lowered STAT1 levels in Poly I:C-stimulated cells, whereas STAT2 and STAT3 remained unchanged (Fig. 3.4.5.1 A–C). Administering melatonin after Poly I:C uniformly suppressed STAT1–STAT3, with no melatonin dose-dependent differences.

All STAT proteins were moderately interrelated, with the strongest association between STAT1 and STAT3 ($r = 0.683$, $p < 0.001$). None of the STAT protein levels correlated with apoptosis in either pretreated or treated cells.

In pretreated cells, IFNλ1 correlated modestly with STAT1–3 (highest correlation with STAT2, $r = 0.509$). STAT2 and STAT3 also showed moderate correlation with IFNLR1 ($r = 0.506$ and $r = 0.438$, respectively). In contrast, in cells treated after Poly I:C stimulation, weak or negative correlations between IFNλ1 and the STATs were observed with a significant relationship between STATs and IFNLR1.

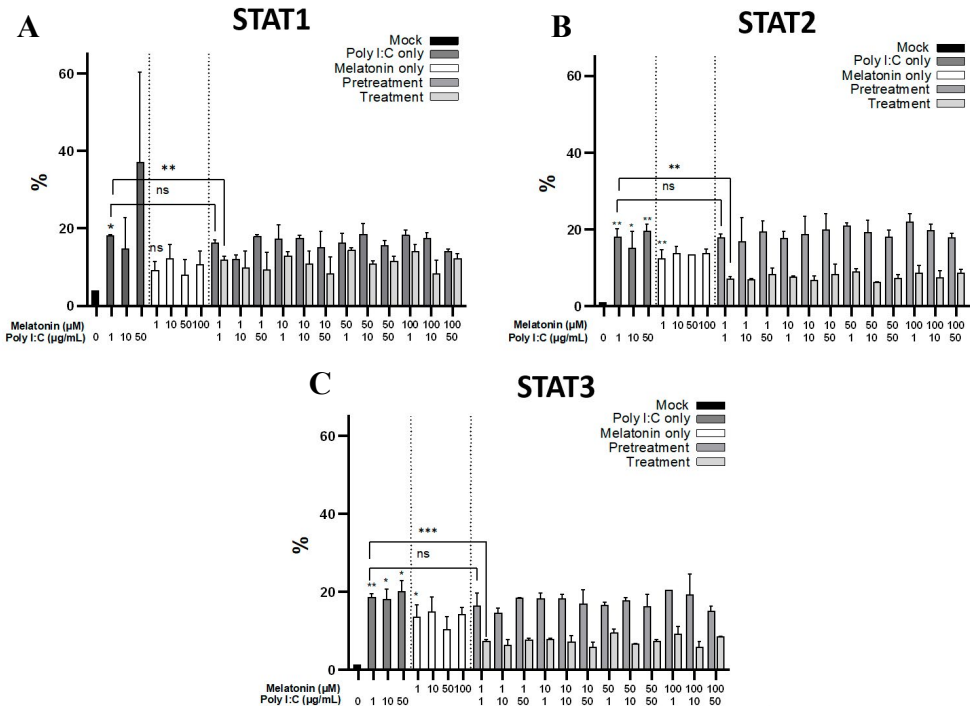

Fig. 3.4.5.1. *Expression of STAT1 (A), STAT2 (B) and STAT3 (C) proteins by flow cytometry in Caco-2 monoculture: comparison of melatonin pretreated, treated and melatonin-naïve controls (n = 3 each)*

ns indicates $p > 0.05$, * indicates $p < 0.05$, ** indicates $p < 0.01$, and *** indicates $p < 0.001$. Abbreviations: Poly I:C – polyinosinic polycytidylic acid; STAT3 – signal transducer and activator of transcription 3.

3.5. The effect of melatonin in co-culture

3.5.1. Poly I:C-induced apoptosis and cell viability

We next assessed the effect of melatonin in the co-culture system, applying both a pretreatment (prior to Poly I:C stimulation) and treatment (following Poly I:C) strategy. A single dose (50 µM) of melatonin was selected based on monoculture experiments, which showed no substantial differences in cellular responses across tested doses.

Pretreatment with 50 µM of melatonin reduced apoptosis and preserved cell viability (Fig. 3.5.1.1). In co-culture, protection from apoptosis was stronger than in monocultures (29.65 ± 0.92 % in untreated vs. 27.65 ± 0.64 % in pretreated cells, $p = 0.009$) or dual co-cultures (Caco-2 + HSIF or Caco-2 + HUVEC only) (Fig. 3.5.1.1 A, E). Consistently, viability in the triple co-culture rose to 158.7 ± 17 % of mock under pretreatment settings before high-dose Poly I:C and was higher than in comparative models (Fig. 3.5.1.1 C). These findings suggest enhanced protection and stress resistance due to multicellular environment.

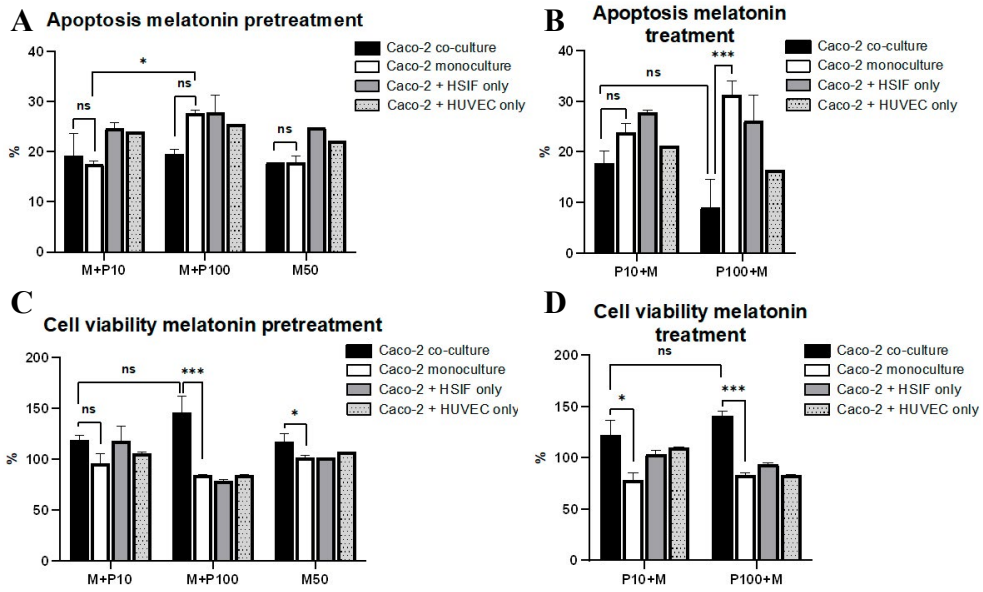

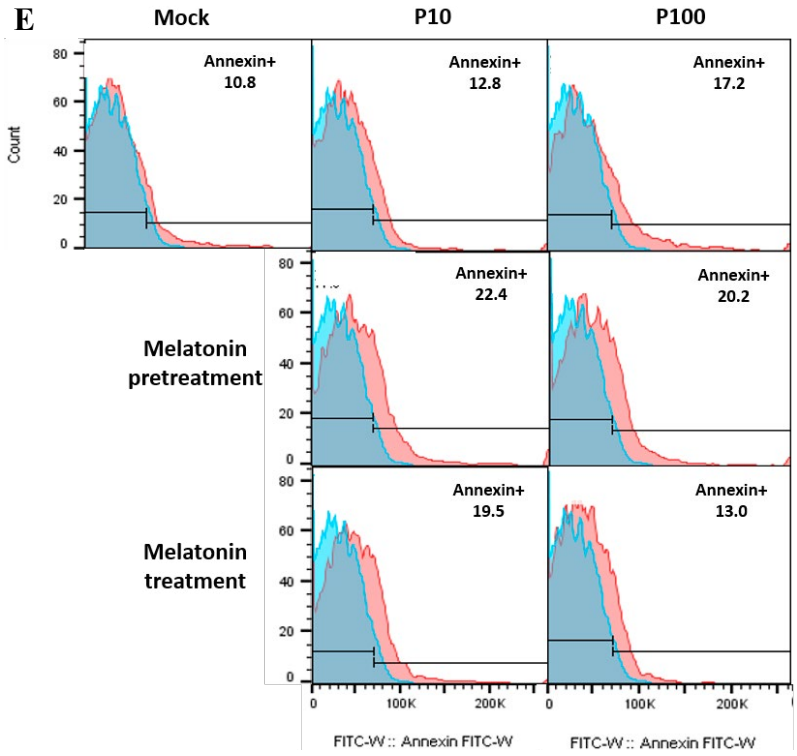

Fig. 3.5.1.1. *Effects of melatonin on apoptosis and viability in mono- and co-culture models stimulated with Poly I:C: (A) apoptosis after melatonin pre-treatment (n = 3); (B) apoptosis after melatonin treatment (n = 3); (C) cell viability after melatonin pretreatment (n = 3); (D) cell viability after melatonin treatment (n = 3), (E) histograms comparing apoptosis in melatonin-naïve, pretreated and treated co-culture (blue histogram shows unstained control, red – annexin positive cells)*

ns indicates $p > 0.05$, * indicates $p < 0.05$, and *** indicates $p < 0.001$. Abbreviations: Poly I:C – polyinosinic polycytidylic acid; P10 – Poly I:C 10 µg/mL; P100 – Poly I:C 100 µg/mL; M – melatonin; M50 – 50 nM melatonin; HSIF – human small intestinal fibroblasts; HUVEC – human umbilical vein endothelial cells.

Adding melatonin after Poly I:C provided stronger protection (Fig. 3.5.1.1 B). In the high-dose setting, apoptosis dropped to 9.1 ± 5.5 % in the triple co-culture versus 31.3 ± 2.7 % in monoculture ($p < 0.001$) (Fig. 3.5.1.1 B, E). Viability likewise increased, surpassing 150 % of mock in the triple co-culture (Fig. 3.5.1.1 D).

Collectively, these results indicate that melatonin shows stronger cytoprotection in co-cultures compared to previous findings in monoculture, and that its efficacy is time-dependent. While pretreatment provides moderate

protection, treatment confers a more robust anti-apoptotic and pro-survival response, likely potentiated by supportive interactions with fibroblasts and endothelial cells.

3.5.2. IFNλ1 and IFNLR1 signalling

To clarify how melatonin modulates the antiviral signalling, we investigated key signalling proteins of the type III IFN axis and organelle activation under both pretreatment and treatment regimens.

When melatonin was applied before Poly I:C stimulation, all culture models retained high IFNλ1 levels (~45 ng/mL) (Fig. 3.5.2.1 A), indicating that melatonin pre-exposure does not suppress, and may even increase IFN release. In contrast, administering melatonin after Poly I:C lowered IFNλ1 expression, particularly in co-cultures (~25–35 ng/mL) (Fig. 3.5.2.1 B), yet levels remained within an antiviral range, suggesting feedback attenuation once protection is established.

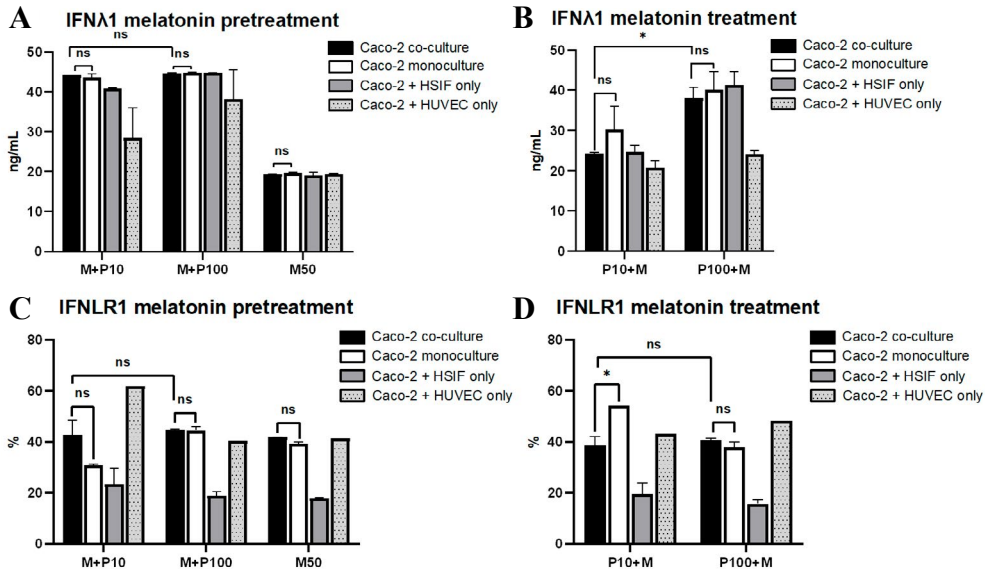

Fig. 3.5.2.1. *Levels of IFNλ1 quantified by ELISA at 24 hours in Poly I:C-stimulated melatonin-pretreated (A) and treated (B) cells (n = 3). Expression IFNLR1 by flow cytometry at 24 hours in Poly I:C-stimulated melatonin-pretreated (C) and treated (D) cells (n = 3)*

ns indicates $p > 0.05$ and * indicates $p < 0.05$. Abbreviations: Poly I:C – polyinosinic polycytidylic acid; P10 – Poly I:C 10 μg/mL; P100 – Poly I:C 100 μg/mL; M – melatonin; M50 – 50 nM melatonin; IFNλ1 – interferon λ1; INFLR1 – interferon λ receptor 1; HSIF – human small intestinal fibroblasts; HUVEC – human umbilical vein endothelial cells.

IFNLR1 expression followed the same pattern (Fig. 3.5.2.1 C, D, Fig. 3.5.2.2). The triple co-culture kept IFNLR1 levels at ~40–45 % under both melatonin regimens, whereas monoculture and the Caco-2 + HSIF model showed stronger downregulation, especially when melatonin was added after low-dose Poly I:C (Fig. 3.5.2.1 C, D). Thus, melatonin helps preserve IFNλ responsiveness, and the multicellular environment is more resistant to receptor loss during immune stress.

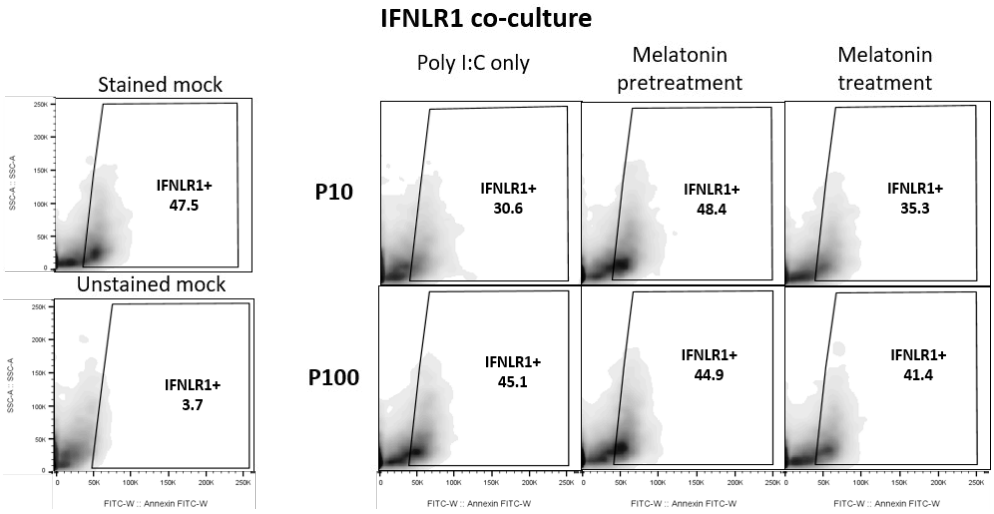

Fig. 3.5.2.2. *Density plots showing the effect of melatonin on the expression of IFNLR1 in co-culture (Caco-2+HSIF+HUVEC) treated with 50 μM melatonin before and after Poly I:C stimulation in comparison to stained and unstained uninfected control*

Abbreviations: Poly I:C – polyinosinic polycytidylic acid; P10 – Poly I:C 10 μg/mL; P100 – Poly I:C 100 μg/mL; INFLR1 – interferon λ receptor 1; HSIF – human small intestinal fibroblasts; HUVEC – human umbilical vein endothelial cells.

3.5.3. Changes in IRF1 and IRF3 signalling

Melatonin altered antiviral transcription-factor (IRF1 and IRF3) profiles in a model-dependent manner. In pretreated triple co-culture, it produced only a slight decline in IRF1, whereas treatment after Poly I:C stimulation markedly downregulated IRF1 (Fig. 3.5.3.1 A, B). This suggests that melatonin can limit excessive IRF1-driven inflammation under stress conditions.

By contrast, IRF3 levels reduced by half in the co-culture in pretreatment conditions, but the effect was even higher when melatonin was used after Poly I:C stimulation, whereas in monoculture melatonin induced an increase in IRF3 levels (Fig. 3.5.3.1 C, D). This data indicate that melatonin preserves

IRF3–IFNλ1 antiviral axis, consistent with its reported role in stabilizing mitochondrial and cytosolic signalling pathways.

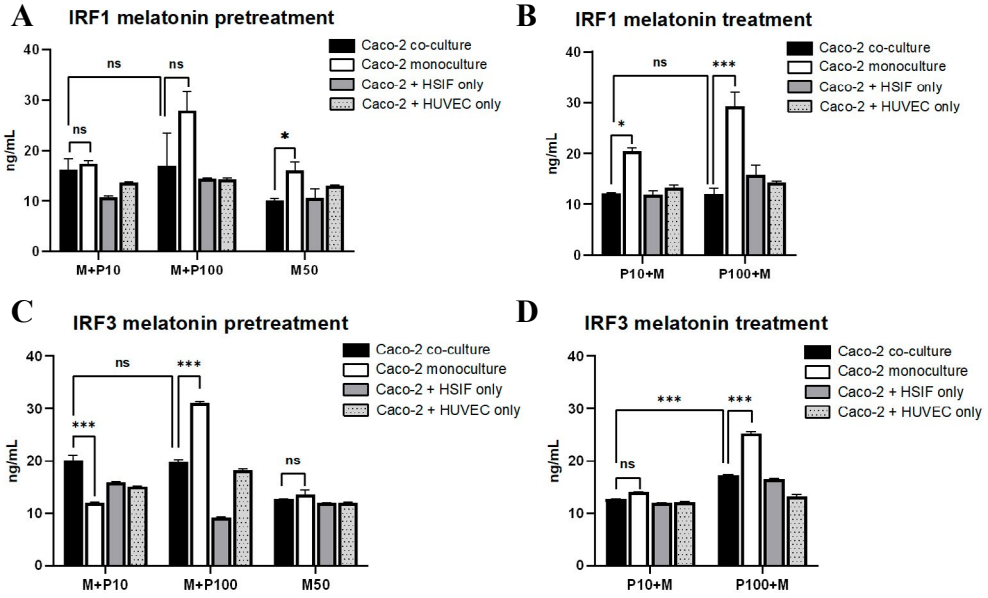

Fig. 3.5.3.1. *IRF levels measured by ELISA 4 hours after Poly I:C in monoculture and co-culture treated with melatonin either before or after stimulation: (A) IRF1 following melatonin pretreatment (n = 3); (B) IRF1 following melatonin treatment (n = 3); (C) IRF3 following melatonin pretreatment (n = 3); (D) IRF3 following melatonin treatment (n = 3)*

Abbreviations: Poly I:C – polyinosinic polycytidylic acid; P10 – Poly I:C 10 μg/mL; P100 – Poly I:C 100 μg/mL; M – melatonin; M50 – 50 nM melatonin; IRF1 – interferon regulatory factor 1; IRF3 – interferon regulatory factor 3; HSIF – human small intestinal fibroblasts; HUVEC – human umbilical vein endothelial cells.

3.5.4. TBK1 and TRIF expression

Melatonin markedly increased TBK1 expression in the triple co-culture model, when it was used after high-dose Poly I:C (71.5 ± 0.96 ng/mL melatonin-treated vs 49.2 ± 0.28 ng/mL in untreated cells), whereas no comparable rise occurred in monoculture or either dual co-culture (Fig. 3.5.4.1 A, B). By contrast, TRIF levels reduced substantially compared to melatonin-untreated co-culture but were relatively stable across the conditions (Fig. 3.5.4.1 C, D), implying that melatonin acts downstream of or independently from TRIF. The data therefore point to post-transcriptional up-regulation of TBK1 or its activation through upstream stress signals, potentially involving peroxisome-mediated pathways discussed below.

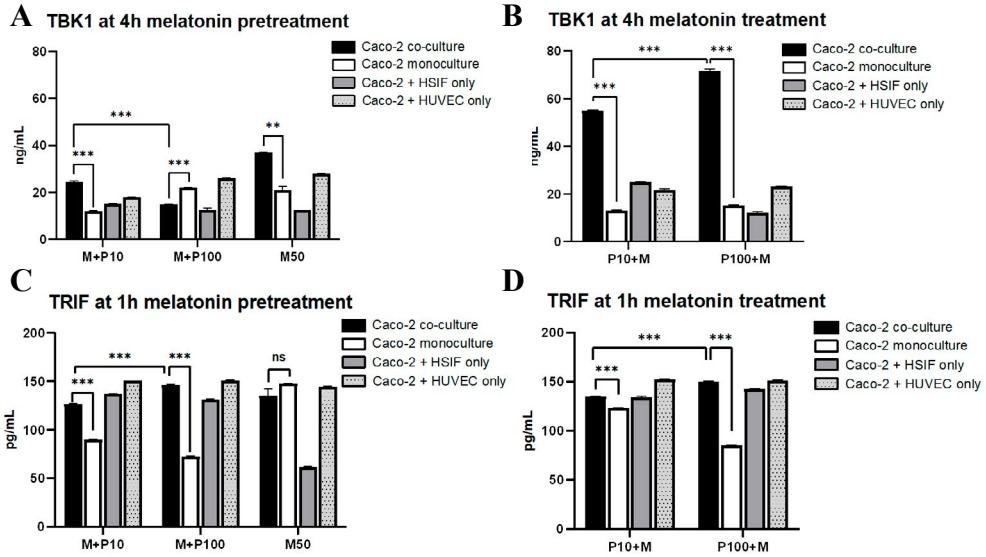

Fig. 3.5.4.1. *TBK1 and TRIF concentrations (ELISA) in co-culture and monoculture models after melatonin application: (A) TBK1 4 hours after Poly I:C in melatonin-pretreated cells (n = 3); (B) TBK1 in melatonin-treated cells 4 hours after Poly I:C (n = 3); (C) TRIF 1 hour after Poly I:C in melatonin-pretreated cells (n = 3); (D) TRIF in melatonin-treated cells 1 hour after Poly I:C (n = 3)*

ns indicates $p > 0.05$, ** indicates $p < 0.01$, and *** indicates $p < 0.001$. Abbreviations: P10 – Poly I:C 10 μg/mL; P100 – Poly I:C 100 μg/mL; M – melatonin; M50 – 50 nM melatonin; TBK1 – TANK-binding kinase 1; TRIF – TIR-domain-containing adapter-inducing IFNβ; HSIF – human small intestinal fibroblasts; HUVEC – human umbilical vein endothelial cells.

3.5.5. Changes in organelle activation

Melatonin reshaped organelle activation in a time- and model-dependent manner (Fig. 3.5.5.1). In Caco-2 monocultures, melatonin further boosted Poly I:C-induced mitochondrial activity, especially at the high dose (Fig. 3.5.5.1 A, B), consistent with the possibility of oxidative stress. In the triple co-culture, however, melatonin dampened or stabilised mitochondrial activation, in line with observed anti-apoptotic effects.

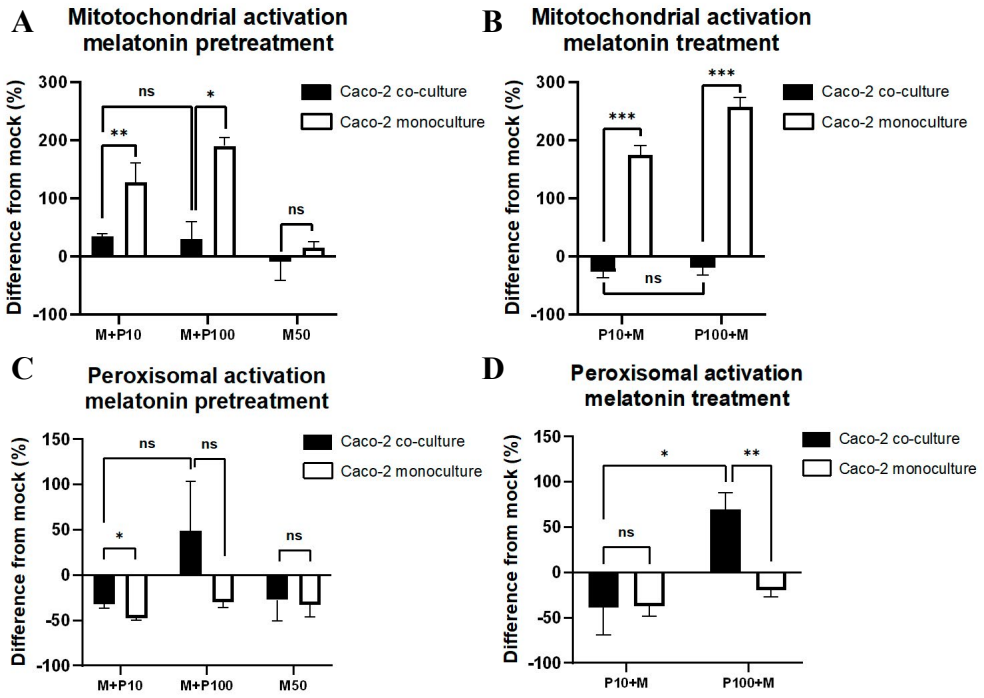

Fig. 3.5.5.1. *Organelle activation in co-culture and monoculture following melatonin application: (A) mitochondrial signal change from mock after melatonin pretreatment in Poly I:C-stimulated cells (n = 3); (B) mitochondrial signal change after melatonin treatment following Poly I:C-stimulation (n = 3); (C) peroxisomal signal change after melatonin pretreatment in Poly I:C-stimulated cells (n = 3); (D) peroxisomal signal change after melatonin treatment following Poly I:C-stimulation (n = 3)*

ns indicates $p > 0.05$, * indicates $p < 0.05$, ** indicates $p < 0.01$, and *** indicates $p < 0.001$. Abbreviations: P10 – Poly I:C 10 μg/mL; P100 – Poly I:C 100 μg/mL; M – melatonin; M50 – 50 nM melatonin; HSIF – human small intestinal fibroblasts; HUVEC – human umbilical vein endothelial cells.

Peroxisomal activity reduced under both pre- and post-treatment regimens, with the largest drop occurring in the co-culture (Fig. 3.5.5.1 C, D). This shift away from peroxisome-centred signalling may reflect the mechanism for melatonin to favour the TBK1–IRF3–IFNλ1 antiviral axis in the co-culture while avoiding the mitochondrial stress pathways that were found to be more prominent in monocultures.

3.5.6. STAT3 activation

While pretreatment boosted STAT3 activation in monoculture (229 ± 0.2 % of mock after high-dose Poly I:C vs 185.3 ± 12.5 % in untreated cells, $p = 0.046$) as also shown previously by flow cytometry, in co-culture STAT3 remained moderate regardless treatment, indicating that melatonin restrains pro-inflammatory STAT3 overactivation in a multicellular setting, resulting in a more balanced antiviral response (Fig. 3.5.6.1).

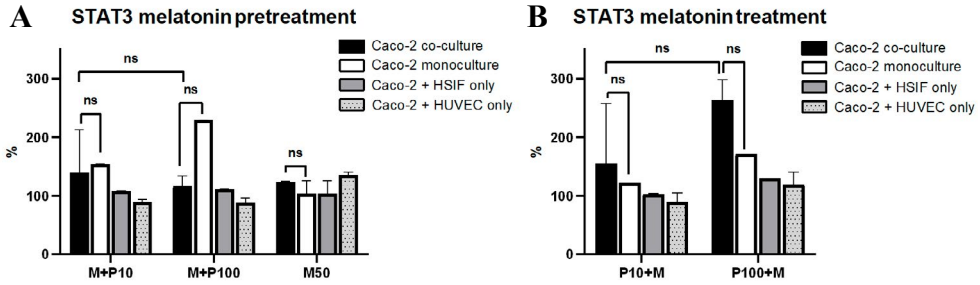

Fig. 3.5.6.1. *STAT3 levels (ELISA) in co-culture and monoculture models: (A) melatonin pretreatment (n = 3); (B) melatonin treatment (n = 3)*

ns indicates $p > 0.05$. Abbreviations: P10 – Poly I:C 10 μg/mL; P100 – Poly I:C 100 μg/mL; M – melatonin; M50 – 50 nM melatonin; STAT3 – signal transducer and transcription activator 3; HSIF – human small intestinal fibroblasts; HUVEC – human umbilical vein endothelial cells.

3.5.7. Modulation of ISG-encoded protein expression

Melatonin modulated the expression of ISG-encoded proteins in the co-culture model, with distinct effects depending on the timing of administration relative to Poly I:C stimulation. Pretreatment with melatonin prior to Poly I:C stimulation led to a downregulation of both MX1 and OAS1 protein levels, suggesting a dampening of the initial antiviral response (Fig. 3.5.7.1 A, B). In contrast, melatonin treatment significantly increased the expression of both ISG products, indicating an amplification of the IFN response once the viral mimic had activated PRR.

These findings align with and reinforce our earlier observations that melatonin, when administered post viral mimicry, enhances a peroxisome-centred, TBK1-driven ISG response, thereby promoting a survival-oriented antiviral state.

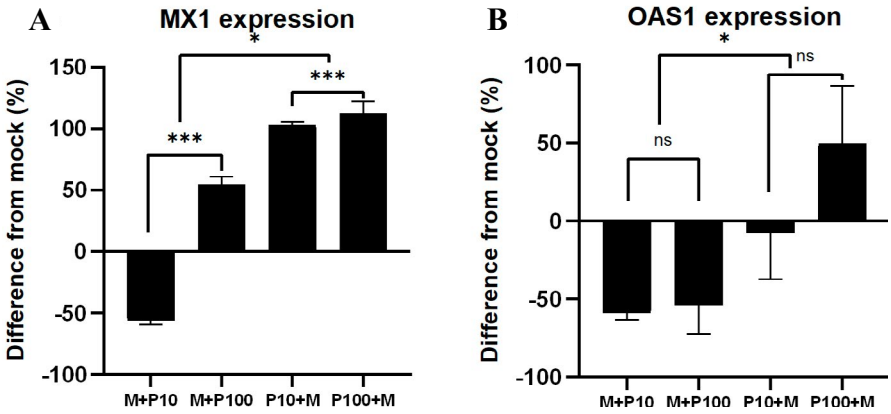

Fig. 3.5.7.1. *The expression of ISG-encoded proteins (MX1 and OAS1) by fluorescent microscopy 24 hours after Poly I:C stimulation in melatonin pretreated or treated co-culture (n = 3)*

ns indicates $p > 0.05$, * indicates $p < 0.05$, and *** indicates $p < 0.001$. Abbreviations: P10 – Poly I:C 10 μg/mL; P100 – Poly I:C 100 μg/mL; M – melatonin 50 μM; M+P10/P100 – melatonin pretreatment before Poly I:C stimulation; P10/P100+M – melatonin treatment after Poly I:C stimulation; MX1 – myxovirus-resistance protein; OAS – 2′-5′-oligoadenylate synthetase 1.

4. DISCUSSION

This study provides novel insights into the antiviral defence mechanisms of intestinal epithelial cells and the modulatory effects of melatonin within a physiologically relevant GI experimental model. Using monoculture and multicellular co-culture models, we demonstrate that Caco-2 epithelial cells preferentially activate type III IFNs in response to viral mimic stimulation, with co-culture systems amplifying and fine-tuning this response via peroxisome-dependent signalling.

4.1. Antiviral response in the experimental models

In this study, we developed two distinct GI models to investigate the response of epithelial cells to viral-mimic inflammation and to assess the modulatory effects of melatonin on these responses. One model involved a Caco-2 monoculture, while the second incorporated fibroblast and endothelial cells to simulate a more physiologically relevant co-culture environment.

Historically, type I IFNs were considered central to antiviral defence. However, the discovery of type III IFNs in 2003 reshaped this view. Type III IFNs were found to have an essential role in protecting various mucosal surfaces, including the gut epithelium [40,46,104–106]. They can provide similar antiviral protection as type I IFNs, but with more localized activity and a reduced risk of pro-inflammatory side effects due to limited induction of ISG. The selective activation of type III IFNs in intestinal mucosa helps to preserve the mucosal barrier by balancing antiviral protection with minimal inflammatory damage, thereby avoiding the systemic side effects commonly associated with type I IFNs [105,107,108].

Although numerous recent studies emphasize the predominance of type III IFNs in GI antiviral responses, the regulatory mechanisms underlying their expression are not yet fully clarified [40]. There is also limited understanding of which subtypes of intestinal epithelial cells primarily produce IFNλ [46]. Animal studies have proposed that in some cases, IFNλ may be secreted by infection-nonsusceptible enterocytes [109]. In contrast, our results provide evidence that fully differentiated human Caco-2 cells can independently produce IFNλ1 in response to TLR3 activation, supporting their active role in mounting mucosal antiviral defence.

Our findings support the growing consensus that intestinal epithelial cells preferentially produce type III IFNs during viral mimic stimulation [47,106]. In our study, Caco-2 cells in monoculture secreted IFNλ1 in response to TLR3 activation by Poly I:C, whereas type I IFNs (IFNα and IFNβ) were undetectable. These results are in line with other studies reporting dominant

IFNλ responses in enterocytes in response to viral infection [11,47,110]. For example, Lin et al. have found very low expression of type I IFNs with predominant type III IFNs in enteroids after norovirus infection and Poly I:C treatment [110]. On the other hand, some studies, such as those by Frias et al. [111], have found IFNβ production under various viral conditions. The discrepancies may be attributable to differences in infection models, cell types, or timing used across studies. For instance, Pervolaraki et al. found that even though viral infection of GI organoids induced strong upregulation of both type I and type III IFNs, only type III IFN secretion was found in the supernatant of the infected organoids [42]. This suggests that I IFN may be retained intracellularly or act in an autocrine fashion, which could explain why I IFN production was not detected in our study as we evaluated only supernatants, potentially missing intracellular cytokine expression.

To better replicate epithelial-stromal interactions *in vivo*, we established a co-culture system including fibroblasts (HSIF) and endothelial cells (HUVECs). Previous studies have demonstrated that direct contact with mesenchymal cells might improve Caco-2 cell epithelial barrier integrity [10]. Our findings extend this by showing that stromal support in co-cultures also promotes epithelial viability and confers resistance against Poly I:C-induced cytotoxicity as well as enhances antiviral responses.

Compared to monocultures, co-cultures maintained higher cell viability and markedly lower apoptotic rates even under high-dose viral-mimic stimulation, highlighting the protective effects of stromal support. These observations align with growing evidence that stromal cells influence epithelial resilience and shape immune responses through both paracrine (via growth factors or cytokines), direct cell-to-cell interactions, and enhanced cellular polarization [10,112–114].

One of the key immunological advantages of the co-culture model was the more robust and rapid induction of IFNλ1, along with sustained expression of its receptor IFNLR1. This pattern suggests an optimized and prolonged antiviral capacity. Meanwhile, IFNα remained undetectable and IFNβ was modestly upregulated, reinforcing the idea of a compartmentalized IFN response in mucosal tissues, favouring type III IFNs [40,104,105,115].

We observed a distinct regulatory pattern of antiviral responses between models at the transcriptional level. Co-cultures exhibited rapid upregulation of IRF3 and TBK1, correlating with IFNλ1 expression. In contrast, IRF1 which is often associated with more inflammatory signalling was more strongly induced in monoculture. This suggests that stromal cells shift epithelial antiviral responses toward a more controlled, IRF3-driven pathway.

Although IRF1 is necessary for ISG expression and can enhance IRF3 activation [52,107], studies show that it is also largely driven by type I IFNs

[108], which were limited in our model. Thus, reduced IRF1 in co-culture may reflect low presence of type I IFNs or intentional downregulation toward less inflammatory antiviral strategies. Several mechanisms may underlie the preferential induction of type III IFNs in intestinal epithelial cells, including high IFNLR1 expression, mucosal-specific co-factors, and MAVS activation in peroxisomes [104,105].

Recent literature highlights peroxisomes as important platforms to regulate innate antiviral responses and type III IFN production in the GI epithelial cells [52,53,107]. Odendall et al. [107] demonstrated that an increased number of peroxisomes due to intestinal epithelial cell differentiation can boost type III IFN production without affecting type I IFN response. Although we did not quantify peroxisome numbers, we observed increased peroxisomal activation (as indicated via PEX1 immunostaining) in co-cultures after Poly I:C stimulation. This activation strongly correlated with IRF3 and TBK1 levels, supporting the hypothesis that peroxisomes played a leading role in antiviral signalling in our model.

Furthermore, while IRF3 can also be activated in mitochondria, peroxisomal MAVS is known to trigger faster IFN responses than its mitochondrial counterpart [52]. Our findings that IFNλ1 is induced earlier in co-cultures support this concept. Notably, a less pronounced effect observed in dual co-cultures suggests that the enhanced peroxisomal role observed in co-cultured cells cannot be attributed solely to epithelial differentiation. Rather, synergistic interactions among multiple stromal cell types are likely required to ensure robust peroxisomal activation.

TBK1 levels were both higher at baseline and more sustained after Poly I:C stimulation in the co-culture. This suggests a “primed” antiviral state, likely driven by stromal-epithelial interactions. Its strong correlation with peroxisomal activation further supports the preferential MAVS–TBK1 signalling via peroxisomes over mitochondria in this setting. Peroxisomal signalling is known to activate robust yet less inflammatory antiviral responses, making it well suited to protect the epithelial barrier [52]. Although TBK1 is known to act downstream of MAVS in both organelles [52], its functional link to peroxisomal activation, to our knowledge, has not been directly characterized, highlighting a novel aspect of mucosal antiviral regulation. However, despite the observed shift toward peroxisome-dominant antiviral signaling in co-cultures, we evaluated organelle activity by immunofluorescence microscopy only and did not confirm the compartment-specific MAVS activation. Thus, additional studies are required to determine whether these effects are indeed driven by MAVS signalling.

MX1 expression rose markedly after Poly I:C stimulation, confirming robust activation of the innate antiviral programme in our model. Notably,

MX1 levels correlated strongly with peroxisomal activation rather than with IFNλ1, in line with earlier reports that peroxisome-associated MAVS can drive ISG induction independently of canonical IFN signaling [52]. These data reinforce the pivotal role of peroxisome-mediated pathways in mucosal antiviral defence.

Overall, our study reinforces the critical role of type III IFNs in gut epithelial antiviral defence and highlights the importance of epithelial–stromal interactions in modulating immune responses. The co-culture model not only better mimics physiological conditions but also promotes protective, organelle-specific antiviral pathways involving peroxisomes and TBK1–IRF3 signalling, resulting in antiviral ISGs production.

4.2. Antiviral effect of melatonin

Melatonin, a pleiotropic indoleamine produced not only by the pineal gland but also by extra-pineal tissues such as the GI tract, possesses well-documented antioxidant, anti-inflammatory, and immunomodulatory properties [76,79,83,95,102,116]. Although it has been widely studied in the context of various viral infections [13,77,81,85–87], research specifically addressing its role in GI viral pathologies remains limited. For instance, Xi-Zhang et al. [82] demonstrated that melatonin reduces the inflammation in intestinal organoids caused by bacterial pathogens by downregulating the expression of inflammatory cytokines, such as NFκB, IL-6, and IL-8. Building on this foundation, our study explored melatonin's antiviral effects with a focus on IFN signalling – a key pathway in antiviral immunity.

First, we explored the antiviral effect of melatonin in a Caco-2 cell monoculture. In these experiments, melatonin exhibited time-dependent effects. Pretreatment (prophylactic application) at low concentrations enhanced cell viability and reduced apoptosis. In contrast, treatment following Poly I:C stimulation (mimicking viral infection) preserved organoid size, cellular morphology, upregulated IFNLR1 expression, and attenuated inflammation by suppressing IFNλ1 and STAT1–3 production, suggesting a protective and immunomodulatory role.

Fibroblasts and endothelial cells enhanced Caco-2 cell responsiveness to melatonin by modulating both IFNλ1 and IFNLR1 expression, underscoring the importance of multicellular models when investigating complex antiviral responses. These findings reinforce the notion that stromal–epithelial interactions are crucial for understanding melatonin's full immunomodulatory potential in the gut.

Despite growing interest in melatonin as an antiviral agent, its specific effects on type III IFNs remain poorly defined. Our data revealed that melatonin

reduced IFNλ1 levels when applied after TLR3 stimulation, potentially linked to IFNλ1's known role in limiting cell proliferation via IFNLR1 activation [117]. While we couldn't confirm a direct causal relationship, the suppression of IFNλ1 expression alongside increased IFNLR1 suggests a complex regulatory feedback loop. Interestingly, pretreatment enhanced cell viability without significantly altering IFNλ1 levels, suggesting possible involvement of alternative regulatory pathways. Notably, an inverse correlation between IFNλ1 and IFNLR1 was observed in pretreated cells – a pattern not replicated in cells treated after the Poly I:C stimulation – suggesting differential pathway activation depending on treatment timing.

Previous studies have concluded that IFNλ1-mediated inhibition of cell proliferation is largely mediated through IFNLR1 activation and downstream JAK/STAT signalling [117,118]. However, the molecular mechanisms underlying this pathway remain incompletely understood. In our study, we found that melatonin alone could induce STAT2 and STAT3 expression, even in the absence of viral mimicry, despite lower IFNLR1 levels. In melatonin-pretreated, Poly I:C-stimulated cells, we observed a positive correlation between IFNLR1 and STAT1–3 expression, consistent with earlier studies [117]. However, an inverse but statistically insignificant association was observed in the post-stimulation-treated cells.

Several studies have reported that melatonin regulates STAT1 and STAT3 in other systems. In murine macrophages, it suppressed STAT1 via nitric oxide and IL-6 inhibition during LPS-induced inflammation [119]. In neuroinflammation models, melatonin pretreatment downregulated STAT1 and increased STAT3 phosphorylation in microglia [120]. It was also shown to inhibit STAT3 phosphorylation in diabetic kidney injury, reducing apoptosis and senescence [121]. While evidence on melatonin's modulation of STAT proteins in the gut is scarce, our results highlight its notable effect on STAT2, which strongly correlated with IFNλ1 in monocultures. STAT2 might play a key role in antiviral response to certain viruses and may, independently from other STAT proteins, promote ISGs production [122]. Since STAT3 plays dual roles in inflammation and epithelial proliferation [123], its overactivation may lead to dysregulated immune responses in monoculture. STAT3 signalling was better balanced in co-cultures, highlighting the influence of the multicellular microenvironment.

Melatonin significantly enhanced protective effects conferred by fibroblast and endothelial cell interactions in co-culture, reinforcing its value as a mucosal immunomodulator. Importantly, melatonin's cytoprotective action did not compromise antiviral signalling. On the contrary, pretreatment maintained high levels of IFNλ1 and IFNLR1 expression, especially in co-cultures, supporting its role in enhancing mucosal antiviral immunity without driving

excessive inflammation. Melatonin administration in co-culture, particularly after Poly I:C stimulation, markedly reduced apoptosis and preserved cell viability.

We also observed melatonin-driven modulation of key transcription factors – IRF3 and IRF1 – expression. IRF3 was upregulated (especially in co-culture), supporting IFNλ1 signalling, whereas IRF1, which is often associated with high inflammatory response and tissue damage [108], expression was suppressed which likely contributes to the controlled antiviral response observed during the experiments.

A novel finding from our study was the observed shift in innate immune signalling in co-culture: melatonin supported redirection of signalling from mitochondria to peroxisomes. Whereas monocultures showed sharp mitochondrial activation (and likely oxidative stress) following Poly I:C stimulation and melatonin treatment, co-cultures maintained mitochondrial stability and engaged reduced but efficient peroxisomal activity. Given the emerging recognition of peroxisomes as low-inflammation antiviral platforms [52,107], this switch may underlie the observed decrease in apoptosis and inflammation in melatonin-treated co-cultures.

This peroxisome-associated response converged on TBK1, whose expression was enhanced following melatonin treatment in co-cultures, while TRIF remained largely unchanged. This implies that melatonin may modulate TBK1 post-transcriptionally or enhance MAVS-peroxisome signalling, resulting in robust IRF3-mediated IFNλ1 production with minimized inflammatory cost. These findings suggest a previously underexplored mechanism by which melatonin can modulate antiviral immunity at the subcellular level, particularly relevant for gut epithelial defence, though further validation using functional inhibition strategies (e.g., TBK1 or IRF3 silencing) would be necessary to confirm causality.

We did not observe significant changes in IFNλ1 or IFNLR1 expression across different melatonin concentrations, but distinct dynamics of cytokines were evident between pretreated and treated cells. Prior work by Winkle et al. [46] suggested a prophylactic role for IFNλ signalling in rotaviral infections, showing that IFNLR1 limits viral evasion of intestinal epithelial cells. This aligns with our finding of higher IFNLR1 expression in melatonin-treated vs. pretreated cells.

We also found that melatonin treatment upregulated the ISG-encoded proteins MX1 and OAS1. To our knowledge, no prior study has reported a direct effect of melatonin on these two effectors. Nevertheless, work in dengue-infected models and COVID-19 shows that melatonin can boost the innate response by broad induction of ISGs, thereby helping to control viral replication [124,125]. This suggests that melatonin may broaden the

IFN-driven antiviral response in intestinal epithelium, making it a promising adjunct for enhancing mucosal antiviral immunity.

Despite melatonin's favourable safety profile even at high doses, its long-term effects remain under investigation [91,126]. Data from animal studies suggest that it might adversely impact fertility [127]. Additionally, optimal dosing and timing for viral infection remains to be elucidated. Maestroni et al. hypothesized [81] that higher doses of melatonin may be required for prophylactic use to stimulate the innate immune response, while lower doses post-infection may be sufficient to reinforce adaptive immunity [81]. In our experiments, we used different melatonin concentrations at varying time points and found that both concentration and timing are critical: lower concentrations applied before Poly I:C stimulation could reduce cell viability, while higher doses or post-infection applications yielded more protective effects. These findings are consistent with reports indicating that low doses promote epithelial regeneration while high doses (e.g. 4 mM) may induce toxicity [99,128,129]. Studies using cancer cells found melatonin to be cytotoxic in a dose-dependent manner when applied at ≥ 4 mM [128,129], though this may not directly translate to healthy epithelial cells. Hence, careful dose optimization is crucial to avoid unintended cytotoxicity and maximize therapeutic benefits and should be targeted in future preclinical and clinical studies before clinical applications.

Moreover, the timing of melatonin administration warrants careful consideration. Early application, which is associated with reduced antiviral protein expression, may inadvertently exacerbate viral inflammation or induce cellular apoptosis. These findings underscore the importance of delineating the precise therapeutic window for melatonin treatment, where its immunomodulatory benefits are maximized without triggering detrimental side effects. This highlights the need for detailed pharmacokinetic and pharmacodynamic studies to guide its clinical use.

The GI tract serves both as a major viral entry point and a primary site of local melatonin synthesis via enterochromaffin cells [130]. This raises intriguing physiological implications: melatonin may naturally function as a local regulator of mucosal immunity, especially under stress or infection. Notably, melatonin levels decline with aging and chronic illness [131], which may compromise epithelial defence. Our results suggest that melatonin supplementation could restore mucosal resilience, particularly in vulnerable populations facing enteric viral threats.

Its low cost, broad biological activity, and favourable safety profile have prompted interest in melatonin's repurposing for respiratory and GI viral infections [14,77,81,91]. Our findings extend this concept, suggesting its utility as an adjunct therapy in managing viral intestinal diseases, particularly

when paired with strategies that preserve or mimic multicellular mucosal architecture.

The study has several limitations. Firstly, the use of Caco-2 cells, which are of adenocarcinoma origin, might not fully represent signalling pathways healthy intestinal epithelium. Secondly, because of biosafety limitations we used Poly I:C to simulate viral inflammation instead of live virus, which may have not fully reflected host-pathogen interactions *in vivo*. Additionally, while we observed key roles of stromal cells and peroxisomal signalling, *in vivo* immune cell interactions (e.g. macrophages or lymphocytes) were not replicated. Also, we evaluated only a subset of the type III IFN pathway; additional ISGs and downstream mediators remain to be studied. Finally, while our findings suggest peroxisomal signalling as one of key immune response modulators, its activation was measured using immunofluorescence only, which may not fully reflect the extent or kinetics of antiviral signalling. Future studies should incorporate complementary methods (e.g., gene expression, live-cell imaging, or functional assays) to verify these mechanisms and clarify how melatonin regulates subcellular antiviral pathways.

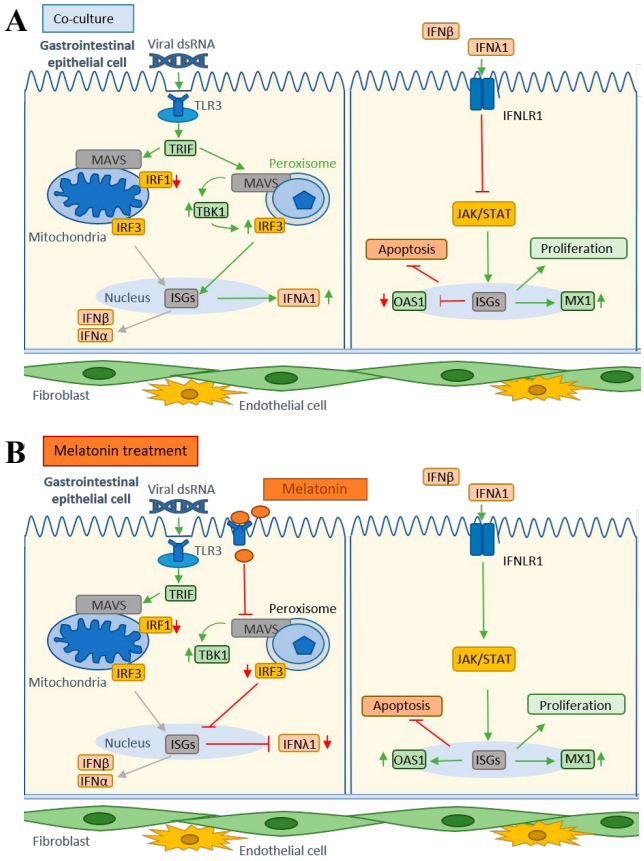

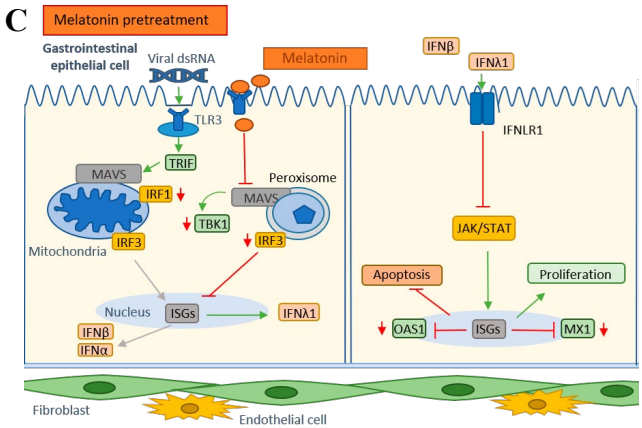

Fig. 4.2.1. *Schematic summary of the study results. (a) Caco-2 cells cultured with HSIF and HUVEC, compared to monoculture, demonstrated enhanced peroxisomal activation, higher TBK1 expression, and stronger and more rapid IRF3 response which resulted in reduced apoptosis. (b) Melatonin treatment in the co-culture modulated organelle-specific antiviral signalling by suppressing peroxisomal activation and promoting mitochondrial activity, which resulted in reduced TBK1, IRF1 and IFNλ1 levels, as well as further reduction of apoptosis. (c) Melatonin pretreatment in the co-culture model reduced apoptosis and preserved cell viability with modest effect to type III IFN axis signalling*

Abbreviations: dsRNA – double-stranded RNA; IFN – interferon; IFNLR1– interferon-λ receptor 1; IRF1 – interferon regulatory factor 1; IRF3 – interferon regulatory factor 3; ISGs – interferon-stimulated genes; MAVS – mitochondrial antiviral signalling protein; JAK/STAT – Janus kinase / signal transducer and activator of transcription pathway; TBK1 – TANK-binding kinase 1; TLR3 – Toll-like receptor 3; TRIF – TIR-domain-containing adapter-inducing IFNβ; MX1 – myxovirus-resistance protein 1; OAS – 2′-5′-oligoadenylate synthetase.

CONCLUSIONS

1. Two experimental GI models were established for antiviral response analysis: monoculture organoid model and co-culture model, consisting of GI epithelial cells, fibroblasts and endothelial cells. The suitability of the models for antiviral studies was confirmed by Poly I:C induced dose-dependent apoptosis. Fibroblasts and endothelial cells in co-culture promoted epithelial cell growth, viability and resistance to virus mimic-induced cytotoxicity.
2. In GI epithelial cells, Poly I:C provoked a robust, dose-dependent type III IFN response: increased IFNλ1 and upregulated IFNLR1 and STAT1–3 were detected, whereas type I IFN expression remained minimal. In co-cultures, the antiviral response was shown to be promoted via the peroxisome–TBK1–IRF3–IFNλ1 axis, resulting in MX1 activation.
3. Co-cultures exhibited faster and higher expression of transcription factors (IRF3, TBK1, and TRIF) compared to monoculture, while IRF1 expression was reduced. Interaction with fibroblasts and endothelial cells induced a strong, dose-dependent increase in peroxisomal activity in epithelial cells, whereas in monoculture mitochondrial involvement was more prominent.
4. Melatonin modulated TBK1–IRF3–type III IFN axis in GI epithelial cells with varying effects depending on the timing of administration. Treatment with melatonin after viral-mimic stimulation, dampened cytokine release and prevented apoptosis, whereas pretreatment prevented apoptosis but maintained cytokine output. Protective effects were stronger in co-culture and involved suppression of peroxisomal activity while favouring mitochondrial signalling, suggesting a potentially organelle-dependent mechanism of action.

FUTURE DIRECTIONS

1. While chronic GI diseases are extensively studied, experimental models for viral GI infections remain limited. Our findings suggest that although monoculture organoids can provide valuable insights into epithelial responses, the absence of signalling from stromal or immune cells limits their ability to fully reflect host antiviral responses. Co-culture systems using transwells with fibroblasts and endothelial cells showed enhanced responses to viral-mimic stimulation and represent a promising, accessible alternative compared to more complex and costly systems, such as gut-on-chip, to study viral GI infections in the future. Further improvement of this model through the inclusion of circulatory immune cells (e.g., macrophages or dendritic cells), would help to increase the physiological relevance.
2. Our research, supported by recent studies, highlights the essential role of peroxisomes in regulating antiviral responses. This emerging field of research requires further mechanistic investigations to elucidate how peroxisomes contribute to immune signalling, particularly in GI epithelial cells. A better understanding of peroxisome-driven immunity may reveal novel therapeutic targets for managing viral GI infections in the future.
3. Melatonin demonstrated potential antiviral and barrier-protective effects in our *in vitro* GI models, supporting its possible therapeutic application in viral GI diseases. Although we identified potential mechanisms of action, they remain incompletely understood. Given the limitations of *in vitro* systems used, our findings cannot be directly translated into recommendations to use it in clinical practice. Further *in vivo* studies are needed to determine optimal dosing and timing before considering melatonin administration for the treatment of GI infections.

SANTRAUKA

ĮVADAS

Virusinės žarnyno infekcijos yra viena iš svarbiausių visuomenės sveikatos problemų, sukelianti didelį sergamumą ir mirštamumą – ypač mažų vaikų bei senjorų tarpe [1,21]. Tai taip yra viena dažniausių apsilankymų pas gydytoją priežasčių [25]. Šiuo metu šių infekcijų gydymas yra tik simptominis (pvz., rehidracija, antipiretiniai vaistai ir pan.) [20–22,27], o universalių, plataus spektro antivirusinių medžiagų vis dar nėra [1].

Žmogaus virškinamojo trakto (VT) epitelis atlieka svarbią funkciją ne tik kaip maistinių medžiagų pasisavinimo vieta, bet ir kaip vienas iš svarbiausių organizmo gynybinių barjerų nuo įvairių patogenų, įskaitant virusus [3,4]. Patekę į žarnyną, virusai atpažįstami ant epitelio ląstelių esančių specialių receptorių, tokių kaip Toll tipo receptorius 3 (TLR3), kurie aktyvuoja įgimtą imuninį atsaką per transkripcijos faktorius, pavyzdžiui, interferonų reguliacinius faktorius IRF3 ir IRF1 [2,3]. Šie signalai skatina I ir III tipo interferonų gamybą, kurie aktyvuoja Janus kinazių ir signalo perdavimo bei transkripcijos aktyvavimo veiksnių (JAK/STAT) signalinę grandinę, inicijuodami pirminį antivirusinį atsaką [2,5]. Šiame procese itin svarbų vaidmenį vaidina TANK surišanti kinazė-1 (TBK1), fosforilinanti IRF3 ir galinti būti aktyvuojama mitochondrijose ar peroksisomose [55]. Visgi šių signalinių procesų dinamika žarnyno epitelyje kol kas nėra iki galo aiški [45]. Tą iš dalies lemia eksperimentinių modelių trūkumas.

Pastaraisiais metais VT ligų tyrimus iš esmės pakeitė organoidų modeliai, kurie suteikia unikalią galimybę tirti audinių sąveikas į fiziologines panašiose sąlygose, nenaudojant eksperimentinių gyvūnų [7,8]. Diferencijuotos epitelio ląstelės gali išlaikyti pagrindines absorbcines ir sekrecines savybes, būdingas plonajai žarnai [9]. Organoidai, atkartodami *in vivo* struktūrą ir funkcijas, leidžia tiksliau modeliuoti žmogaus VT infekcijas ir tampa vertingu įrankiu siekiant analizuoti infekcijų patogenezę, signalinius kelius ir galimų terapinių medžiagų poveikį [7,8].

Be to, epitelio imuninis atsakas stipriai priklauso nuo aplinkinių stromos ląstelių, tokių kaip fibroblastai ir endotelio ląstelės. Jų įtraukimas į kokultūrų modelius pastaraisiais metais padėjo sukurti dar fiziologiškesnes sistemas, leidžiančias tirti tarpląstelinę sąveiką ir šeimininko-patogeno ryšius [10]. Fibroblastai ir endotelio ląstelės palaiko žarnyno audinių homeostazę ir moduliuoja antivirusinį atsaką, todėl jų naudojimas žarnyno infekcijų modeliuose ypač svarbus [10,11], bet kol kas mažai tyrinėtas.

Melatoninas – natūralus hormonas, geriausiai žinomas dėl savo cirkadinių ritmų reguliavimo ir taikymo miego sutrikimų gydymui [12], – pastaruoju

metu sulaukia vis daugiau dėmesio dėl savo platesnio terapinio potencialo, įskaitant ir antivirusinį poveikį [13,14]. Tyrimai rodo, kad melatoninas gali moduliuoti imuninį atsaką ir stiprinti apsauginius ląstelės mechanizmus [15], galimai veikdamas mitochondrijų signalinius kelius, susijusius su antivirusiniu atsaku. Visgi jo poveikis žarnyno infekcijų atveju dar nėra pakankamai ištirtas.

Šiame darbe sukurti pažangūs VT organoidų ir kokultūrų modeliai, siekiant ištirti antivirusinius signalinius kelius žarnyno epitelio ląstelėse, palyginti antivirusinį atsaką monokultūroje ir kokultūroje, bei įvertinti melatonino – kaip terapinės ar profilaktinės medžiagos – poveikį šiems procesams.

DARBO TIKSLAS IR UŽDAVINIAI

Darbo tikslas – ištirti žarnyno epitelio antivirusinį atsaką eksperimentiniuose žarnyno modeliuose ir įvertinti melatonino poveikį jo moduliacijai.

Uždaviniai:

1. Sukurti eksperimentinius žarnyno epitelio modelius antivirusinio atsako tyrimui.
2. Ištirti imuniniame enterocitų atsake į virusinę infekciją dalyvaujančius signalinius baltymus bei organeles, jų ekspresijos dinamiką bei tarpusavio sąsajas.
3. Palyginti antivirusiniame atsake dalyvaujančių baltymų bei organelių dinamiką sukurtuose VT modeliuose.
4. Įvertinti melatonino poveikį virusų sukeltai enterocitų pažaidai, antivirusinio atsako moduliacijai ir ląstelių regeneracijai sukurtuose VT modeliuose.

MOKSLINIS DARBO NAUJUMAS IR AKTUALUMAS

Virusinės žarnyno infekcijos išlieka reikšminga visuomenės sveikatos problema, sąlygojanti didelį sergamumą ir mirtingumą visame pasaulyje, tačiau jų patogenezė, ypač VT gleivinės lygmenyje, vis dar nėra iki galo aiški. Šiame tyrime analizuotas žarnyno gleivinės imuninis atsakas, pasitelkiant pažangius *in vitro* epitelio organoidų bei sudėtinį – epitelio, fibroblastų ir endotelio ląsteles apjungiantį – kokultūrų modelį.

Tyrimas atskleidė ypatingą III tipo interferonų vaidmenį žarnyno epitelio imuniniame atsake į virusinę infekciją ir stromos ląstelių įtaką gleivinės imuninei funkcijai. Nustatyta, kad stromos komponentai keičia įvairių signalinių baltymų išskyrimo dinamiką ir jų integracija į infekcinius žarnyno modelius ateityje yra itin svarbi.

Šiame darbe taip pat įvertintas melatonino, kaip galimos terapinės medžiagos, gebėjimas reguliuoti antivirusinį atsaką, mažinti infekcijos sukeltą pažeidimą ir skatinti epitelio regeneraciją. Šie duomenys yra svarbūs, nes apie melatonino poveikį žarnyne kol kas žinoma nedaug. Be to, tyrimo metu nustatyti galimi melatonino veikimo mechanizmai, susiję su mitochondrijų ir peroksisomų signaliniais keliais.

Apibendrinant, tyrimo rezultatai praplečia žinias apie antivirusinį atsaką žarnyne ir gali būti reikšmingi tiek kuriant naujas gydymo strategijas ar vakcinas, tiek taikomi ir kitose biomedicinos srityse.

TYRIMO METODIKA

Didžioji dalis eksperimentų buvo atlikti Lietuvos sveikatos mokslų universiteto (LSMU) Farmakologijos ir fiziologijos institute. Kadangi naudotos komercinės ląstelių linijos, etikos leidimas tyrimui nebuvo reikalingas.

Ląstelių priežiūra

Eksperimentiniam virškinamojo trakto modeliui sukurti naudotos trys komercinės žmogaus ląstelių linijos:

- Žarnyno epitelio ląstelės (**Caco-2**, HTB-37, ATCC, JK),
- Žmogaus plonosios žarnos fibroblastai (**HSIF**, P10760, Innovative Technologies and Biological Systems, S.L., Ispanija),
- Žmogaus virkštelės venos endotelio ląstelės (**HUVEC**, C0035C, Thermo Fisher Scientific, JAV).

Visos ląstelės buvo kultivuojamos 150 cm^2 audinių kultūrų flakonuose 37 °C temperatūroje drėkinamame inkubatoriuje su 5 proc. CO_2. Kiekviena ląstelių linija auginta atitinkamoje augimo terpėje (1 lentelė), kuri buvo keičiama kas 2–3 dienas. Ląstelėms pasiekus 70–80 proc. suaugimą, jos buvo persėjamos naudojant TrypLE™ Express fermentą. Prieš persėjimą ląstelės buvo suskaičiuojamos naudojant 0,4 proc. tripano mėlio tirpalą ir hemocitometrą. Visi eksperimentai atlikti su 7–25 pasažų ląstelėmis.

1 lentelė. *Eksperimentiniuose modeliuose naudotų skirtingų ląstelių tipų auginimo terpės sudėtis*

Ląstelių tipas	**Augimo terpės sudėtis**
Caco-2	MEM + 10 proc. FBS + 1 proc. NEAA + 1 proc. P/S
HSIF	DMEM + 10 proc. FBS + 1 proc. P/S
HUVEC	HLVEC bazinė medija + 10 proc. FBS + 1 proc. P/S + LSGS

Santrumpos: DMEM – Dulbecco modifikuota Eagle terpė; FBS – galvijų vaisiaus serumas; HLVEC – didžiųjų kraujagyslių endotelio terpė; LSGS – mažo serumo augimo papildas; MEM – minimalioji esminė terpė; NEAA – neesminės aminorūgštys; P/S – penicilinas/streptomicinas.

Virškinamojo trakto modelio kūrimas

Caco-2 monokultūra ant plastikinio paviršiaus

In vitro modeliui naudotos iš žmogaus storosios žarnos adenokarcinomos išgautos Caco-2 ląstelės, laikomos auksiniu standartu žarnyno modeliuose. Caco-2 ląstelės buvo išsėtos po 10 000 ląstelių šulinėliui tankiu į 96 šulinėlių plokšteles ir kultivuojamos 21 dieną, leidžiant joms diferencijuotis į enterocitus ir formuoti organoidus.

Kokultūra

Siekiant geriau atkartoti *in vivo* sąlygas, žarnyno epitelio ląstelių modelis buvo papildytas fibroblastais (HSIF) ir endotelio ląstelėmis (HUVEC). Pirmiausia, HSIF ir HUVEC buvo sumaišytos santykiu 3:1 ir išsėtos po 30 000 ląst./šulinėlyje, naudojant 1:1 abiejų ląstelių augimo terpės mišinį. Tuomet Caco-2 ląstelės (po 10 000 ląst.) buvo išsėtos ant 0,4 µm porų kultūros intarpų (angl. *transwell*). Šios kultūros auginimo laikotarpis sutrumpintas iki 14 dienų, kadangi auginimas 21 dieną lėmė organoidų suirimą. Palyginimui tomis pačiomis sąlygomis intarpuose auginta Caco-2 monokultūra ir Caco-2 kokultūros tik su fibroblastais arba endotelio ląstelėmis.

Kultūrų užkrėtimas Poly I:C

Virusinei infekcijai imituoti modeliuose naudota Poly I:C (poliinozino-policitidilo rūgštis) – sintetinis dvigrandės ribonukleino rūgšties (RNR) analogas ir TLR3 receptoriaus agonistas. Monokultūrose, praėjus 21 d. nuo jų išsėjimo, Caco-2 ląstelės buvo 24 val. stimuliuotos 1, 10 ir 50 µg/ml Poly I:C. Kokultūros stimuliuotos praėjus 14 dienų nuo išsėjimo tik 10 ir 100 µg/ml Poly I:C, uždedant jį 24 val. tik ant Caco-2 ląstelių, esančių inserte (1 pav.).

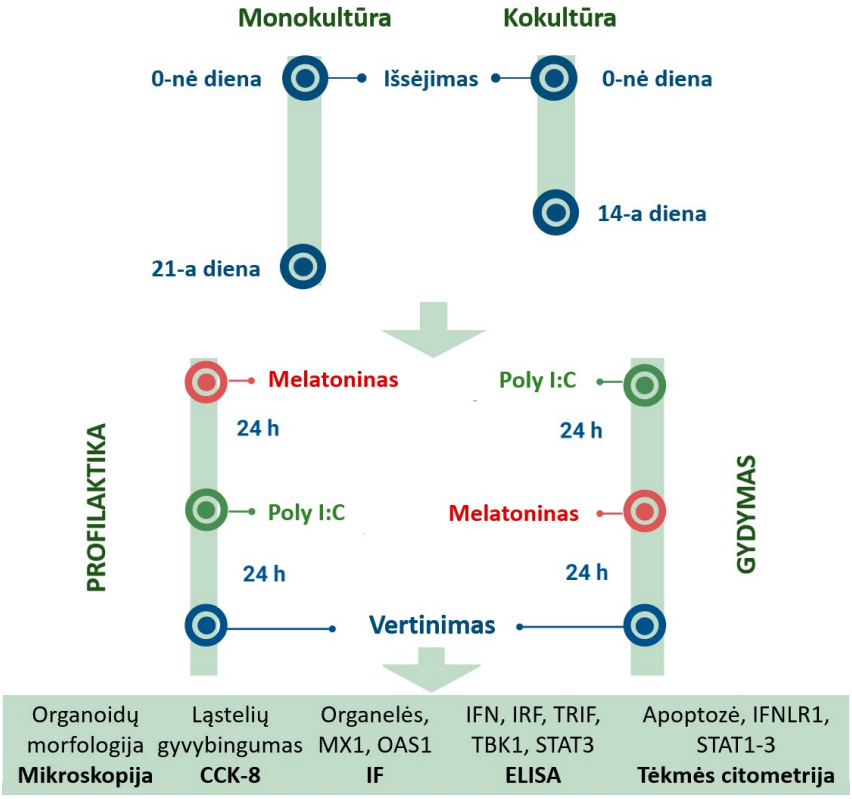

1 pav. *Tyrimo eksperimentų schema*

Santrumpos: CCK-8 – ląstelių skaičiavimo rinkinys-8; ELISA – fermentinis imunosorbentinis tyrimas; IF – imunofluorescencija; IFNLR1 – interferono λ receptorius 1; IFN – interferonai; IRF – interferono reguliaciniai faktoriai; MX1 – miksovirusų atsparumo baltymas 1; OAS – 2′-5′-oligoadenilato sintetazė; Poly I:C – poliinozino policitidilo rūgštis; STAT1–3 – signalų perdavimo ir transkripcijos aktyvatoriai 1–3; TBK1 – TANK-jungimosi kinazė 1; TRIF – TIR domeną turintis adapteris, indukuojantis IFNβ.

Profilaktika ir gydymas melatoninu

Eksperimentams naudotas melatoninas buvo paruoštas pagal gamintojo instrukcijas ir atskiestas Caco-2 ląstelių augimo terpėje. Monokultūrose epitelio ląstelės buvo veikiamos melatoninu (1, 10, 50 arba 100 µM koncentracijomis) 24 val. prieš arba 24 val. po stimuliacijos Poly I:C (1 pav.). Kokultūrose tokiu pačiu principu naudota tik 50 µM dozė.

Mikroskopija bei organoidų kiekio ir dydžio skaičiavimai

Ląstelių augimas buvo stebimas naudojant šviesinę mikroskopiją. Monokultūra buvo fotografuojama 7-ąją, 14-ąją ir 21-ąją dienomis, o kokultūra – 3-iąją, 7-ąją ir 14-ąją. Organoidų kiekis ir dydis monokultūrose buvo vertintas mikroskopiškai praėjus 24 val. po Poly I:C stimuliacijos (ar melatonino taikymo). Šviesiniu mikroskopu (Olympus IX2-SP) su skaitmenine kamera 4× priartinimu atliktos šulinėlių nuotraukos, kuriose esančių organoidų kiekis ir dydis įvertintas naudojant ImageJ programą. Analizė atlikta naudojant bent trijų šulinėlių nuotraukas kiekvienai sąlygai.

Ląstelių gyvybingumo vertinimas

Ląstelių gyvybingumas buvo vertinamas naudojant ląstelių skaičiavimo rinkinį (*angl.* Cell Counting Kit-8, CCK8; Abcam, DB) praėjus 24 ir 48 val. po Poly I:C stimuliacijos. Kaip nurodyta gamintojo, į kiekvieną šulinėlį, pakeitus terpę, įdėta po 10 µl dažo. Praėjus 2 valandoms, gautas spalvinis reakcijos intensyvumas įvertintas spektrofotometriškai mikroplokštelių skaitytuvu matuojant optinį tankį 450 nm bangos ilgio šviesoje.

Imunofluorescencinis dažymas

Caco-2 ląstelės buvo fiksuotos 4 proc. paraformaldehidu, permeabilizuotos 0,2 proc. Triton™ X-100 tirpalu, blokuotos 10 proc. galvijų vaisiaus serumo (FBS) tirpalu ir per naktį inkubuotos su specifiniais pirminiais antikūnais (EpCAM, ZO-1, MUC2, vimentinu). Kitą dieną ląstelės nuplautos buferiniu tirpalu (PBS) ir branduoliai nudažyti DAPI (4′,6-diamidino-2-fenilindolu).

Kokultūrų mėginiuose siekiant parodyti tiek fibroblastų, tiek endotelio ląstelių augimą, HUVEC ląstelės prieš sėjimą buvo nudažytos PKH26 fluorescenciniais membraniniais dažais, o HSIF po fiksacijos ir permeabilizacijos dažytos anti-α-SMA antikūnu.

Peroksisomų bei interferoną stimuliuojančių genų produktų aktyvumui įvertinti ląstelės buvo žymėtos atitinkamai PEX1, MX1, OAS1 antikūnais, mitochondrijos gyvose ląstelėse nudažytos MitoTracker™ (200 nM) dažais.

Visi dažymo veiksmai buvo atlikti tamsoje. Vaizdai gauti fluorescenciniu mikroskopu ir apdoroti su cellSens ir ImageJ programomis.

Tėkmės citometrija

Tėkmės citometrija buvo taikyta ląstelių apoptozės įvertinimui ir antivirusiniuose signaliniuose keliuose dalyvaujančių baltymų žymėjimui. Tėkmės citometrijos analizė atlikta naudojant BD FACSMelody ląstelių rūšiuoklį

LSMU Virškinamojo trakto tyrimų instituto Klinikinės ir molekulinės gastroenterologijos laboratorijoje.

Receptoriaus IFNLR1 ir STAT1–3 baltymų ekspresija vertinta ląsteles dažant specifiniais antikūnais: IFNLR1 monokloniniu antikūnu; fosfo-STAT1 (Tyr701), žymėtu eFluor™ 660; fosfo-STAT2 (Tyr689), žymėtu fluoresceino izotiocianatas (FITC); fosfo-STAT3 (Tyr705), žymėtu fikoeritrinu (PE). Dažymas atliktas laikantis gamintojo instrukcijų.

Viduląsteliniam žymėjimui (STAT1–3) ląstelės buvo permeabilizuotos 0,2 proc. Triton™ X-100 tirpalu. Apoptozė vertinta naudojant Aneksino V-FITC / propidiumo jodido (PI) žymėjimo rinkinį. Kokultūrų modeliuose endoteliui nuo fibroblastų atskirti tėkmės citometrijos metu, endotelio ląstelės prieš dažymą buvo pažymėtos PECAM-1 antikūnu. Duomenys analizuoti naudojant FlowJo (10.10 versija) programinę įrangą. Visi tyrimai atlikti triplikatuose.

ELISA tyrimai

Antivirusinis atsakas buvo kiekybiškai įvertintas nustatant interferonų (IFNλ1, IFNβ, IFNα) koncentracijas ląstelių kultūros supernatantuose bei antivirusiniuose signaliniuose keliuose dalyvaujančių baltymų (IRF1, IRF3, STAT3, TRIF ir TBK1) kiekius ląstelių lizatuose. Tyrimams naudoti komerciniai žmogaus ELISA (fermentinio imunosorbentinio tyrimo) rinkiniai. Citokinų bei signalinių baltymų koncentracijos buvo nustatytos vadovaujantis rinkinių gamintojų instrukcijomis: mėginiai buvo inkubuojami su specifiniais monokloniniais antikūnais, po to – su krienų peroksidaze sujungtais antriniais antikūnais. Gautas spalvinės reakcijos intensyvumas buvo įvertintas spektrofotometriškai, matuojant optinį tankį mikroplokštelių skaitytuvu LSMU Biochemijos laboratorijoje. Koncentracijos buvo apskaičiuotos pagal standartines kreives. Visi tyrimai atlikti triplikatuose.

Statistinė analizė

Statistinė analizė atlikta IBM SPSS (29.0.2.0 versija) ir GraphPad Prism (10.4.2 versija) programomis. Tyrimo rezultatai pateikti kaip bent 3 nepriklausomų eksperimentų vidurkiai su standartine deviacija (SD). Statistiškai reikšmingas skirtumas tarp 2 grupių vertintas *t* testu, o tarp kelių grupių – vienpuse ir dvipuse ANOVA ir post-hoc Bonferonni testu. Koreliacijos apskaičiuotos naudojantis Pearsono koeficientu. Statistiniai analizuotų baltymų kiekių skirtumai tarp skirtingų modelių tame pačiame laiko taške buvo vertinti naudojant kompaktiško raidinio žymėjimo (angl. *Compact Letter Display, CLD*) metodą, kur skirtingos raidės žymi reikšmingus skirtumus, t. y. skirtin-

gos mažosios raidės reiškia $p < 0,05$, o skirtingos didžiosios – $p < 0,01$. Duomenys laikyti statistiškai reikšmingais, kai p reikšmė buvo mažiau nei 0,05 ir grafikuose žymimi kaip * – $p < 0,05$, ** – $p < 0,01$, *** – $p < 0,001$. Grafikai sukurti naudojantis GraphPad Prism, iliustracijos – Microsoft PowerPoint (Office 2019). Teksto redagavimui naudotas ChatGPT, visas AI sugeneruotas turinys buvo kruopščiai peržiūrėtas.

Finansavimas

Tyrimas finansuotas Lietuvos mokslo tarybos (projektas IPTAVI, sutarties Nr. S-MIP-23-110) ir Lietuvos sveikatos mokslų universiteto Mokslo fondo lėšomis.

PAGRINDINIAI REZULTATAI

Virusinio virškinamojo trakto modelio sukūrimas

Tyrimo metu buvo sukurti trys virškinamojo trakto (VT) modeliai, iš kurių tolimesniems eksperimentams atrinkti du: monokultūros modelis su organoidais ir kokultūra, kurioje epitelio ląstelės augintos kartu su fibroblastais (HSIF) ir endotelio ląstelėmis (HUVEC).

Monokultūroje Caco-2 ląstelės buvo kultivuojamos 21 dieną, kol diferencijavosi ir suformavo poliarizuotas epitelio struktūras – organoidus, patvirtintus mikroskopiškai bei taikant specifinius žymenis, tokius kaip ZO-1, EpCAM, MUC2 ir vimentinas.

Vėliau modelis buvo patobulintas įtraukiant fibroblastų ir endotelio ląsteles. Jos kartu buvo auginamos šulinėlio dugne, o epitelio ląstelės – virš jų pakabintame inserte. Kokultūroje Caco-2 ląstelių proliferacija padidėjo 32 proc. ($p = 0,031$).

Poly I:C, kaip virusinę infekciją imituojančios medžiagos, veiksmingumas buvo patvirtintas vertinant ląstelių gyvybingumą bei organoidų morfologiją. Monokultūroje Poly I:C stimuliacija sukėlė stiprią, nuo dozės priklausomą pažaidos reakciją: sumažėjo ląstelių gyvybingumas (iki 84 proc., $p = 0,003$), organoidų skaičius (~35 proc.) ir dydis (~55 proc.). Net ir mažiausia Poly I:C dozė (1 μg/ml) sukėlė statistiškai reikšmingą apoptozę, o esant didžiausiai dozei (50 μg/ml), apoptozė net padvigubėjo.

Kokultūroje epitelio ląstelės buvo atsparesnės. Dėl to siekiant užtikrinti pakankamą virusinę infekciją imituojančią pažaidą, Poly I:C koncentracija padidinta iki 100 μg/ml. Net ir po šios koncentracijos Poly I:C stimuliacijos, apoptozės apimtys (15,05 proc. lyginant su 12,1 proc., $p > 0,05$) ir gyvybingumas kokultūros modelyje išliko panašūs į kontrolines, kai tuo tarpu monokultūroje ir dviejų ląstelių linijų kokultūrose apoptozė siekė 35–40 proc.,

o gyvybingumas sumažėjo iki ~75–80 proc. Tai rodo, kad fibroblastų ir endotelio ląstelių kombinacija stiprina epitelio atsparumą prieš virusinę pažaidą.

Antivirusinis atsakas monokultūroje

Toliau pradėti žarnyno epitelio imuninio atsako tyrimai monokultūroje. Pirmiausia įvertintas interferonų – IFNλ1, IFNβ ir IFNα – išsiskyrimas. Poly I:C stimuliacija sukėlė nuo dozės priklausomą IFNλ1 ekspresijos padidėjimą Caco-2 ląstelėse. IFNλ1 pokytis pastebėtas jau po 6 val. nuo stimuliacijos. IFNβ ar IFNα ekspresijos padidėjimo nebuvo nustatyta.

Praėjus 24 val. nuo Poly I:C stimuliacijos tėkmės citometrija nustatytas ir padidėjęs IFNLR1 kiekis, rodantis, kad ląstelės suaktyvina receptorių ekspresiją, reaguodamos į virusinę pažaidą imituojančią stimuliaciją. Be to, Poly I:C stimuliacija ne tik aktyvavo IFNλ1 gamybą, bet ir reikšmingai suaktyvino visų trijų tirtų STAT transkripcijos faktorių (STAT1, STAT2 ir STAT3) ekspresiją. Tai reiškia, kad sukurtame žarnyno epitelio modelyje Poly I:C efektyviai sukėlė antivirusinį atsaką per III tipo IFN signalinį kelią.

Antivirusinis atsakas kokultūroje

Atliekant imuninio atsako vertinimą kokultūroje nustatyta, kad stromos ląstelių buvimas ne tik padidina epitelio atsparumą, bet ir reguliuoja antivirusinį atsaką. Poly I:C stimuliacija reikšmingai padidino IFNλ1 ekspresiją visuose modeliuose (> 40 ng/ml), tačiau kokultūroje šis atsakas buvo greitesnis. Kaip ir monokultūroje, IFNα indukcija nebuvo nustatyta, o IFNβ ekspresija nežymiai padidėjo tik po didelės Poly I:C dozės.

Dėl išskirtinio III tipo IFN kelio aktyvumo, toliau tirta jį reguliuojančių transkripcijos faktorių (IRF1, IRF3, TRIF, TBK1) ekspresija bei su ja galintis būti susijęs organelių (mitochondrijų ir peroksisomų) atsakas. Nustatyta skirtinga transkripcijos faktorių dinamika monokultūros ir kokultūros modeliuose. Kokultūroje IRF3 ekspresija padidėjo greičiau, o IRF1 lygis išliko žemesnis nei monokultūroje. Tai rodo, kad fibroblastai ir endotelio ląstelės mažina IRF1 ekspresiją epitelio ląstelėse ir taip galimai reguliuoja III tipo IFN gamybą.

TBK1 ekspresija monokultūroje didėjo priklausomai nuo Poly I:C dozės ir piką pasiekė po 24 val. Tuo tarpu kokultūroje TBK1 ekspresija buvo didelė jau prieš stimuliaciją ir vėliau mažai keitėsi, kas rodo, kad prie TBK1 aktyvacijos galimai prisideda fibroblastų ir endotelio sąveika. TRIF ekspresija taip pat buvo reikšmingai didesnė kokultūroje nei monokultūroje ($p < 0{,}001$). Tarp TRIF ir TBK1 nustatyta labai stipri koreliacija ($r = 0{,}998$, $p < 0{,}001$).

IFNLR1 ekspresija išliko aukšta tiek monokultūroje, tiek kokultūroje, kas rodo išlaikomą jautrumą IFNλ1, net esant aktyviai jo ekspresijai.

Analizuojant organelių vaidmenį, nustatyta, kad monokultūroje antivirusinis atsakas labiau priklauso nuo mitochondrijų, o kokultūroje – nuo peroksisomų. Pastarųjų aktyvacija kokultūroje stipriai koreliavo su IRF3 ($r = 0{,}949$), TBK1 ($r = 0{,}949$) ir TRIF ($r = 0{,}947$) ekspresija. Tai leidžia daryti išvadą, kad kokultūros aktyvuoja peroksisomų–TBK1–IRF3–IFNλ1 kelią, kuris galimai mažiau toksiškas nei su mitochondrijomis susiję signaliniai keliai.

Didelė Poly I:C dozė (100 μg/ml) beveik dvigubai padidino MX1 baltymo ekspresiją lyginant su kontrolinėmis ląstelėmis ($p < 0{,}001$). Tuo tarpu OAS1 kiekis po Poly I:C stimuliacijos reikšmingai sumažėjo ($p = 0{,}023$). MX1 kiekis teigiamai koreliavo su peroksisomų aktyvacija ($r = 0{,}456$) ir TBK1 ekspresija ($r = 0{,}578$), tačiau stipriai neigiamai – su mitochondrijų aktyvacija ($r = -0{,}664$). OAS1 ekspresija buvo teigiamai susijusi su TBK1 ($r = 0{,}808$) ir STAT3 ($r = 0{,}623$) bei neigiamai – su apoptoze ($r = -0{,}818$).

Melatonino poveikis monokultūroje

Atsižvelgiant į vis gausėjančius duomenis apie melatonino antivirusines savybes, įvertintas jo poveikis Poly I:C sukeltai Caco-2 ląstelių pažaidai ir antivirusiniam atsakui.

Išbandžius ant Poly I:C nepaveiktų ląstelių, melatoninas neturėjo įtakos nei jų gyvybingumui, nei organoidų morfologijai, patvirtindamas savo saugumą. Tyrimo metu išbandytos dvi strategijos: 1) profilaktinis gydymas – melatoninas taikytas likus 24 val. iki Poly I:C stimuliacijos; 2) gydymas po infekcijos – melatoninas taikytas praėjus 24 val. po Poly I:C stimuliacijos.

Profilaktinis taikymas paskatino ląstelių proliferaciją ir mažino apoptozę, tačiau neapsaugojo nuo Poly I:C sukelto organoidų pažeidimo. Tuo tarpu gydymas po Poly I:C stimuliacijos nesumažino apoptozės, tačiau galimai turėjo apsauginį poveikį organoidams, nes nors jų kiekis ir sumažėjo, jie padidėjo.

Melatoninas savaime neskatino IFNλ1 ekspresijos. Profilaktika melatoninu taip pat neturėjo ypatingo poveikio IFNλ1 ekspresijai, bet gydymas po Poly I:C stimuliacijos – ją sumažino. Įdomu tai, kad melatoninas padidino IFNLR1 ekspresiją Poly I:C nepaveiktose ląstelėse, o taikant melatoniną po Poly I:C stimuliacijos, IFNLR1 lygis dar padidėjo. Be to, profilaktika melatoninu sumažino STAT1 ekspresiją Poly I:C paveiktose Caco-2 ląstelėse, o gydymas po Poly I:C stimuliacijos – visų trijų STAT baltymų ekspresiją, nepriklausomai nuo koncentracijos.

Melatonino poveikis kokultūroje

Melatonino poveikis kokultūroje buvo šiek tiek kitoks. Profilaktinis melatonino taikymas taip pat sumažino epitelio ląstelių apoptozę ir padidino jų gyvybingumą, bet poveikis buvo stipresnis nei kontroliniuose modeliuose, kas rodo papildomą stromos ląstelių įtaką. Melatonino gydomasis poveikis kokultūroje, priešingai nei monokultūroje, buvo dar stipresnis. Taikant melatoniną taip pat padidėjo ir ląstelių gyvybingumas, kas patvirtina jo stiprų apsauginį poveikį.

Melatonino poveikis IFNλ1 ekspresijai kokultūroje buvo panašus į stebėtą monokultūroje: profilaktinis taikymas įtakos IFNλ1 ekspresijai neturėjo, o gydymas jo kiekį kiek sumažino, tačiau jis išliko pakankamas antivirusiniam atsakui. IFNLR1 ekspresijos tendencija buvo panaši. Kokultūroje receptoriaus lygis išliko aukštas tiek profilaktiškai, tiek gydomuoju tikslu paveiktose ląstelėse. Tai rodo, kad melatoninas padeda išlaikyti jautrumą IFNλ1, o kokultūros pasižymi didesniu atsparumu receptoriaus mažėjimui imuninio streso sąlygomis.

Melatoninas taip pat turėjo įtakos pagrindinių antivirusinių transkripcijos faktorių ekspresijai. IRF1 kiekis kokultūroje sumažėjo tiek po profilaktinio, tiek po gydomojo melatonino taikymo. Priešingai, IRF3 ir TBK1 ekspresija reikšmingai padidėjimo. Tuo tarpu TRIF ekspresija išliko stabili visuose modeliuose, kas rodo, kad melatoninas galimai veikia žemiau TRIF arba nepriklausomai nuo jo.

Melatoninas taip pat turėjo įtakos organelių aktyvacijai. Monokultūrose jis dar labiau sustiprino Poly I:C sukeltą mitochondrijų aktyvaciją, kas galimai didino oksidacinį stresą. Kokultūroje, priešingai, melatoninas sumažino arba stabilizavo mitochondrijų aktyvumą, atitinkantį stebėtą antiapoptotinį poveikį. Peroksisomų aktyvacija sumažėjo tiek melatoniną taikant profilaktiškai, tiek kaip gydymą, ypač kokultūroje. Šis antivirusinio atsako aktyvavimo per peroksisomas sumažėjimas gali atspindėti reguliacinį mechanizmą, kuriuo melatoninas palaiko TBK1–IRF3–IFNλ1 ašies aktyvavimą ko-kultūroje.

IŠVADOS

1. Antivirusinio atsako VT epitelyje analizei buvo sukurti 2 VT modeliai: Caco-2 organoidų monokultūra ir kokultūra, sudaryta iš epitelio, fibroblastų bei endotelio ląstelių. Modelių tinkamumą patvirtinto nuo Poly I:C dozės priklausomas VT epitelio ląstelių apoptozės padidėjimas. Kokultūroje fibroblastai ir endotelio ląstelės paskatino epitelio ląstelių augimą ir gyvybingumą bei padidino jų atsparumą citotoksiniam Poly I:C poveikiui.

2. VT epitelio ląstelėse Poly I:C sukėlė ryškų, nuo dozės priklausomą III tipo IFN atsaką: padidėjo IFNλ1, IFNLR1 ir STAT1–3 ekspresija, kai tuo tarpu I tipo IFN ekspresija buvo minimali. Kokultūrose antivirusinis atsakas buvo skatinamas per peroksisomų–TBK1–IRF3–IFNλ1 ašį, kuri padidino MX1 expresiją.
3. Kokultūrose, lyginant su monokultūra, nustatyta greitesnė bei didesnė transkripcijos faktorių IRF3, TBK1 ir TRIF ekspresija, o IRF1 kiekis buvo mažesnis. Epitelio sąveika su fibroblastais ir endoteliu skatino ryškų, nuo dozės priklausomą peroksisomų aktyvumo padidėjimą, kai tuo tarpu monokultūros antivirusiniame atsake dominavo mitochondrijos.
4. Melatoninas VT epitelio ląstelėse moduliavo TBK1–IRF3–III tipo IFN ašį. Jo poveikis priklausomai nuo taikymo laiko ir modelio skyrėsi. Taikant kaip gydymą, melatoninas pasižymėjo apsauginiu poveikiu – slopino antivirusinių citokinų gamybą, tačiau neturėjo įtakos apoptozei. Taikant kaip profilaktiką, melatoninas apsaugojo nuo apoptozės, tačiau neslopino virusinio uždegimo sukeltos antivirusinių citokinų gamybos. Kokultūroje nustatytas ryškesnis apsauginis melatonino poveikis, kuris siejosi su peroksisomų aktyvumo slopinimu bei mitochondrinių procesų stabilizacija, kas leidžia manyti, kad jo veikimo mechanizmas galėtų priklausyti nuo organelių aktyvacijos.

ATEITIES TYRIMŲ KRYPTYS

1. Kadangi tyrimo metu sukurtame kokultūros modelyje su fibroblastais ir endotelio ląstelėmis buvo nustatytas stipresnis imuninis atsakas, lyginant su monokultūros modeliais, šis modelis galėtų būti naudojamas kaip prieinama alternatyva kitoms kompleksinėms ir brangioms sistemoms (pvz., žarnyno mikroscheminiam modeliui) tyrinėti virusines žarnyno infekcijas ateityje. Siekiant dar fiziologiškesnio efekto, į modelį papildomai reikėtų įtraukti imunines ląsteles, tokias kaip makrofagai ar dendritinės ląstelės.
2. Tyrimo rezultatai patvirtina, kad peroksisomos vaidina svarbų vaidmenį ląstelės atsake į virusinę infekciją, tačiau reikalingi tolimesni tyrimai, kurie padėtų išsiaiškinti tikslesnį mechanizmą, kaip peroksisomos veikia antivirusinį atsaką žarnyno epitelio ląstelėse. Tai galbūt galėtų būti naudinga antivirusinių vaistų paieškoje ateityje.
3. Atliktuose *in vitro* tyrimuose melatoninas turėjo antivirusinių ir epitelio barjerą apsaugančių savybių. Tai rodo, kad ateityje jis galėtų būti

pritaikytas virusinėms žarnyno infekcijoms gydyti. Deja, melatonino naudojimas klinikinėje praktikoje šiai indikacijai negali būti rekomenduojamas remiantis tik šiais *in vitro* rezultatais. Reikalingi išsamesni tyrimai siekiant patikslinti jo veikimo mechanizmą bei nustatyti tinkamą jo dozę bei skyrimo laiką.

REFERENCES

1. Santos-Ferreira N, Van Dycke J, Neyts J, Rocha-Pereira J. Current and Future Antiviral Strategies to Tackle Gastrointestinal Viral Infections. Microorganisms. 2021;9(8):1599.
2. Wang J, Li H, Xue B, Deng R, Huang X, Xu Y, et al. IRF1 Promotes the Innate Immune Response to Viral Infection by Enhancing the Activation of IRF3. J Virol. 2020;94(22):e01231-20.
3. Julio-Pieper M, López-Aguilera A, Eyzaguirre-Velásquez J, Olavarría-Ramírez L, Ibacache-Quiroga C, Bravo JA, Cruz G. Gut Susceptibility to Viral Invasion: Contributing Roles of Diet, Microbiota and Enteric Nervous System to Mucosal Barrier Preservation. Int J Mol Sci. 2021;22(9):4734.
4. Neurath MF, Artis D, Becker C. The intestinal barrier: a pivotal role in health, inflammation, and cancer. Lancet Gastroenterol Hepatol. 2025;10(6):573-592.
5. Pervolaraki K, Rastgou Talemi S, Albrecht D, Bormann F, Bamford C, Mendoza JL, et al. Differential induction of interferon stimulated genes between type I and type III interferons is independent of interferon receptor abundance. PLoS Pathog. 2018;14(11):e1007420.
6. Perry AK, Chow EK, Goodnough JB, Yeh WC, Cheng G. Differential requirement for TANK-binding kinase-1 in type I interferon responses to toll-like receptor activation and viral infection. J Exp Med. 2004;199(12):1651–8.
7. Gebert JT, Scribano F, Engevik KA, Perry JL, Hyser JM. Gastrointestinal organoids in the study of viral infections. Am J Physiol Gastrointest Liver Physiol. 2023;324(1):G51-G59.
8. Adeniyi-Ipadeola G, Nwanosike H, Ramani S. Human intestinal organoids as models to study enteric bacteria and viruses. Curr Opin Microbiol. 2023;75:10236.
9. Samy KE, Levy ES, Phong K, Demaree B, Abate AR, Desai TA. Human intestinal spheroids cultured using Sacrificial Micromolding as a model system for studying drug transport. Sci Rep. 2019;9(1):9936.
10. Darling NJ, Mobbs CL, González-Hau AL, Freer M, Przyborski S. Bioengineering Novel in vitro Co-culture Models That Represent the Human Intestinal Mucosa With Improved Caco-2 Structure and Barrier Function. Front Bioeng Biotechnol. 2020;8:992.
11. Su R, Shereen MA, Zeng X, Liang Y, Li W, Ruan Z, et al. The TLR3/IRF1/Type III IFN Axis Facilitates Antiviral Responses against Enterovirus Infections in the Intestine. mBio. 2020;11(6):e02540-20.
12. Riemann D, Espie CA, Altena E, Arnardottir ES, Baglioni C, Bassetti CLA, et al. The European Insomnia Guideline: An update on the diagnosis and treatment of insomnia 2023. J Sleep Res. 2023 Dec;32(6):e14035.
13. Kitidee K, Samutpong A, Pakpian N, Wisitponchai T, Govitrapong P, Reiter RJ, Wongchitrat P. Antiviral effect of melatonin on Japanese encephalitis virus infection involves inhibition of neuronal apoptosis and neuroinflammation in SH-SY5Y cells. Sci Rep. 2023;13(1):6063.
14. Lempesis IG, Georgakopoulou VE, Reiter RJ, Spandidos DA. A mid-pandemic night's dream: Melatonin, from harbinger of anti-inflammation to mitochondrial savior in acute and long COVID-19 (Review). Int J Mol Med. 2024;53(3):28.
15. Hardeland R. Melatonin and inflammation-Story of a double-edged blade. J Pineal Res. 2018;65(4):e12525.
16. Black RE, Perin J, Yeung D, Rajeev T, Miller J, Elwood SE, Platts-Mills JA. Estimated global and regional causes of deaths from diarrhoea in children younger than 5 years during 2000-21: a systematic review and Bayesian multinomial analysis. Lancet Glob Health. 2024;12(6):e919-e928.

17. Ardura-Garcia C, Kreis C, Rakic M, Jaboyedoff M, Mallet MC, Low N, Kuehni CE. Rotavirus disease and health care utilisation among children under 5 years of age in highly developed countries: A systematic review and meta-analysis. Vaccine. 2021;39(22):2917-2928.
18. Hassan F, Kanwar N, Harrison CJ, Halasa NB, Chappell JD, Englund JA, et al. Viral Etiology of Acute Gastroenteritis in <2-Year-Old US Children in the Post-Rotavirus Vaccine Era. J Pediatric Infect Dis Soc. 2019;8(5):414-421.
19. Jagirdhar GSK, Pulakurthi YS, Chigurupati HD, Surani S. Gastrointestinal tract and viral pathogens. World J Virol. 2023;12(3):136-150.
20. Flynn TG, Olortegui MP, Kosek MN. Viral gastroenteritis. Lancet. 2024;403(10429):862-876.
21. Leung AK, Hon KL. Paediatrics: how to manage viral gastroenteritis. Drugs Context. 2021;10:2020-11-7.
22. Bányai K, Estes MK, Martella V, Parashar UD. Viral gastroenteritis. Lancet. 2018;392(10142):175-186.
23. Pawłuszkiewicz K, Ryglowski PJ, Idzik N, Błaszczyszyn K, Kucharczyk E, Gaweł-Dąbrowska D, et al. Rotavirus Infections: Pathophysiology, Symptoms, and Vaccination. Pathogens. 2025;14(5):480.
24. Hassan E, Baldridge MT. Norovirus encounters in the gut: multifaceted interactions and disease outcomes. Mucosal Immunol. 2019;12(6):1259-1267.
25. Schmutz C, Bless PJ, Mäusezahl D, Jost M, Mäusezahl-Feuz M; Swiss Sentinel Surveillance Network. Acute gastroenteritis in primary care: a longitudinal study in the Swiss Sentinel Surveillance Network, Sentinella. Infection. 2017;45(6):811-824.
26. Hallowell BD, Chavers T, Parashar U, Tate JE. Global Estimates of Rotavirus Hospitalizations Among Children Below 5 Years in 2019 and Current and Projected Impacts of Rotavirus Vaccination. J Pediatric Infect Dis Soc. 2022;11(4):149-158.
27. Guarino A, Ashkenazi S, Gendrel D, Lo Vecchio A, Shamir R, Szajewska H; European Society for Pediatric Gastroenterology, Hepatology, and Nutrition; European Society for Pediatric Infectious Diseases. European Society for Pediatric Gastroenterology, Hepatology, and Nutrition/European Society for Pediatric Infectious Diseases evidence-based guidelines for the management of acute gastroenteritis in children in Europe: update 2014. J Pediatr Gastroenterol Nutr. 2014;59(1):132-52.
28. Acevedo-Rodriguez JG, Contreras CA, Ochoa TJ. Viral diarrheas - newer advances in diagnosis and management. Curr Opin Infect Dis. 2024;37(5):385-391.
29. Allaire JM, Crowley SM, Law HT, Chang SY, Ko HJ, Vallance BA. The Intestinal Epithelium: Central Coordinator of Mucosal Immunity. Trends Immunol. 2018;39(9):677-696.
30. Zhang E, Fang M, Jones C, Minze LJ, Xing J, Zhang Z. Mechanisms involved in controlling RNA virus-induced intestinal inflammation. Cell Mol Life Sci. 2022;79(6):313.
31. Imre G. Cell death signalling in virus infection. Cell Signal. 2020;76:109772.
32. Villena J, Vizoso-Pinto MG, Kitazawa H. Intestinal Innate Antiviral Immunity and Immunobiotics: Beneficial Effects against Rotavirus Infection. Front Immunol. 2016;7:563.
33. Schneider WM, Chevillotte MD, Rice CM. Interferon-stimulated genes: a complex web of host defenses. Annu Rev Immunol. 2014;32:513-45.
34. García-Álvarez M, Berenguer J, Jiménez-Sousa MA, Pineda-Tenor D, Aldámiz-Echevarria T, Tejerina F, Diez C, et al. Mx1, OAS1 and OAS2 polymorphisms are associated with the severity of liver disease in HIV/HCV-coinfected patients: A cross-sectional study. Sci Rep. 2017;7:41516.

35. Isaacs A, Lindenmann J. Virus interference. I. The interferon. Proc R Soc Lond B Biol Sci. 1957;147(927):258-67.
36. Stanifer ML, Boulant S. Differential signaling by type-I and type-III interferons in mucosa. Curr Opin Immunol. 2024;86:102400.
37. Kotenko SV, Durbin JE. Contribution of type III interferons to antiviral immunity: location, location, location. J Biol Chem. 2017;292(18):7295-7303.
38. Stanifer ML, Pervolaraki K, Boulant S. Differential Regulation of Type I and Type III Interferon Signaling. Int J Mol Sci. 2019;20(6):1445.
39. Gewaid H, Bowie AG. Regulation of type I and type III interferon induction in response to pathogen sensing. Curr Opin Immunol. 2024;87:102424.
40. Wright AP, Nice TJ. Role of type-I and type-III interferons in gastrointestinal homeostasis and pathogenesis. Curr Opin Immunol. 2024;86:102412.
41. Martínez-Espinoza I, Guerrero-Plata A. Current Landscape of IFN-λ: Induction, Inhibition, and Potential Clinical Applications to Treat Respiratory Viral Infections. Immunohorizons. 2023;7(4):265-272.
42. Pervolaraki K, Stanifer ML, Münchau S, Renn LA, Albrecht D, Kurzhals S, et al. Type I and Type III Interferons Display Different Dependency on Mitogen-Activated Protein Kinases to Mount an Antiviral State in the Human Gut. Front Immunol. 2017;8:459.
43. Pervolaraki K, Guo C, Albrecht D, Boulant S, Stanifer ML. Type-Specific Crosstalk Modulates Interferon Signaling in Intestinal Epithelial Cells. J Interferon Cytokine Res. 2019;39(10):650-660.
44. Goel RR, Kotenko SV, Kaplan MJ. Interferon lambda in inflammation and autoimmune rheumatic diseases. Nat Rev Rheumatol. 2021;17(6):349-362.
45. Nolan LS, Baldridge MT. Advances in understanding interferon-mediated immune responses to enteric viruses in intestinal organoids. Front Immunol. 2022;13:943334.
46. Van Winkle JA, Peterson ST, Kennedy EA, Wheadon MJ, Ingle H, Desai C, et al. Homeostatic interferon-lambda response to bacterial microbiota stimulates preemptive antiviral defense within discrete pockets of intestinal epithelium. Elife. 2022;11:e74072.
47. Doldan P, Dai J, Metz-Zumaran C, Patton JT, Stanifer ML, Boulant S. Type III and Not Type I Interferons Efficiently Prevent the Spread of Rotavirus in Human Intestinal Epithelial Cells. J Virol. 2022;96(17):e0070622.
48. Baldridge MT, Lee S, Brown JJ, McAllister N, Urbanek K, Dermody TS, et al. Expression of IFNLR1 on Intestinal Epithelial Cells Is Critical to the Antiviral Effects of Interferon Lambda against Norovirus and Reovirus. J Virol. 2017;91(7):e02079-16.
49. Nice TJ, Baldridge MT, McCune BT, Norman JM, Lazear HM, Artyomov M, et al. Interferon-λ cures persistent murine norovirus infection in the absence of adaptive immunity. Science. 2015;347(6219):269-73.
50. Günther C, Ruder B, Stolzer I, Dorner H, He GW, Chiriac MT, et al. Interferon Lambda Promotes Paneth Cell Death Via STAT1 Signaling in Mice and Is Increased in Inflamed Ileal Tissues of Patients With Crohn's Disease. Gastroenterology. 2019;157(5):1310-1322.e13.
51. Broggi A, Ghosh S, Sposito B, Spreafico R, Balzarini F, Lo Cascio A, et al. Type III interferons disrupt the lung epithelial barrier upon viral recognition. Science. 2020;369(6504):706-712.
52. Dixit E, Boulant S, Zhang Y, Lee AS, Odendall C, Shum B, et al. Peroxisomes are signaling platforms for antiviral innate immunity. Cell. 2010;141(4):668-81.
53. Ferreira AR, Marques M, Ramos B, Kagan JC, Ribeiro D. Emerging roles of peroxisomes in viral infections. Trends Cell Biol. 2022;32(2):124-139.
54. Tiku V, Tan MW, Dikic I. Mitochondrial Functions in Infection and Immunity. Trends Cell Biol. 2020;30(4):263-275.

55. Jiang H, Nair V, Sun Y, Ding C. The diverse roles of peroxisomes in the interplay between viruses and mammalian cells. Antiviral Res. 2024;221:105780.
56. Schrader M, Kamoshita M, Islinger M. Organelle interplay-peroxisome interactions in health and disease. J Inherit Metab Dis. 2020;43(1):71-89.
57. Zheng C, Su C. Herpes simplex virus 1 infection dampens the immediate early antiviral innate immunity signaling from peroxisomes by tegument protein VP16. Virol J. 2017;14(1):35.
58. Mohan KV, Som I, Atreya CD. Identification of a type 1 peroxisomal targeting signal in a viral protein and demonstration of its targeting to the organelle. J Virol. 2002;76(5):2543-7.
59. Asal M, Rep M, Bontkes HJ, van Vliet SJ, Mebius RE, Gibbs S. Towards Full Thickness Small Intestinal Models: Incorporation of Stromal Cells. Tissue Eng Regen Med. 2024;21(3):369-377.
60. Dutta D, Heo I, Clevers H. Disease Modeling in Stem Cell-Derived 3D Organoid Systems. Trends Mol Med. 2017 May;23(5):393-410.
61. Rahmani S, Breyner NM, Su HM, Verdu EF, Didar TF. Intestinal organoids: A new paradigm for engineering intestinal epithelium in vitro. Biomaterials. 2019;194:195-214.
62. Pinto M, Robine S, Appay MD, Kedinger M, Triadou N, Dussaulx E, et al. Enterocyte-like differentiation and polarization of the human colon carcinoma cell line Caco-2 in culture. Biol Cell. 1983;47(3):323-30.
63. Antfolk M, Jensen KB. A bioengineering perspective on modelling the intestinal epithelial physiology in vitro. Nat Commun. 2020;11(1):6244.
64. Grasset E, Pinto M, Dussaulx E, Zweibaum A, Desjeux JF. Epithelial properties of human colonic carcinoma cell line Caco-2: electrical parameters. Am J Physiol. 1984;247(3 Pt 1):C260-7.
65. Yin Y, Xu L, Steinway SN. Editorial: 3D organoid and organ-on-a-chip and their applications for virology and antiviral research. Front Microbiol. 2023;14:1266136.
66. Randall KJ, Turton J, Foster JR. Explant culture of gastrointestinal tissue: a review of methods and applications. Cell Biol Toxicol. 2011;27(4):267-84.
67. Sato T, Vries RG, Snippert HJ, van de Wetering M, Barker N, Stange DE, et al. Single Lgr5 stem cells build crypt-villus structures in vitro without a mesenchymal niche. Nature. 2009;459(7244):262-5.
68. Hu X, Zhou L, Wang X, Jiang J, An S, Ye L, Liang H. Exploring the potential of organoids in advancing disease modeling for viral diseases. Future Virol. 2024:19(10–11), 419–433.
69. Barrila J, Crabbé A, Yang J, Franco K, Nydam SD, Forsyth RJ, et al. Modeling Host-Pathogen Interactions in the Context of the Microenvironment: Three-Dimensional Cell Culture Comes of Age. Infect Immun. 2018;86(11):e00282-18.
70. Blutt SE, Crawford SE, Ramani S, Zou WY, Estes MK. Engineered Human Gastrointestinal Cultures to Study the Microbiome and Infectious Diseases. Cell Mol Gastroenterol Hepatol. 2017;5(3):241-251.
71. Hentschel V, Arnold F, Seufferlein T, Azoitei N, Kleger A, Müller M. Enteropathogenic Infections: Organoids Go Bacterial. Stem Cells Int. 2021;2021:8847804.
72. Vilardi A, Przyborski S, Mobbs C, Rufini A, Tufarelli C. Current understanding of the interplay between extracellular matrix remodelling and gut permeability in health and disease. Cell Death Discov. 2024;10(1):258.
73. Zhang J, Penny J, Lu JR. Development of a novel in vitro 3D intestinal model for permeability evaluations. Int J Food Sci Nutr. 2020;71(5):549-562.
74. Baddal B, Marrazzo P. Refining Host-Pathogen Interactions: Organ-on-Chip Side of the Coin. Pathogens. 2021;10(2):203.

75. Chu JTS, Lamers MM. Organoids in virology. Npj Viruses. 2024;2(1):5.
76. Tan DX, Manchester LC, Esteban-Zubero E, Zhou Z, Reiter RJ. Melatonin as a Potent and Inducible Endogenous Antioxidant: Synthesis and Metabolism. Molecules. 2015;20(10):18886-906.
77. Bahrampour Juybari K, Pourhanifeh MH, Hosseinzadeh A, Hemati K, Mehrzadi S. Melatonin potentials against viral infections including COVID-19: Current evidence and new findings. Virus Res. 2020;287:198108.
78. Alomari T, Al-Abdallat H, Hamamreh R, Alomari O, Hos BH, Reiter RJ. Assessing the antiviral potential of melatonin: A comprehensive systematic review. Rev Med Virol. 2024;34(1):e2499.
79. Reiter RJ, Ma Q, Sharma R. Melatonin in Mitochondria: Mitigating Clear and Present Dangers. Physiology (Bethesda). 2020 Mar 1;35(2):86-95.
80. Martín Giménez VM, de Las Heras N, Lahera V, Tresguerres JAF, Reiter RJ, Manucha W. Melatonin as an Anti-Aging Therapy for Age-Related Cardiovascular and Neurodegenerative Diseases. Front Aging Neurosci. 2022;14:888292.
81. Maestroni GJM. Role of Melatonin in Viral, Bacterial and Parasitic Infections. Biomolecules. 2024;14(3):356.
82. Xi-Zhang, Yuan XQ, Zhang XM. Melatonin reduces inflammation in intestinal cells, organoids and intestinal explants. Inflammopharmacology. 2021;29(5):1555-1564.
83. Carrillo-Vico A, Guerrero JM, Lardone PJ, Reiter RJ. A review of the multiple actions of melatonin on the immune system. Endocrine. 2005;27(2):189-200.
84. Maestroni GJM, Conti A, Pierpaoli W. Pineal Melatonin, Its Fundamental Immunoregulatory Role in Aging and Cancer. Ann N Y Acad Sci. 1988;521(1):140–8.
85. Reiter RJ, Sharma R, Simko F, Dominguez-Rodriguez A, Tesarik J, Neel RL, et al. Melatonin: highlighting its use as a potential treatment for SARS-CoV-2 infection. Cell Mol Life Sci. 2022;79(3):143.
86. Wongchitrat P, Yasawong M, Jumpathong W, Chanmanee T, Samutpong A, Dangsakul W, et al. Melatonin inhibits Zika virus replication in Vero epithelial cells and SK-N-SH human neuroblastoma cells. Melatonin Research. 2022;5(2):171–85.
87. Pérez-Martínez Z, Boga JA, Potes Y, Melón S, Coto-Montes A. Effect of Melatonin on Herpesvirus Type 1 Replication. Int J Mol Sci. 2024;25(7):4037.
88. Radogna F, Diederich M, Ghibelli L. Melatonin: a pleiotropic molecule regulating inflammation. Biochem Pharmacol. 2010;80(12):1844-52.
89. Tarocco A, Caroccia N, Morciano G, Wieckowski MR, Ancora G, Garani G, Pinton P. Melatonin as a master regulator of cell death and inflammation: molecular mechanisms and clinical implications for newborn care. Cell Death Dis. 2019;10(4):317.
90. Henderson R, Kim S, Lee E. Use of melatonin as adjunctive therapy in neonatal sepsis: A systematic review and meta-analysis. Complement Ther Med. 2018;39:131-136.
91. Andersen LP, Gögenur I, Rosenberg J, Reiter RJ. The Safety of Melatonin in Humans. Clin Drug Investig. 2016;36(3):169-75.
92. Calvo JR, González-Yanes C, Maldonado MD. The role of melatonin in the cells of the innate immunity: a review. J Pineal Res. 2013;55(2):103-20.
93. Mannino G, Caradonna F, Cruciata I, Lauria A, Perrone A, Gentile C. Melatonin reduces inflammatory response in human intestinal epithelial cells stimulated by interleukin-1β. J Pineal Res. 2019;67(3):e12598.
94. Slominski RM, Reiter RJ, Schlabritz-Loutsevitch N, Ostrom RS, Slominski AT. Melatonin membrane receptors in peripheral tissues: distribution and functions. Mol Cell Endocrinol. 2012;351(2):152-66.
95. Carrillo-Vico A, Reiter RJ, Lardone PJ, Herrera JL, Fernández-Montesinos R, Guerrero JM, Pozo D. The modulatory role of melatonin on immune responsiveness. Curr Opin Investig Drugs. 2006 May;7(5):423-31.

96. Acuña-Castroviejo D, Escames G, Venegas C, Díaz-Casado ME, Lima-Cabello E, López LC, et al. Extrapineal melatonin: sources, regulation, and potential functions. Cell Mol Life Sci. 2014;71(16):2997-3025.
97. Zheng J, Zhou Y, Zhang D, Ma K, Gong Y, Luo X, et al. Intestinal melatonin levels and gut microbiota homeostasis are independent of the pineal gland in pigs. Front Microbiol. 2024;15:1352586.
98. Pan J, Li F, Wang C, Li X, Zhang S, Zhang W, et al. Effects of Duodenal 5-Hydroxytryptophan Perfusion on Melatonin Synthesis in GI Tract of Sheep. Molecules. 2021;26(17):5275.
99. Park SY, Jang WJ, Yi EY, Jang JY, Jung Y, Jeong JW, Kim YJ. Melatonin suppresses tumor angiogenesis by inhibiting HIF-1alpha stabilization under hypoxia. J Pineal Res. 2010 Mar;48(2):178-84.
100. Carrillo-Vico A, Calvo JR, Abreu P, Lardone PJ, García-Mauriño S, Reiter RJ, Guerrero JM. Evidence of melatonin synthesis by human lymphocytes and its physiological significance: possible role as intracrine, autocrine, and/or paracrine substance. FASEB J. 2004 Mar;18(3):537-9.
101. Kennaway DJ. The dim light melatonin onset across ages, methodologies, and sex and its relationship with morningness/eveningness. Sleep. 2023 May 10;46(5):033.
102. Bubenik GA. Gastrointestinal melatonin: localization, function, and clinical relevance. Dig Dis Sci. 2002;47(10):2336-48.
103. Bartfeld S, Clevers H. Organoids as Model for Infectious Diseases: Culture of Human and Murine Stomach Organoids and Microinjection of Helicobacter Pylori. J Vis Exp. 2015;(105):53359.
104. Hemann EA, Gale M Jr, Savan R. Interferon Lambda Genetics and Biology in Regulation of Viral Control. Front Immunol. 2017;8:1707.
105. Lazear HM, Schoggins JW, Diamond MS. Shared and Distinct Functions of Type I and Type III Interferons. Immunity. 2019;50(4):907-923.
106. Stanifer ML, Guo C, Doldan P, Boulant S. Importance of Type I and III Interferons at Respiratory and Intestinal Barrier Surfaces. Front Immunol. 2020;11:608645.
107. Odendall C, Dixit E, Stavru F, Bierne H, Franz KM, Durbin AF, et al. Diverse intracellular pathogens activate type III interferon expression from peroxisomes. Nat Immunol. 2014 Aug;15(8):717-26.
108. Forero A, Ozarkar S, Li H, Lee CH, Hemann EA, Nadjsombati MS, et al. Differential Activation of the Transcription Factor IRF1 Underlies the Distinct Immune Responses Elicited by Type I and Type III Interferons. Immunity. 2019;51(3):451-464.e6.
109. Ingle H, Makimaa H, Aggarwal S, Deng H, Foster L, Li Y, et al. IFN-λ derived from nonsusceptible enterocytes acts on tuft cells to limit persistent norovirus. Sci Adv. 2023;9(37):2562.
110. Lin SC, Qu L, Ettayebi K, Crawford SE, Blutt SE, Robertson MJ, et al. Human norovirus exhibits strain-specific sensitivity to host interferon pathways in human intestinal enteroids. Proc Natl Acad Sci U S A. 2020;117(38):23782-23793.
111. Frias AH, Jones RM, Fifadara NH, Vijay-Kumar M, Gewirtz AT. Rotavirus-induced IFN-β promotes anti-viral signaling and apoptosis that modulate viral replication in intestinal epithelial cells. Innate Immun. 2012;18(2):294–306.
112. Bhushal S, Wolfsmüller M, Selvakumar TA, Kemper L, Wirth D, Hornef MW, et al. Cell Polarization and Epigenetic Status Shape the Heterogeneous Response to Type III Interferons in Intestinal Epithelial Cells. Front Immunol. 2017;8:671.
113. Kayama H, Takeda K. Regulation of intestinal epithelial homeostasis by mesenchymal cells. Inflamm Regen. 2024;44(1):42.
114. Eenjes E, Grommisch D, Genander M. Functional Characterization and Visualization of Esophageal Fibroblasts Using Organoid Co-Cultures. J Vis Exp. 2023;(191).

115. Pott J, Stockinger S. Type I and III Interferon in the Gut: Tight Balance between Host Protection and Immunopathology. Front Immunol. 2017;8:258.
116. Maestroni GJ. The immunotherapeutic potential of melatonin. Expert Opin Investig Drugs. 2001;10(3):467-76.
117. Qin M, Chen W, Li Z, Wang L, Ma L, Geng J, et al. Role of IFNLR1 gene in PRRSV infection of PAM cells. J Vet Sci. 2021;22(3):e39.
118. Dumoutier L, Tounsi A, Michiels T, Sommereyns C, Kotenko SV, Renauld JC. Role of the interleukin (IL)-28 receptor tyrosine residues for antiviral and antiproliferative activity of IL-29/interferon-lambda 1: similarities with type I interferon signaling. J Biol Chem. 2004;279(31):32269-74.
119. Choi EY, Jin JY, Lee JY, Choi J Il, Choi IS, Kim SJ. Melatonin inhibits Prevotella intermedia lipopolysaccharide-induced production of nitric oxide and interleukin-6 in murine macrophages by suppressing NF-κB and STAT1 activity. J Pineal Res. 2011;50(2):197–206.
120. Li J, Liu H, Wang X, Xia Y, Huang J, Wang T, et al. Melatonin ameliorates Parkinson's disease via regulating microglia polarization in a RORα-dependent pathway. NPJ Parkinsons Dis. 2022;8(1):90.
121. Fang X, Huang W, Sun Q, Zhao Y, Sun R, Liu F, et al. Melatonin attenuates cellular senescence and apoptosis in diabetic nephropathy by regulating STAT3 phosphorylation. Life Sci. 2023; 332:122108.
122. Steen HC, Gamero AM. The role of signal transducer and activator of transcription-2 in the interferon response. J Interferon Cytokine Res. 2012;32(3):103-10.
123. Yu H, Lee H, Herrmann A, Buettner R, Jove R. Revisiting STAT3 signalling in cancer: new and unexpected biological functions. Nat Rev Cancer. 2014;14(11):736-46.
124. Morchang A, Malakar S, Poonudom K, Noisakran S, Yenchitsomanus PT, Limjindaporn T. Melatonin Inhibits Dengue Virus Infection via the Sirtuin 1-Mediated Interferon Pathway. Viruses. 2021;13(4):659.
125. Su WL, Wu CC, Wu SV, Lee MC, Liao MT, Lu KC, Lu CL. A Review of the Potential Effects of Melatonin in Compromised Mitochondrial Redox Activities in Elderly Patients With COVID-19. Front Nutr. 2022;9:865321.
126. Menczel Schrire Z, Phillips CL, Chapman JL, Duffy SL, Wong G, D'Rozario AL, et al. Safety of higher doses of melatonin in adults: A systematic review and meta-analysis. J Pineal Res. 2022;72(2):e12782.
127. Brzezinski A, Rai S, Purohit A, Pandi-Perumal SR. Melatonin, Clock Genes, and Mammalian Reproduction: What Is the Link? Int J Mol Sci. 2021;22(24):13240.
128. Ghorbani-Anarkooli M, Dabirian S, Zendedel A, Moladoust H, Bahadori MH. Effects of melatonin on the toxicity and proliferation of human anaplastic thyroid cancer cell line. Acta Histochem. 2021;123(3):151700.
129. Liu L, Xu Y, Reiter RJ. Melatonin inhibits the proliferation of human osteosarcoma cell line MG-63. Bone. 2013;55(2):432-8.
130. Pal PK, Sarkar S, Chattopadhyay A, Tan DX, Bandyopadhyay D. Enterochromaffin cells as the source of melatonin: key findings and functional relevance in mammals. Melatonin Research. 2019;2(4):61–82.
131. Pandi-Perumal SR, BaHammam AS, Brown GM, Spence DW, Bharti VK, Kaur C, et al. Melatonin antioxidative defense: therapeutical implications for aging and neurodegenerative processes. Neurotox Res. 2013;23(3):267-300.

PUBLICATIONS

Thesis publications:

1. **Šeškutė, M.**, Laucaitytė, G., Inčiūraitė, R., Malinauskas, M., & Jankauskaitė, L. (2025). Enhancing Antiviral Immunity in the Gastrointestinal Epithelium: The Role of Fibroblast–Endothelium Interaction and Melatonin. Cells, 14(13), 990. https://doi.org/10.3390/cells14130990
2. **Šeškutė, M.**, Žukaitė, D., Laucaitytė, G., Inčiūraitė, R., Malinauskas, M., & Jankauskaitė, L. (2024). Antiviral Effect of Melatonin on Caco-2 Cell Organoid Culture: Trick or Treat? International Journal of Molecular Sciences, 25(22), 11872. https://doi.org/10.3390/ijms252211872

The results of the thesis were presented in international scientific conferences:

1. **Šeškutė, Milda**; Žukaitė, Dominyka; Laucaitytė, Goda; Jankauskaitė, Lina. Melatonin demonstrates antiviral potential in human gastrointestinal organoids through modulation of STAT protein expression. Medicina: Abstracts of the International Scientific Conference on Medicine organized within the frame of the 82nd International Scientific Conference of the University of Latvia [: 5 April 2024, Riga, Latvia] / Editor-in-chief Edgaras Stankevičius
2. **Šeškutė, Milda**; Žukaitė, Dominyka; Laucaitytė, Goda; Malinauskas, Mantas; Jankauskaitė, Lina. Melatonin shows potential as an antiviral agent through modulation of the IFN-III pathway in human intestinal organoids. // TOLL 2024 “Road to translation”: 17 - 20 April 2024, Rotterdam, The Netherlands: Abstract E-Book.
3. **Šeškutė, Milda**; Žukaitė, Dominyka; Laucaitytė, Goda; Malinauskas, Mantas; Jankauskaitė, Lina. Melatonin induces antiviral effect in human intestinal organoids via type III IFN pathway // ESCMID Global 2024 - 34th European Congress of Clinical Microbiology and Infectious Diseases, Barcelona, 27-30 April 2024.
4. **Šeškutė, Milda**; Žukaitė, Dominyka; Laucaitytė, Goda; Malinauskas, Mantas; Jankauskaitė, Lina. Melatonin promotes antiviral effect by inducing interferon lambda receptor 1 expression. // ESPID 2024: 42nd Annual Meeting of the European Society for Paediatric Infectious Diseases: Copenhagen & online, 20-24 May 2024: Abstract Book / European Society for Paediatric Infectious Diseases (ESPID).
5. **Šeškutė, Milda**; Kūlokienė, Ugnė; Inčiūraitė, Rūta; Malinauskas, Mantas; Jankauskaitė, Lina. Modulatory antiviral effects of fibroblast-

endothelial interaction and melatonin on Caco-2 cells. // ESPID 2024: 43rd Annual Meeting of the European Society for Paediatric Infectious Diseases: Bucharest & online, 26-30 May 2025: Abstract Book / European Society for Paediatric Infectious Diseases (ESPID).

CURRICULUM VITAE

Name, Surname	**Milda Šeškutė**
Date of birth	1991 01 22
E-mail	milda.seskute@lsmu.lt
Research interests	pediatric infectious diseases, viral infections, vaccination

Education

2020–2024	Lithuanian University of Health Sciences, Department of Pediatrics, Kaunas, Lithuania Doctoral (PhD) studies
2019–2021	University of Oxford, Department of Continuing Education, Oxford, UK Postgraduate Diploma in Pediatric Infectious Diseases
2015–2019	Lithuanian University of Health Sciences, Department of Pediatrics, Kaunas, Lithuania Postgraduate studies and professional qualification of Pediatrician and Pediatric Infectious Disease Specialist
2009–2015	Lithuanian University of Health Sciences, Kaunas, Lithuania Master's degree in Medicine and qualification of medical doctor (MD)

Professional experience

2021–present	*Pediatric Infectious Disease Specialist* Hospital of Lithuanian University of Health Sciences Kauno klinikos
2020–present	*Pediatrician and Pediatric Infectious Disease Specialist* Kaunas Hospital of the Lithuanian University of Health Sciences
2020–present	*Assistant* Department of Pediatrics, Lithuanian University of Health Sciences Infectious Disease Department, Lithuanian University of Health Sciences
2015–2019	*Resident physician* Hospital of Lithuanian University of Health Sciences Kauno klinikos, Kaunas Hospital of the Lithuanian University of Health Sciences
09/2017-11/2017	*ERASMUS+ traineeship* Department of Pediatric Nephrology, Universita degli Studi di Padova, Padova, Italy
09/2014–01/2015	*Internship* Klaipėda Republic Hospital
07/2013	*Internship* Ospedale Filippo Del Ponte, Department of Pediatrics, Varese, Italy

Scientific projects

2023-present	Project Junior Researcher Inovatyvi personalizuota terapija, IPTAVI (project No. S-MIP-23-110, project leader: prof. dr. L. Jankauskaitė)

Courses	ESPID Summer School of Vaccinology (Athens, 2024) Good clinical practice course (2024) EdTech (Digital Competence Framework for Educators) (2023)
Awards	Young Investigator Award in 17th Baltic states conference "Vaccination Day" (2018)
Memberships	European Society for Pediatric Infectious Diseases European Society of Clinical Microbiology and Infectious Diseases Congenital Cytomegalovirus Network (cCMVnet)
Languages	Lithuanian (native) English Italian

ACKNOWLEDGEMENTS

I would like to sincerely thank to my supervisor, prof. dr. Lina Jankauskaitė, who has been an inspiring example of a true scientist. She provided not only valuable scientific knowledge and expertise but also guidance that extended far beyond scientific matters – her emotional support and calm attitude helped me to navigate the most challenging moments during these years. I am also grateful to my consultant, Assoc. Prof. Dr. Mantas Malinauskas, whose thoughtful advice, especially during the critical stages of this work, was truly appreciated.

I am thankful to my teammates Goda Laucaitytė and Dominyka Žukaitė for their input into this work, constant willingness to help, and support of scientific ideas.

This study would not have been possible without the financial support provided by the Research Council of Lithuania (IPTAVI project, No. S-MIP-23-110) and the Research Centre of the Lithuanian University of Health Sciences. I am also grateful for the opportunity to conduct my research at the Institute of Pharmacology and Physiology of LSMU, and for the instrumental support received from other departments – particularly the Clinical and Molecular Gastroenterology Laboratory of the Institute for Digestive Research and the Laboratory of Biochemistry. I would like to especially acknowledge Dr. Rūta Inčiūraitė for her kind assistance and flexibility in flow cytometry experiments.

A special expression of gratitude goes to my teachers, Assoc. Prof. Dr. Giedra Levinienė and Assoc. Prof. Dr. Eglė Tamulevičienė, who were the first to recognize my scientific potential and consistently supported me in becoming an independent scientist. Their continuous encouragement has played a fundamental role in shaping my academic path.

Heartfelt thanks go to my family (those who are still with me and those who are no longer) for their endless patience, understanding, and support throughout this long process. I am deeply thankful to Povilas, who has been always by my side since the beginning of the journey. His ability to understand my work, cheer the achievements and understand failures were very important to me.

I would also like to thank to Assoc. Prof. Dr. Vilma Tamulionytė who gave me physical strength and mood boost to finish this journey.

And lastly, to all the good people – Aušra, Tatjana, my colleagues and other supporters – who surrounded me with kindness and gave me the strength and time to keep going: thank you.

AUTHOR'S CONTRIBUTION

Under the guidance of my supervisor, I learned the fundamentals of cell-culture modeling and good laboratory practice to carry out this research. I was personally responsible for maintaining cell growth, establishing the experimental models described, and conducting all laboratory procedures, including immunofluorescent staining, flow cytometry and ELISA assays. I also analyzed the experimental data, prepared drafts of the resulting publications, and created all of the figures and visualizations presented.

Through these experiments, I gained extensive experience in cell culture, significantly deepened my understanding of cellular mechanisms and protein analysis techniques, and greatly strengthened my competence as an independent investigator.